



Serviço Público Federal  
Ministério da Educação

FUNDAÇÃO UNIVERSIDADE FEDERAL DE MATO GROSSO DO SUL

Programa de Pós-Graduação em Farmácia



**Larissa Bianca Barbosa dos Santos Amorim**

**Síntese e atividade anti-trypanosoma de novos derivados  
nitroimidazol isoxazólicos com substituintes difenil éter e tioeter**

Campo Grande, MS  
2023



Serviço Público Federal  
Ministério da Educação

FUNDAÇÃO UNIVERSIDADE FEDERAL DE MATO GROSSO DO SUL

Programa de Pós-Graduação em Farmácia



**Larissa Bianca Barbosa dos Santos Amorim**

**Síntese e atividade anti-trypanosoma de novos derivados  
nitroimidazol isoxazólicos com substituintes difenil éter e tioeter**

Dissertação apresentada ao Curso de Pós-Graduação em Farmácia da Universidade Federal de Mato Grosso do Sul como requisito final à obtenção do título de Mestre em Farmácia.

Orientador: Prof. Dr. Adriano Cesar De Moraes Baroni

Co-orientador: Dr. Diego Bento de Carvalho

Campo Grande, MS  
2023

## Agradecimentos

Em primeiro lugar, a Deus, por abrir os caminhos e as oportunidades de uma forma tão especial em minha vida, sempre no momento certo. Por ter me guiado e dado coragem para buscar meus sonhos e me dar saúde e determinação para realizar este trabalho.

Um agradecimento especial à minha família. Meu pai, Ailton e minha mãe, Valdirene que sempre me ensinaram através do próprio exemplo, a me esforçar e superar os obstáculos da vida na busca dos meus objetivos. À minha irmã, Nicolly, pelo amor e companheirismo, sempre me esforcei para ser um bom exemplo pra ti.

Ao meu esposo e melhor amigo, Éverton, por sempre acreditar em mim e me incentivar a ser minha melhor versão... sem você eu não teria chegado até aqui. Obrigada por ser meu apoio, por me trazer alegria e fazer sorrir mesmo quando estou "*in the depths of despair*", por me aguentar cantando as mesmas músicas da Taylor por horas sem fim. Como disse o pequeno príncipe: "Amar não é olhar um para o outro, é olhar juntos na mesma direção". Obrigada por ser meu companheiro nessa aventura que é a vida.

Agradeço ao meu orientador, Prof. Adriano. Seu apoio, orientação, risadas e até as broncas fizeram desta uma experiência inesquecível para mim.

Ao Diego, o co-orientador e técnico mais divertido do mundo...jamais esquecerei nossas risadas, discussões profundas, fofocas quentíssimas e dramas no lab. Obrigada por compartilhar seu conhecimento comigo e me ensinar quase tudo que sei sobre síntese.

À Cris, técnica de laboratório da QF, uma supermãe de dois japinhas e também para nós alunos. Seu bom humor e sorriso estampado no rosto foi sempre contagiante para mim, obrigada por todo o apoio.

Aos meus colegas de laboratório e amigos Omar, Camila, Jefferson e Bruno. Obrigada pela parceria nesses últimos anos, todas as gargalhadas compartilhadas, os momentos de consolo que me trouxeram quando estava pra baixo, as músicas cantadas, às vezes bem desafinadas e o mais importante: obrigada pelos FIDs de RMN!!!

A todos os ICs que participaram também no desenvolvimento desse trabalho, a Ágatha e a Maria. Os ICs Rafael e Luiz que sempre foram muito parceiros, a presença de vocês era diversão garantida.

À minha querida amiga paraguaia, Maria de los Angeles, que mesmo de longe me incentivou a seguir minha carreira na área da síntese e escolher o prof. Adriano como orientador. Seu eterno bom humor me contagia até hoje, obrigada pela parceria todos esses anos.

*'Cause there were pages turned  
With the bridges burned  
Everything you lose is a step you take  
So make the friendship bracelets  
Take the moment and taste it  
You've got no reason to be afraid*

*You're on your own, kid  
Yeah, you can face this  
You're on your own, kid  
You always have been*

*-Taylor Swift*

## Table of content

|   |    |
|---|----|
| <b>Chapter I</b> .....  | 1  |
| Introduction .....  | 2  |
| Neglected Tropical Diseases .....                                     | 2  |
| Chagas Disease .....  | 3  |
| Epidemiology .....  | 4  |
| Etiological agent, life cycle and transmission .....                  | 7  |
| Clinical manifestations .....   | 11 |
| Treatments .....  | 12 |
| References .....  | 15 |
| <b>Chapter II</b> .....   | 19 |
| Graphical Abstract (GA) .....   | 20 |
| Abstract .....  | 22 |
| Introduction .....  | 23 |
| Results and Discussion .....  | 25 |
| Chemistry .....   | 25 |
| <i>In vitro</i> Antitrypanosomal activity, cytotoxicity and SAR ..... | 33 |
| Conclusions .....   | 41 |
| Experimental .....  | 42 |
| Supplementary Information .....                                       | 52 |
| Acknowledgments .....   | 52 |
| References .....  | 53 |
| Annexes .....   | 56 |

# Chapter I

# Introduction

## Neglected Tropical Diseases

The World Health Organization (WHO) defines neglected tropical diseases (NTDs) as a diverse group of 20 diseases and conditions of global public health significance. These conditions are most prevalent in tropical regions and are considered endemic in many developing countries, where they impact over a billion individuals living in impoverished conditions. Consequently, the majority of individuals affected by NTDs have far less access to resources, facing challenges such as poor sanitary conditions, inadequate nutrition and lack of access to necessary health care.<sup>1,2</sup>

Furthermore, neglected tropical diseases are a major obstacle to the socioeconomic development and overall quality of life for the individuals affected. Because poverty is a key determinant of NTDs, its consequences include keeping affected individuals out of school and out of the workforce for years, as well as burdening households with high medical costs and trapping communities in cycles of poverty, whilst also costing developing economies billions of dollars annually. Additionally, many NTDs are known to cause physical disfigurement and even disability, leading to stigma and social discrimination of those affected. Thus, because developed countries have comparatively limited NTD transmission, NTDs disproportionately affect the poor and most vulnerable. In spite of their significant worldwide numbers, since overall mortality rates are lower than those for other infectious diseases like HIV/AIDS or malaria, NTDs are disregarded with limited diagnostic, treatment, and public health initiatives.<sup>2-4</sup>

Neglected tropical diseases are caused by viral, protozoan, helminth, bacterial, ectoparasitic and fungal infections such as dengue, leprosy, leishmaniasis and chagas disease; many of which are zoonotic and/or vector borne diseases with complex life cycles (Fig. 1). This hinders efforts to control the spread of NTDs, despite the fact that many of these diseases are preventable or treatable with low-cost interventions. Therefore, the WHO established five key strategies for the prevention and control

of NTDs, consisting of the provision of sanitation and hygiene, vector control, intensified case management, veterinary public health and preventive chemotherapy.<sup>2-4</sup>

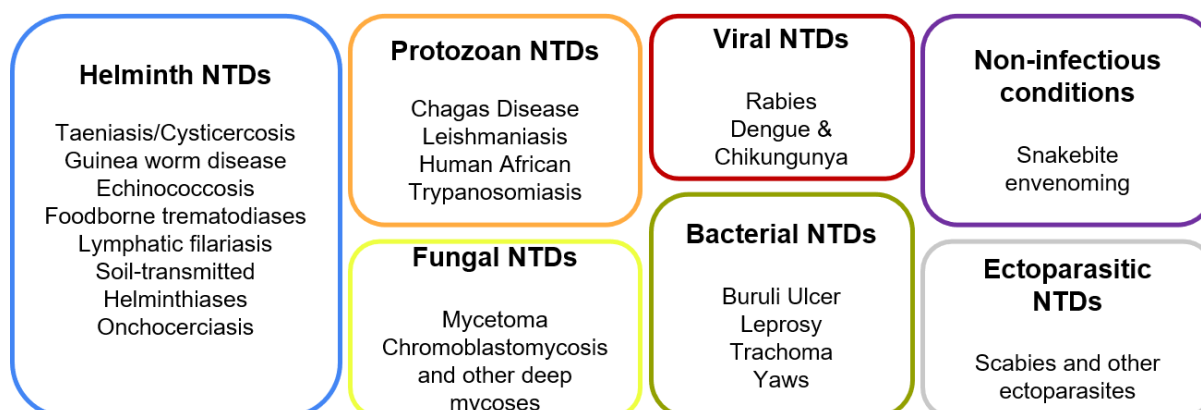


**Figure 1. Neglected tropical diseases (NTDs) according to the WHO classification.**

## Chagas Disease

Chagas disease (CD) or American trypanosomiasis is a zoonotic infectious disease caused by the protozoan parasite *Trypanosoma cruzi*. CD is considered a NTD, whose etiological agent as well as its life cycle, was discovered over a hundred years ago, in 1909, by Brazilian physician Dr. Carlos Chagas. His discovery is considered unique in the history of medicine because it includes the entire cycle of the disease; its etiological agent *T. cruzi* and its evolutionary cycle; the vector insect, the Triatomine bug; and the disease's pathology.<sup>5-8</sup>

Despite its recent discovery, evidence of *T. cruzi* infection in humans goes as far back as 9000 years with the identification of the protozoan's kinetoplastid DNA in Chinchorro mummies. The Chinchorro people are traced back to 7020 B.C. and are known to be the first settlers of the Andean region. Research suggests these first settlers of the Andean region intruded upon the sylvatic cycle of *T. cruzi* infection, thus becoming participants and leading to the gradual evolution of the domestic cycle.<sup>9</sup> Research has also shown changes in land use and biodiversity loss have a significant impact on ecosystem functioning and serve as crucial contributors to infectious disease outbreaks.<sup>10</sup> Thus, given the propensity of some triatomine bugs to adapt to more open vegetation and develop a preference for human housing, it is noteworthy that the emergence of CD's domestic cycle was most



likely brought about by deforestation, as a result of agricultural development of those first settlers.<sup>9,10</sup>

## **Epidemiology**

Currently, it is estimated that CD affects approximately 6-7 million people worldwide, with most cases concentrated in 21 countries of Latin America (Fig. 2), where the disease is endemic.<sup>5,6</sup> Moreover, according to the Pan American Health Organization (PAHO), in these endemic regions around 70 million people are at risk of infection and 30,000 new cases are registered annually. This high incidence is due to the number of people who live in areas of exposure to the disease in the Americas alone, where CD is responsible for approximately 12,000 deaths per year.<sup>11</sup> Nonetheless, it is noteworthy that these figures may be underestimated because quantifying the burden of CD is still a major challenge; Even in endemic regions there is a lack of a precise overview of the disease's current status.<sup>12</sup>

Although CD was originally restricted to the Americas' continental rural areas, the subsequent rise of population mobility in recent decades has caused a shift in the disease profile. Whilst decades ago residents of impoverished rural areas were considered to be more at risk of exposure to CD, because of urbanization, most infected persons now reside in cities and suburban areas.<sup>7</sup> Beyond that, CD is increasingly being identified in countries and regions where it typically wouldn't be found. Due to rises in migration, cases of CD have been reported in the USA, Canada, as well as many European, African, and Western Pacific nations, evidently becoming a growing worldwide health concern.<sup>5,13</sup> For instance, In 2009 the Centers for Disease Control and Prevention (CDC) reported over 300,000 potentially infected individuals in the USA alone.<sup>14</sup> More recent studies have reaffirmed these numbers with an estimated prevalence ranging from 240,000 to 350,000 individuals infected by *T. cruzi* in the USA.<sup>15,16</sup>

Global distribution of cases of Chagas disease, based on official estimates, 2018

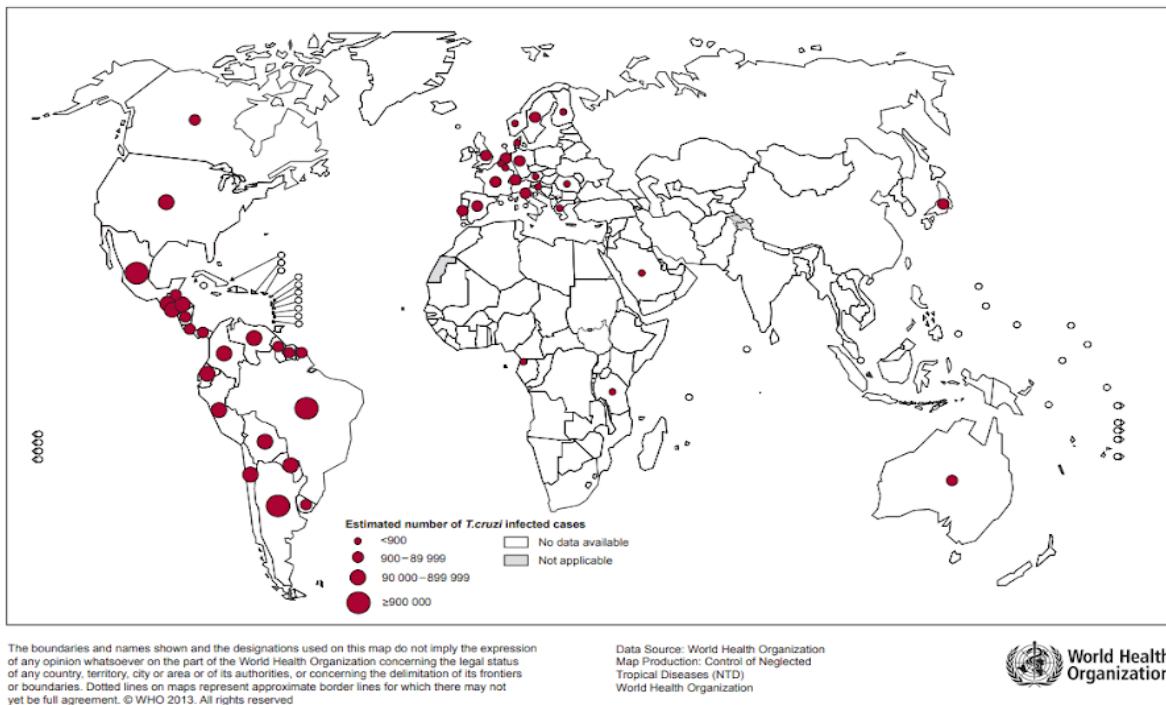


**Figure 2. Map of the global distribution of Chagas Disease, 2018. (Figure from reference 6).**

Contrarily, since the 1990s effective intergovernmental initiatives throughout the Americas have significantly reduced parasite and vector transmission whilst improving access to diagnostic and antiparasitic treatment.<sup>5</sup> Endemic southern cone countries, which include Brazil, Chile, Uruguay, Paraguay and Bolivia have shown the most progress with an average reduction of incidence of 94% from 1990-2006. The progress of these countries alone has reduced the incidence of CD in all of Latin America by 70%, mainly due to the interruption of vectorial transmission in some countries, although other forms of infection such as congenital and oral transmission still pose a challenge to the effective control of the disease.<sup>11,17</sup>

In spite of this significant reduction in incident cases, one of the major obstacles in these endemic regions is accurately estimating seroprevalence in the population. For instance, the incidence of CD in Brazil, one of the most significant countries within the endemic region, has significantly decreased in recent years as a result of the interruption of vectorial transmission.<sup>17</sup> However, there is currently no reliable estimate of the prevalence of Chagas disease in the country as

a whole due to the lack of updated national serological surveys of *T. cruzi* infection in the general population.<sup>18,19</sup>

A systematic review based on national and subnational studies of the prevalence of CD in Brazil from 1980-2012 affirmed a dramatic reduction in incident cases while maintaining a high prevalence in known endemic regions, mostly in the northeast and southeast regions of the country. The study also evidenced CD affecting mainly an elderly population in urban areas, where over 70% of individuals affected by CD reside. This can be attributed to the migration of infected people from rural endemic areas to urban regions, where vectorial transmission is absent. As for the high prevalence in the elderly population, this may be due to the chronic nature of CD, which developed with the aging of individuals infected in the past. The review also emphasized the heterogeneity of the existing data as a strong limitation of the study, since available research was mostly carried out in endemic regions and underrepresented in other areas.<sup>18</sup> Similarly, these results corroborate with another study published in 2019 by Martins-Melo *et. al.* Based on the epidemiological results of the 2016 Global Burden of Disease Study (GBD), their research aimed to assess the overall burden of CD in Brazil and reported the highest fatal and non-fatal burdens due to CD were observed among males and the elderly population, also in the Brazilian states that are significant endemic areas for the disease. In addition, they concluded the illness continues to be a major neglected cause of premature death and disability in the country.<sup>19</sup>

As for mortality rates, a nationwide study published in 2021 evidenced the impact of Chagas Disease-related mortality in Brazil from 2000-2019. During this twenty-year time period, a total of 22,663,092 deaths were registered in the country and CD was identified in 122,291 death certificates (proportional mortality: 0.54%), with 94,788 (77.5%) being recorded as an underlying cause and 27,503 (22.5%) being reported as an associated cause of death. In conclusion, the study found a decreasing trend in Chagas disease-related mortality rates in Brazil over the study period, despite the fact that it is still a significant and neglected cause of death.<sup>20</sup>

There is indeed insufficient data to determine the true impact of Chagas disease on the general population at the national and international levels. Further population-based research is required, not only in Brazil but also in other endemic countries. Mainly because understanding the overall burden and trends of Chagas disease-related morbidity and mortality is critical for tracking and assessing the effects of interventions as well as the success of surveillance and control efforts, especially in endemic countries.

### **Etiological agent, life cycle and transmission**

*Trypanosoma cruzi* is a protozoan parasite of the Trypanosomatidae family that in nature has been found to infect various populations of vertebrate hosts such as humans, wild and domestic animals, as well as invertebrates vector insects. *T. cruzi* displays morphological and functional differences, depending on the vertebrate or invertebrate host. In the mammalian host, the parasite cycles between intracellular forms called amastigotes, which replicate via binary division, and non-replicative and flagellated infective forms, known as trypomastigotes. In the invertebrate host, the parasite evolves from trypomastigote form to epimastigotes, which then replicate by binary division in the gut, differentiating into infective metacyclic trypomastigotes (figure 4).<sup>21-23</sup>

*T. cruzi* is a heterogeneous species with a variety of strains that circulate in mammalian hosts and insect vectors. The diversity of the parasite's genome and the multiplicity of its genotypes and phenotypes are widely recognized, early research even revealed that DNA content varies by up to 40% amongst *T. cruzi* strains. Because of this variation, molecular biology data has led to its classification into seven close-related groups known as discrete typing units (DTUs), TcI to TcVI as well as Tcbat. Genetic variation has been associated with geographical variances in morbidity and mortality, clinical traits, and even treatment response. Nevertheless, there is currently not enough evidence to prove a correlation between parasite lineage and disease severity.<sup>22-25</sup>

Chagas disease can be transmitted by over 100 species of Triatomine insects, which are hematophagous insects of the order Hemiptera, family Reduviidae, and subfamily Triatominae

(figure 3). Although many species of triatomine bugs are possible *T. cruzi* vectors, five are of particular epidemiological importance: *Triatoma infestans*, *Triatoma brasiliensis*, *Triatoma dimidiata*, *Rhodnius prolixus*, and *Panstrongylus megistus*.<sup>22</sup>

These insects, often known as 'kissing bugs,' are primarily found in the Americas, and reside in the crevices of poorly constructed homes in rural or suburban locations. Due to their adaptation to human housing, several triatomine species have become highly effective CD vectors. Others continue to be more sylvatic, remaining in wild environments, rarely invading houses, and feeding on humans. Triatomines often remain hidden during the day and come out at night to feed on animal blood. The insect typically bites exposed skin or mucosa, defecates or urinates close to the bite and when a human instinctively spreads the bug's feces or urine into a bite or other skin lesion, the eyes, or the mouth, the parasite enters the body. During the vectorial infection process, signs indicative of parasite entry may be recognized, such as a skin lesion called a chagoma; and in rare cases of ocular inoculation, a purple swelling of periorbital tissue called romaña's sign (figure 4).<sup>11</sup>



**Figure 3. Triatomine insect during a blood meal. (figure from reference 26)**

The *T. cruzi* life cycle initiates when the triatomine vector consumes circulating trypomastigotes in a blood meal from an infected mammalian host. In the vector's midgut, trypomastigotes are converted into the epimastigote form, which is the main replicating stage in the invertebrate host. Epimastigotes then proceed to the insect's hindgut where they develop into infective metacyclic trypomastigotes, which are expelled with the vector's feces and urine. Metacyclic trypomastigotes enter the mammalian host via a bite wound or damaged skin or mucous membrane,

where they invade a variety of nucleated cells. Trypomastigotes then differentiate into intracellular amastigote forms in the host cell's cytoplasm, where they replicate by binary fission. These amastigotes evolve into trypomastigotes and at the conclusion of this phase, the host cell ruptures releasing trypomastigotes into the bloodstream. The circulating parasites can then infiltrate new cells, begin new replication cycles, and infect vectors that feed on the host, thus completing the parasite's life cycle.<sup>22-25</sup>

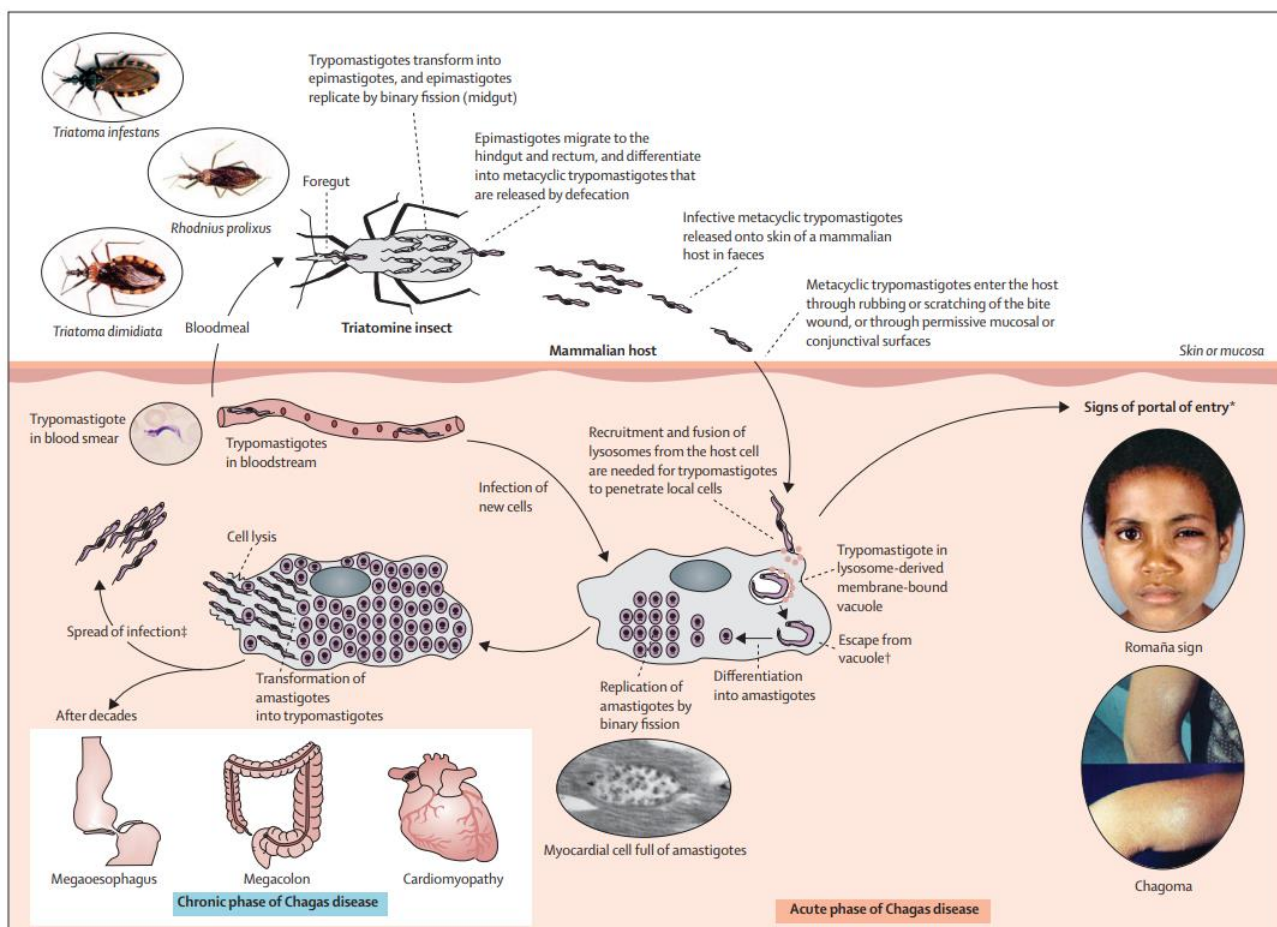


**Figure 4. *T. cruzi* life cycle (figure from reference 25)**

Further studies have highlighted the existence of pleomorphic populations of the parasite that have brought significant impacts on the current understanding of the life cycle of *T. cruzi*. In mammalian hosts, slender and broad blood trypomastigotes have been identified and recent studies have discovered that the proportion of these pleomorphic forms is strain dependent and can be linked to varying infection outcomes in the host. This is due to the fact that slender forms are more infectious (infecting through penetration and phagocytosis), they also determine earlier parasitemia and are

more sensitive to circulating antibodies. On the other hand, broad forms endure longer in the bloodstream, are less infectious (infecting only through phagocytosis) whilst developing later parasitemia, and are more resistant to antibodies. Additionally, slender and broad forms also exhibit tropism for different tissues: broad forms demonstrate tropism for cardiac, skeletal, and smooth muscle cells, whereas slender forms mostly infect mononuclear phagocytic system cells and show tropism for spleen, liver, and bone marrow.<sup>22,27</sup>

Another significant finding in 2017 revealed that some amastigotes may become metabolically dormant or quiescent, which is crucial in terms of treatment resistance and disease relapse. Even after treatment, these forms have the ability to spontaneously reactivate cell cycle and re-establish infection in chronically infected tissues of mammalian hosts. However, the physiological mechanisms of dormancy in *T. cruzi* have not yet been fully elucidated; therefore, more research on the mechanism of dormancy must be conducted in order to therapeutically overcome it.<sup>22</sup>

Regarding the various forms of transmission, in various countries of Central and South America, the Pan American Health Organization has declared the interruption of vector-borne transmission.<sup>11</sup> Although there has been significant improvement in the management of vectorial transmission in endemic areas, other forms of transmission remain a concern for acute CD cases. Recently, oral transmission, organ transplantation and blood transfusion, congenital transmission and laboratory accidents have been implicated in many cases; as for non-endemic areas, these non-vectorial forms of transmission play an important role as well.

In the Amazon Region, over 780 acute cases were related to the intake of contaminated beverages or food between 1998 and 2010. The main sources of disease outbreaks were fruit, such as açaí, and sugar cane juices infected with parasites from triatomine insects and the number of people infected in an oral outbreak might range from a few to more than 100. Although the clinical signs and symptoms of orally transmitted acute CD are comparable to those of other routes, there are significant differences that may be attributed to inoculum size. A notable distinction is that the acute phase of

vectorial infection affects just 2%-5% of patients. As for oral outbreaks, prolonged fever is a common symptom and is generally associated with higher mortality rates than vector-borne infection.<sup>23, 25</sup>

### **Clinical manifestations**

After vector-borne infection, the incubation period lasts for one to two weeks, after which the disease can be asymptomatic or present mostly self-limiting symptoms such as prolonged fever and fatigue. Hepatosplenomegaly, lymphadenopathy, splenomegaly, edema and in rare cases, myocarditis or meningoencephalitis can also be observed during the acute phase of the disease. Throughout the acute phase, the disease can be diagnosed by direct microscopic examination of the individual's blood, through PCR and culture because parasitemia is high during this period. However, the nonspecific symptoms associated with the acute phase make the detection of the disease very difficult, which is why acute infections are rarely diagnosed.<sup>23, 25</sup>

The acute phase lasts approximately 4-8 weeks, during which treatment with antitrypanosomal drugs shows more efficacy. Even if the infection is not treated with medications, symptoms of the acute phase disappear on their own in roughly 90% of infected people. Approximately 60-70% of these patients will never develop clinically noticeable symptoms, despite the fact that they are infected for life. In the few symptomatic cases, the parasite itself, as well as the host's acute immunoinflammatory response generated by the parasite's presence, is responsible for causing organ and tissue damage. After a 90-day period, parasitemia drops significantly and patients may enter what is known as the indeterminate form of CD. This form of CD is distinguished by the presence of *T. cruzi* seropositivity, low parasitemia and an absence of clinical signs and symptoms of cardiac and digestive involvement with normal chest radiography and electrocardiography.<sup>23, 25, 28,29</sup>

The other 30–40% of patients will subsequently develop what is known as a determinate chronic form of CD that often manifests 10–30 years after infection. This chronic determinate form can be distinguished by cardiac, digestive (megaesophagus and megacolon), or cardio digestive manifestations. The most common and severe type of organ involvement, however, is chronic



Chagas' cardiomyopathy that can be defined by chronic inflammation resulting in damage the myocardium and affects up to 45% of infected patients. In this chronic phase, parasitemia is low, although, reactivation of Chagas disease can also happen in individuals who experience immunological compromise, such as those who are co-infected with HIV or on immunosuppressive medications.<sup>23, 25, 28,29</sup>

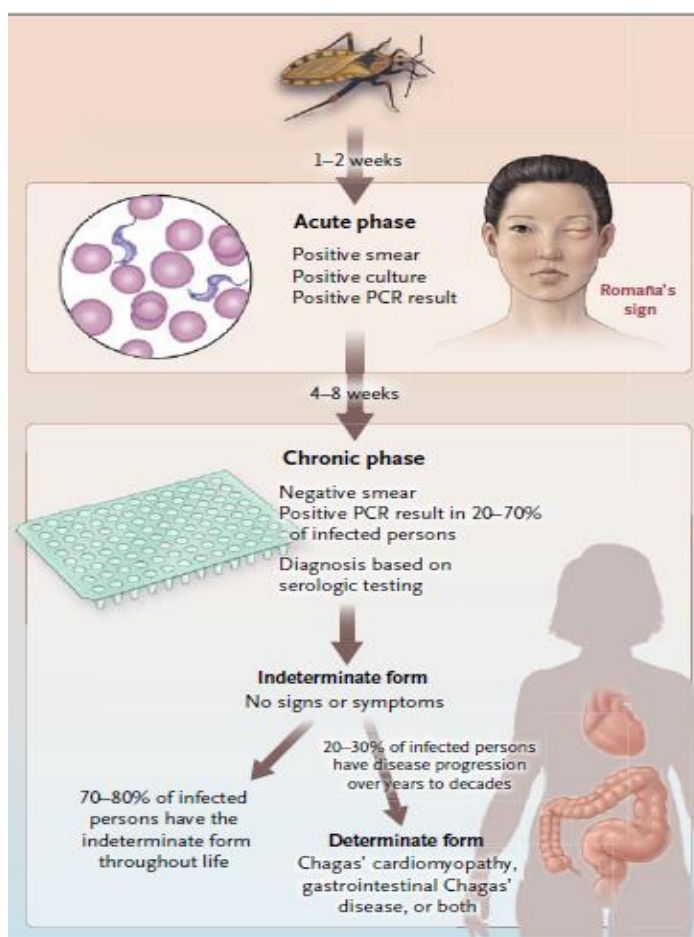


**Figure 5. *T. cruzi* life cycle (figure from reference 29)**

## Treatments

Treatment of CD can be classified as either etiologic (treating *T. cruzi* infection directly) or non-etiological (treating disease symptoms). Elimination of parasites and the avoidance of organ damage are the goals of etiologic treatment. Nonetiological treatment, on the other hand, attempts to prevent morbidity and mortality associated with the chronic phase of the disease. Following the etiologic treatment approach, heterocyclic drugs nifurtimox and benznidazole, introduced in 1969

and 1971, respectively, are the only two drugs that have been proven to be effective against CD. Both are prodrugs, with efficacy and safety profiles that are far from ideal and are mainly affected by the age of the patients as well as the stage of the infection.<sup>28-30</sup>

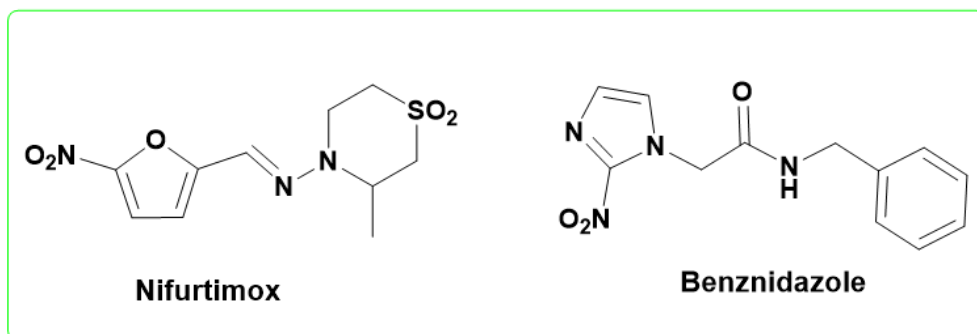


**Figure 6. Antitrypanosomal drugs nifurtimox and benznidazole**

In order to mediate their cytotoxic effects, nitroheterocyclic compounds, including nifurtimox and benznidazole, act as substrates to *T. cruzi* type I and type II nitroreductases. The reduction of the compound's nitro group to an amine group generates cytotoxic reactive oxygen species (ROS) that damage vital structures in the parasite. Both drugs are better tolerated by children and are more effective when administered during the acute phase of the disease. In the chronic indeterminate phase, cure rates range from 86% in children under the age of 14 to 7-8% in adults. Nifurtimox and benznidazole both lessen the intensity of symptoms, shorten the clinical course of illness, and minimize the parasitemia duration in patients with acute Chagas disease and early neonatal Chagas disease.<sup>28-31</sup>

5-Nitrofuran derivative nifurtimox (3-methyl-N- [(5-nitro-2 furanyl)-methylene]-4-morpholinamine 1,1 dioxide) was the first drug used to treat CD and has shown higher toxicity and adverse effects than benznidazole. Because of this, nifurtimox is not the treatment of choice for CD in many endemic countries and was discontinued in Brazil, Argentina, Chile, and Uruguay in the early 1980s. However, due to a lack of alternatives, it has maintained its indication as a second-line treatment when benznidazole fails or exhibits toxicity. The WHO recommends 8 to 10 mg/kg daily in three separate doses for adults and 15 to 20 mg/kg daily in four divided doses for children over a

period of 60 to 90 days. The most common side effects of nifurtimox are gastrointestinal disorders such as vomiting, nausea, and abdominal discomfort. However, up to 30% of patients may also have central nervous system disturbances such as polyneuritis, disorientation, seizures, and even psychosis.<sup>28-</sup>

31

Benznidazole N-benzyl-2-(2-nitro-1H-imidazol-1-yl) acetamide, a 2-nitroimidazole derivative, is utilized as the first line treatment for Chagas disease because of its superior safety profile and better tissue penetration. It is recommended that benznidazole be administered orally every day for 60 days at a dose of 5 to 7 mg/kg for adults and 10 mg/kg for children. Nonetheless, due to the drug's low solubility along with the high doses of the medication given over an extended period of time, side effects such as dermatological hypersensitivity (rashes and exfoliative dermatitis) which are the most common symptoms, bone marrow suppression (thrombocytopenia, neutropenia, and agranulocytosis), and peripheral neuropathy may occur. Although treatment must be interrupted promptly if neuropathy or bone marrow suppression is observed. Intrinsic resistance to benznidazole has also been recorded, and as previously mentioned, the alternate treatment option is nifurtimox.<sup>28-</sup>

31

Despite numerous studies showing its efficacy in the acute phase of the disease, the main drawback in treatment with benznidazole is the low cure rate during the chronic phase. Patients with mild-to-moderate disease showing early signs of cardiomyopathy and those with chronic CD in the indeterminate phase typically receive antitrypanosomal treatment. The majority of medical professionals now agree that most people with chronic *T. cruzi* infections should be treated, with exclusion criteria being a maximum age of 55 and the presence of severe irreversible cardiomyopathy. In the BENEFIT trial (Benznidazole Evaluation for Interrupting Trypanosomiasis), a randomized, double-blind, placebo-controlled study where 2854 patients from several endemic countries (Argentina, Bolivia, Brazil, Colombia, and El Salvador) were treated for 40 to 80 days with either benznidazole or placebo. These patients were assessed for side effects, ECG, liver function, and their blood parasite burden monitored for at least 5 years after therapy. The study concluded that treatment

with benznidazole did not significantly improve the clinical heart damage of individuals with established moderate-to-severe chagas' cardiomyopathy. Despite not being recommended for treatment of patients with signs of advanced cardiomyopathy, in cases of disease reactivation in chronic patients, antitrypanosomal treatment should be promptly initiated. Cases of acute CD, congenital infection, infected children and patients up to the age of 18 with chronic disease are strongly advised to receive antitrypanosomal treatment.<sup>28-31</sup>

Both benznidazole and nifurtimox can cause serious adverse effects which can lead to poor treatment adherence. Despite having good action in the acute phase of the disease, another important obstacle of treatment with the available drugs is the inactivity of these substances during the chronic stage as well as the occurrence of intrinsic resistance to these medications. Furthermore, because *T. cruzi* has a complex life cycle, infecting many different species of mammals, and is capable of adapting from sylvatic to rural and even urban areas, Chagas Disease currently represents a major therapeutic challenge in the combat of neglected tropical diseases even in non-endemic areas. Another rising issue is the drop in awareness and interest in combating CD, as its case numbers have significantly dropped in endemic regions following measures of vector control by Public Health Organizations. Thus, the impact of Chagas disease is still felt strongly on a global scale. As a result, pursuing the search for new, more effective, and tolerable treatments is crucial.

## References

1. World Health Organization, <https://www.who.int/news-room/questions-and-answers/item/neglected-tropical-diseases>, accessed in June 2023.
2. World Health Organization, *Working to overcome the global impact of neglected tropical diseases: first WHO report on neglected tropical diseases*, World Health Organization, 2010, [<https://apps.who.int/iris/handle/10665/44440>].

3. Mackey, T. K.; Liang, B. A.; Cuomo, R.; Hafen, R.; Brouwer, K. C.; & Lee, D. E.; *Clin. Microbiol. Rev.* **2014**, 27, 949, [<https://doi.org/10.1128/cmr.00045-14>].
4. Engels, D.; Zhou, XN.; *Int. J. Med. Parasit. Dis.* **2020**, 28, 9. [<https://mednexus.org/doi/full/10.1186/s40249-020-0630-9>].
5. World Health Organization, [[https://www.who.int/news-room/fact-sheets/detail/chagas-disease-\(american-trypanosomiasis\)](https://www.who.int/news-room/fact-sheets/detail/chagas-disease-(american-trypanosomiasis))], accessed in June 2023.
6. World Health Organization, [[https://www.who.int/health-topics/chagas-disease#tab=tab\\_1](https://www.who.int/health-topics/chagas-disease#tab=tab_1)], accessed in June 2023.
7. Steverding D.; *The history of Chagas disease. Parasit Vectors.* **2014**, 10; 7. [<https://parasitesandvectors.biomedcentral.com/articles/10.1186/1756-3305-7-317>].
8. Fiocruz, [<https://chagas.fiocruz.br/historia/a-descoberta/#descoberta>], accessed in June 2023.
9. Araújo, A.; Jansen, AM.; Reinhard, K.; Ferreira, L.F.; Paleoparasitology of Chagas disease-- a review. *Mem Inst Oswaldo Cruz.* **2009**, 104 , Suppl 9, [<https://doi.org/10.1590/S0074-02762009000900004>].
10. Andreazzi, C. S.; Martinez-Vaquero, L. A.; Winck, G. R.; Cardoso, T. S.; Teixeira, B. R.; Xavier, S. C.; D'Andrea, P. S.; *Ecography.* **2023**, 5, [<https://doi.org/10.1111/ecog.06579>].
11. Pan American Health Organization, <https://www.paho.org/en/topics/chagas-disease#:~:text=In%20the%20Americas%2C%20Chagas%20disease,risk%20of%20contracting%20this%20disease>, accessed in June 2023.
12. Miranda-Schaeubinger, M.; Chakravarti, I.; Freitas, L. K.C.; Omidian, Z.; Robert, H.; *Curr Trop Med Rep.* **2019**, 6, 23.[<https://doi.org/10.1007/s40475-019-00177-y>].
13. Schmunis, GA.; Yadon ZE.; *Acta Trop.* **2010**, 1, 14. [<https://doi.org/10.1016/j.actatropica.2009.11.003>].
14. Caryn, B.; Susan, P.; *Clin. Infect. Dis.* **2009**, 5, 52.[<https://doi.org/10.1086/605091>].
15. Manne-Goehler, J.; Umeh C.A.; Montgomery S.P.; Wirtz V.J.; *PLoS Negl. Trop. Dis.* **2016**, 7, 10. [<https://doi.org/10.1371/journal.pntd.0005033>].

16. Irish, A.; Whitman, J.D.; Clark, E.H.; Marcus, R.; Bern, C.; *United States. Emerg. Infect. Dis.* **2022**, 28, 7. [<https://doi.org/10.3201/eid2807.212221>].
17. Moncayo, Á.; Silveira, A. C.; *American Trypanosomiasis, Chagas Disease: One Hundred Years of Research*, Second Edition, 2017, 59. [<https://doi.org/10.1590/S0074-02762009000900005>].
18. Martins-Melo, F. R.; Ramos, Jr, A. N.; Alencar, C. H.; Heukelbach J.; *Acta Trop.* **2014**, 130, 167. [<https://doi.org/10.1016/j.actatropica.2013.10.002>].
19. Martins-Melo, F. R.; Carneiro, M.; Ribeiro, A. L. P.; Bezerra, J. M. T.; Werneck, G. L.; *Int. J. Parasitol.* **2019**, 49, 301. [<https://doi.org/10.1016/j.ijpara.2018.11.008>].
20. Martins-Melo, F. R.; Castro, M. C.; Werneck, G. L.; *Acta Trop.* **2021**, 220, [<https://doi.org/10.1016/j.actatropica.2021.105948>].
21. Zuma, AA.; Dos Santos Barrias, E.; De Souza, W.; *Curr Pharm Des.* 2021; 27, 1671. [<https://dx.doi.org/10.2174/1381612826999201203213527>].
22. Martín-Escolano, J.; Marín, C.; Rosales, M. J.; Tsaousis, A. D.; Medina-Carmona, E.; Martín-Escolano, R., *ACS Infect. Dis.* **2022**, 8, 1107. [<https://doi.org/10.1021/acsinfecdis.2c00123>].
23. Pérez-Molina, J. A.; Molina, I.; *The Lancet.* **2018**, 391, 82. [[https://doi.org/10.1016/S0140-6736\(17\)31612-4](https://doi.org/10.1016/S0140-6736(17)31612-4)].
24. Jansen, A. M.; Xavier, S. C. D. C.; Roque, A. L. R.; *Front. Cell. Infect. Microbiol.* **2020**, 10, 10. [<https://doi.org/10.3389/fcimb.2020.00010>].
25. Rassi, A.; Marin-Neto, J. A.; Chagas disease. *The Lancet.* **2010**, 375, 1388. [[https://doi.org/10.1016/S0140-6736\(10\)60061-Xc](https://doi.org/10.1016/S0140-6736(10)60061-Xc)].
26. Jurberg, J.; Rodrigues, J. M.; Moreira, F. F.; Dale, C.; Cordeiro, I. R.; Valdir, Jr D.; Rocha, D. S.; *Atlas Iconográfico dos triatomíneos do Brasil: vetores da doença de Chagas*, 2014. [[http://www.fiocruz.br/ioc/media/Atlas\\_triatominio\\_jurberg.pdf](http://www.fiocruz.br/ioc/media/Atlas_triatominio_jurberg.pdf)].

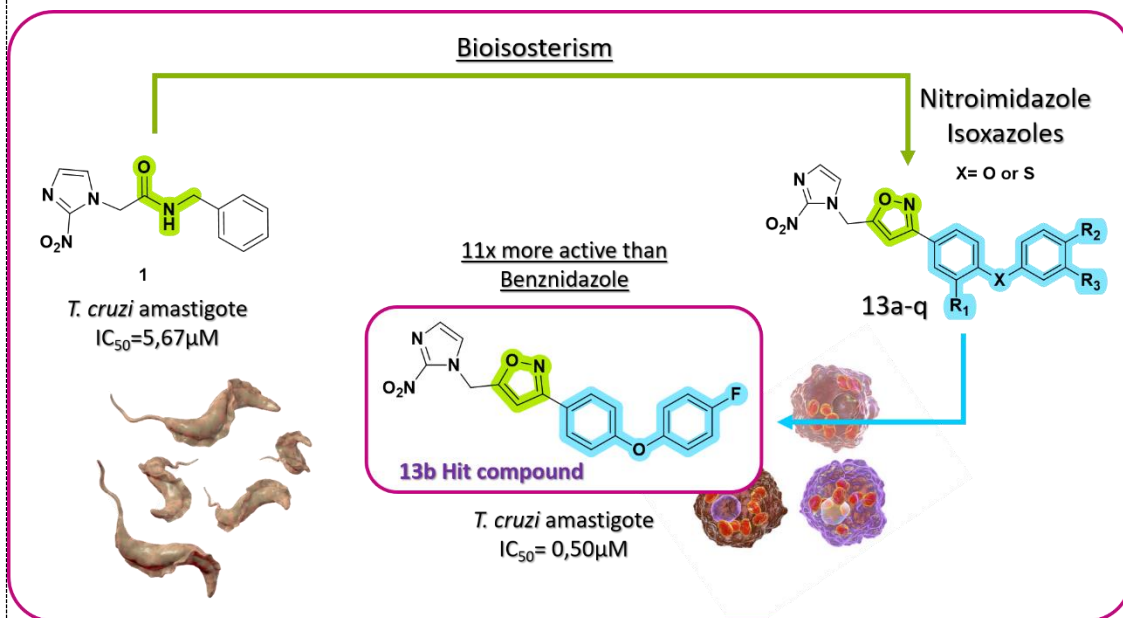
27. Abegg, C. P.; de Abreu, A. P.; da Silva, J. L.; de Araújo, S. M.; Gomes, M. L.; Ferreira, É. C.; de Ornelas Toledo, M. J.; *Exp. Parasitol.* **2017**, *176*, 8.  
[<https://doi.org/10.1016/j.exppara.2017.02.013>].
28. Echeverria, L. E.; Carlos, A. M.; *Infectious Disease Clinics*, **2019**, *33*, 119.  
[<https://doi.org/10.1016/j.idc.2018.10.015>]
29. Bern, C.; *New England Journal of Medicine*, **2015**, *373*, 456.  
[<https://doi.org/10.1056/nejmra1410150>].
30. Pérez, J. A.; Crespillo, C.; Nicolau, P.; Molina, I.; *Enferm. Infecc. Microbiol. Clin.* **2021**, *39*, 458.[<https://doi.org/10.1016/j.eimc.2020.04.011>].
31. Bermudez, J.; Davies, C.; Simonazzi, A.; Real, J. P.; Palma, S.; *Acta trop.* **2016**, *156*, 1.  
[<https://doi.org/10.1016/j.actatropica.2015.12.017>]

# Chapter II



## Graphical Abstract (GA)

GA Figure:



**GA Text:** Seventeen novel nitroimidazole isoxazole compounds with diphenyl ether and thioether substituents were synthesized and evaluated for antitrypanosomal activity in amastigotes, as well as for their cytotoxicity. Twelve of the synthesized compounds showed a higher potency than the reference drug benznidazole (BNZ), many of which also exhibited a better toxicity profile than the reference drug. Compound **13b** was 11-fold more active than BNZ with an  $IC_{50}$  of  $0.50\mu M$ , also showing a higher toxicity profile with a selectivity index of 199.4.

**Synthesis and Antitrypanosomal activity of novel Nitroimidazole Isoxazole derivatives with  
Diphenyl ether and thioether substituents**

***Larissa B. B. Santos,<sup>a</sup> Diego B. Carvalho,<sup>a</sup> Gisele B. Portapilla,<sup>b</sup> Sergio de Albuquerque<sup>b</sup>***

***Adriano C. M. Baroni,<sup>\*a</sup>***

*<sup>a</sup> Laboratório de Síntese e Química Medicinal (LASQUIM), Faculdade de Ciências Farmacêuticas,  
Alimentos e Nutrição, Universidade Federal do Mato Grosso do Sul, UFMS, Campo Grande, Mato  
Grosso do Sul, CEP 79051-470, Brazil*

*<sup>b</sup> Departamento de Análises Clínicas, Toxicológicas e Bromatológicas, Faculdade de Ciências  
Farmacêuticas de Ribeirão Preto – Universidade de São Paulo, Ribeirão Preto, São Paulo, CEP  
14040-900, Brazil*

\* [adriano.baroni@ufms.br](mailto:adriano.baroni@ufms.br)

ORCID ID: 0000-0002-5371-3755

## Abstract

Chagas disease remains a significant public health problem, affecting 6-7 million people worldwide. The key issues with available therapeutic approaches include toxicity, a variety of adverse effects, and inefficiency in the chronic stage of the disease, emphasizing the need to find new drug treatments. Therefore, we synthesized seventeen novel 3,5-disubstituted isoxazole nitroimidazole analogs of benznidazole with diphenyl ether and thioether substituents and evaluated their antitrypanosomal activity and cytotoxicity. Compounds **13a-q** were obtained in moderate to good yields (29–81%), **13a-g** displayed greater activity than benznidazole. **13b** (R1= Ph-O-(4-F-Ph)) and **13g** (R1= Ph-O-(4-OCH<sub>3</sub>-Ph)) were the most active of all the synthesized compounds (IC<sub>50</sub>=0.50μM and IC<sub>50</sub>=0.64μM, respectively). Compounds **13h-n** included 3-fluoro substituent in the first phenyl ring, resulting in lower activity and safety profile. The diphenyl thioether compounds **13o-q** exhibited only moderate activity (IC<sub>50</sub>=11μM- 20.55μM). Further research is needed to better understand the role of diphenyl ether groups in antitrypanosomal activity.

**Keywords:** Isoxazole, antitrypanosomal, Chagas disease, bioisosterism, cycloaddition [3+2]

## Introduction

Chagas disease, also known as American Trypanosomiasis, is a tropical illness caused by *Trypanosoma cruzi*, a Trypanosomatidae protozoan. Whilst the most common form of infection with *T. cruzi* is through vectorial transmission, which occurs through contact with the feces of a triatomine insect, other important means of infection include infected blood transfusion, oral transmission through contaminated food, congenital transmission and organ transplantation.<sup>1-2</sup>

According to the World Health Organization (WHO), it is estimated that there are approximately 6 to 7 million people infected worldwide, making it a major public health problem, especially in Latin American countries where the disease is endemic.<sup>1</sup> The disease also has a significant impact on the social and economic well-being of the poverty-stricken communities it mainly affects, classifying it as a neglected tropical disease.<sup>1-3</sup> Although Chagas disease is widespread in Latin America, migratory patterns have disseminated it worldwide, with cases confirmed in Europe, the United States, Japan and Australia, making it a worldwide health problem.<sup>4-</sup>

6

Currently, therapeutic options for the treatment of Chagas disease are limited to two nitroheterocycle drugs, benznidazole and nifurtimox. Despite their poor safety and effectiveness profiles, these have been the primary treatment for nearly 50 years.<sup>5</sup> Both drugs are most effective during the acute phase of *T. cruzi* infection, present better tolerance in children whilst showing higher toxicity in adults and varied susceptibility among *T. cruzi* strains. Nifurtimox is a nitrofurant derivative that was initially introduced in 1969, however, it is poorly tolerated in adult patients, with low treatment adherence due to the drug's numerous adverse effects. These include gastrointestinal symptoms such as anorexia, vomiting, and diarrhea, neurological disorders including dizziness, headaches, mood swings, disorientation, and insomnia, as well as fatigue and skin rashes.<sup>5,8</sup>

Benznidazole **1** is a 2-nitroimidazole derivative and is currently the first line of treatment for Chagas disease demonstrating a similar efficacy profile to that of Nifurtimox. Although its safety and tolerability are slightly better than those of nifurtimox, adverse events such as allergic dermatopathy,

vomiting, nausea, peripheral polyneuropathy and even bone marrow depression have been reported after treatment.<sup>9</sup> Due to these adverse events, patient adherence is often compromised, emphasizing the need for the discovery of new, more effective treatments for Chagas disease with fewer adverse effects.

Nitroheterocycle compounds exhibit a wide range of biological activities, including antibacterial, antituberculosis, and antiparasitic properties, and have emerged as promising therapeutic options for treating neglected diseases.<sup>10</sup> Besides benznidazole and nifurtimox, other nitroheterocycle compounds have demonstrated significant antitrypanosomal activity. For instance, fexinidazole, a 5-nitroimidazole compound, was developed by The Drugs for Neglected Diseases initiative (DNDi) and was approved for the treatment of human African trypanosomiasis.<sup>11</sup>

Given the re-emergence of nitroheterocycles as effective therapeutic options in the treatment of neglected diseases, our research group devised and synthesized a series of triazole compounds based on the structure of benznidazole **1**. The study confirmed previous findings by demonstrating that bioisosteric replacement of the amide group with a 1,2,3-triazole ring resulted in compounds with good antitrypanosomal activity.<sup>14</sup>

Based on these promising results, the isoxazole scaffold was used in another study conducted by our research group. The isoxazole moiety is also well-known for its several biological activities and has been widely employed in the development of numerous therapeutic agents, including antibacterial, anti-cancer, anti-inflammatory, anti-viral, and anti-parasitic compounds.<sup>13</sup> As a result, in novel benznidazole derivatives, a bioisosteric substitution of the amide group by an isoxazole core was proposed, and the outcomes revealed that isoxazole compounds exhibit higher activity when compared to triazole compounds with similar substituents.<sup>12,14</sup>

Therefore, with the purpose of developing novel antitrypanosomal compounds with a better safety and efficacy profile, this study reports the synthesis of a new series of nitroimidazole isoxazole compounds with diphenyl ether and thioether substituents (Figure 1). The design is based on the structure of benznidazole. Additionally, the cytotoxicity and antitrypanosomal activity of these

compounds against the amastigote form of *Trypanosoma cruzi* were evaluated.

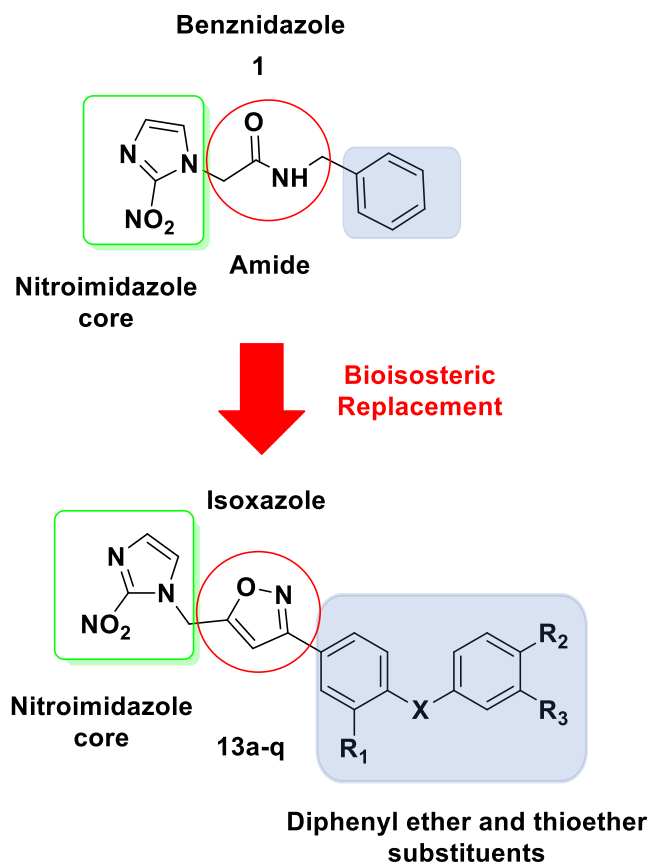


Figure 1. Design of nitroimidazole isoxazoles **13a-q** based on the structure of antitrypanosomal drug benznidazole **1**.

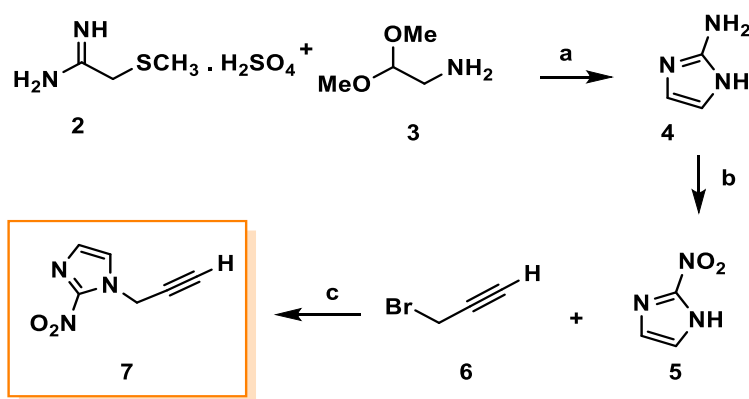
## Results and Discussion

### Chemistry

Nitroimidazole isoxazole compounds were synthesized through a [3+2] cycloaddition reaction between two main building blocks, terminal acetylene (propargyl-2-nitroimidazole) and diphenyl ether or thioether chloro-oximes exhibiting varied substituents. In this study, we report the synthesis of 17 previously unpublished isoxazole compounds with diphenyl ether and thioether substituents.

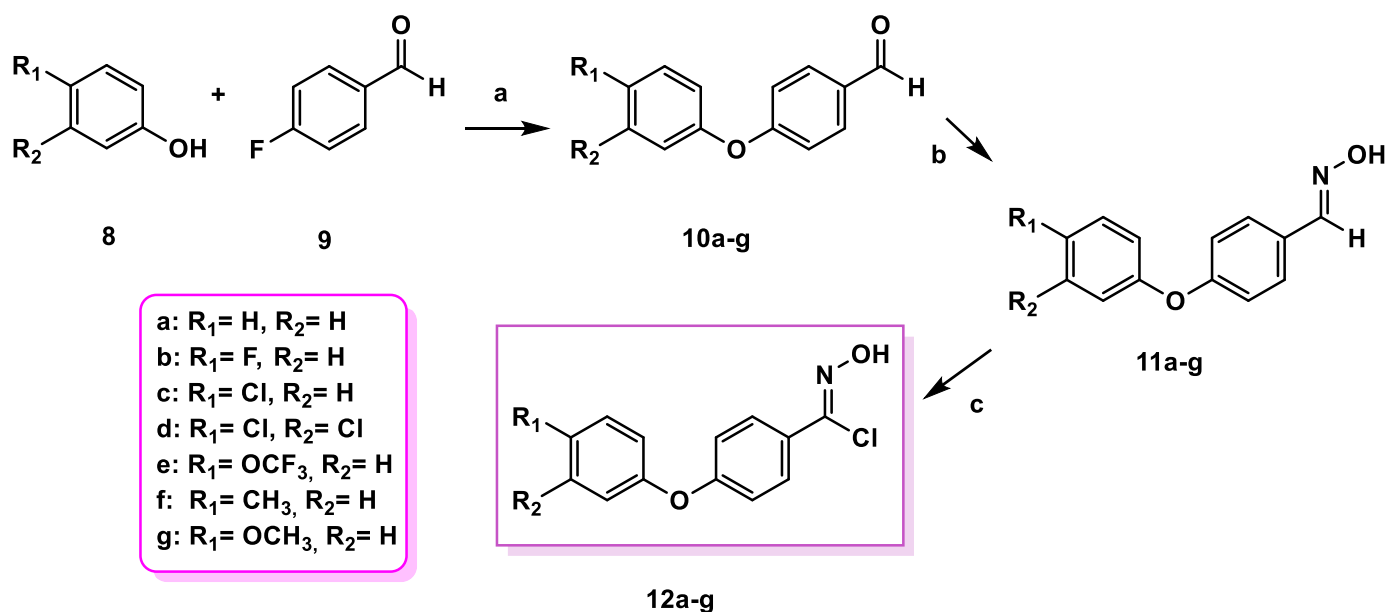
The terminal acetylene **7** was obtained by the cyclization of *S*-methylisothiourea hemisulfate salt **2** and aminoacetaldehyde dimethyl acetal **3**, providing 2-aminoimidazole **4** in 60 % yield (Scheme 1, procedure a).<sup>15</sup> Then, 2-nitroimidazole **5** was synthesized with an 80% yield by diazotization of 2-

aminoimidazole, followed by nitration with  $\text{NaNO}_2$  in the presence of copper sulfate (Scheme 1, procedure b). 2-nitroimidazole was then treated with propargyl bromide **6** in the presence of  $\text{K}_2\text{CO}_3$  in acetone to produce propargyl-2-nitroimidazole (Scheme 1, procedure c), which was subsequently purified through flash chromatography, resulting in an 84% yield of the terminal acetylene **7**.<sup>16-17</sup>



**Scheme 1.** Synthesis of terminal acetylene. Reagents and conditions: a)  $\text{H}_2\text{O}$ ,  $75^\circ\text{C}$ , 1h, (61%). b) 1)  $\text{H}_2\text{O}$ ,  $-5^\circ\text{C}$ ,  $\text{HBF}_4$ . 2)  $\text{NaNO}_2$ ,  $-10^\circ\text{C}$ , 30 min. 3)  $\text{CuSO}_4 \cdot 5\text{H}_2\text{O}$ , r.t., 24h (80%). c)  $\text{K}_2\text{CO}_3$ , acetone, r.t. 24h (84%).

The chloro-oximes were obtained using two distinct approaches, the general procedure A (GP-A) which initiated with the synthesis of 4-phenoxybenzaldehyde or through general procedure B (GP-B) which initiated with the synthesis of 4-phenoxybenzonitrile and 4-(phenylthio)benzonitrile. General procedure A (scheme 2) was applied to render chloro-oximes **12a-g** with moderate to good yields (40-89%) and began with the synthesis of phenoxybenzaldehydes **10a-g** by a nucleophilic aromatic substitution between 4-fluorobenzaldehyde and phenols with desired substituents (scheme 2, procedure a).<sup>18</sup> Next, phenoxybenzaldehydes reacted with hydroxylamine hydrochloride (scheme 2, procedure b) producing aldoximes **11a-g** followed by chlorination with NCS (N-chlorosuccinimide) to produce chloro-oximes **12a-g** (scheme 2, procedure c).<sup>19-20</sup>

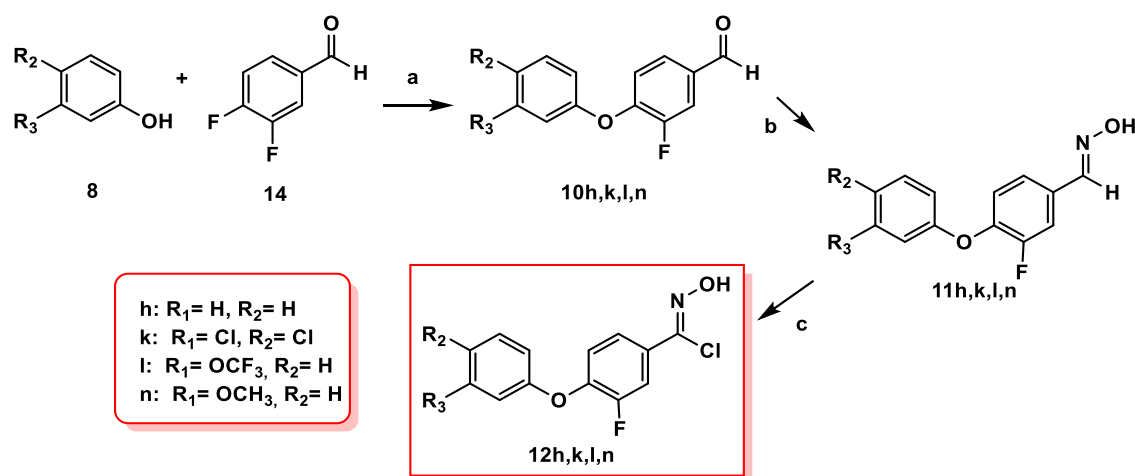


**Scheme 2.** General procedure A (GP-A). Reagents and conditions: a)  $K_2CO_3$ , DMSO, reflux,  $110^\circ C$ . b)  $NH_2OH.HCl$ , NaOH,  $EtOH/H_2O$ , r.t. 3h. c) N-chlorosuccinimide (NCS), ACN, DMF,  $60^\circ C$ , 2h.

Regarding compounds **13h-n**, we proposed to investigate if the incorporation of a fluorine in one of the phenyl rings would affect the potential antitrypanosomal activity of the synthesized compounds. This was proposed because the addition of fluorine groups in a molecule is known to affect a variety of physicochemical properties that are important in drug design, such as the compound's solubility, lipophilicity, pKa and molecular conformation. Thus, potentially altering the compound's pharmacokinetic properties, selectivity, toxicity and even potency of drug candidates.<sup>22,23</sup>

Consequently, nitroimidazole isoxazole compounds **13h-n** were designed with a *meta*-substituted fluorine and similar substituent groups, using GP-A and GP-B. Phenoxybenzaldehydes **10h, k, l, n** were synthesized via GP-A beginning with a nucleophilic aromatic substitution between 3,4-difluorobenzaldehyde and phenols with desired substituents (scheme 3, procedure a).<sup>18</sup> Phenoxybenzaldehydes then reacted with hydroxylamine hydrochloride producing aldoximes **11h, k, l, n**, followed by chlorination with NCS (N-chlorosuccinimide) to produce chloro-oximes **12h, k, l, n** (scheme 3, procedure c).<sup>19-20</sup>



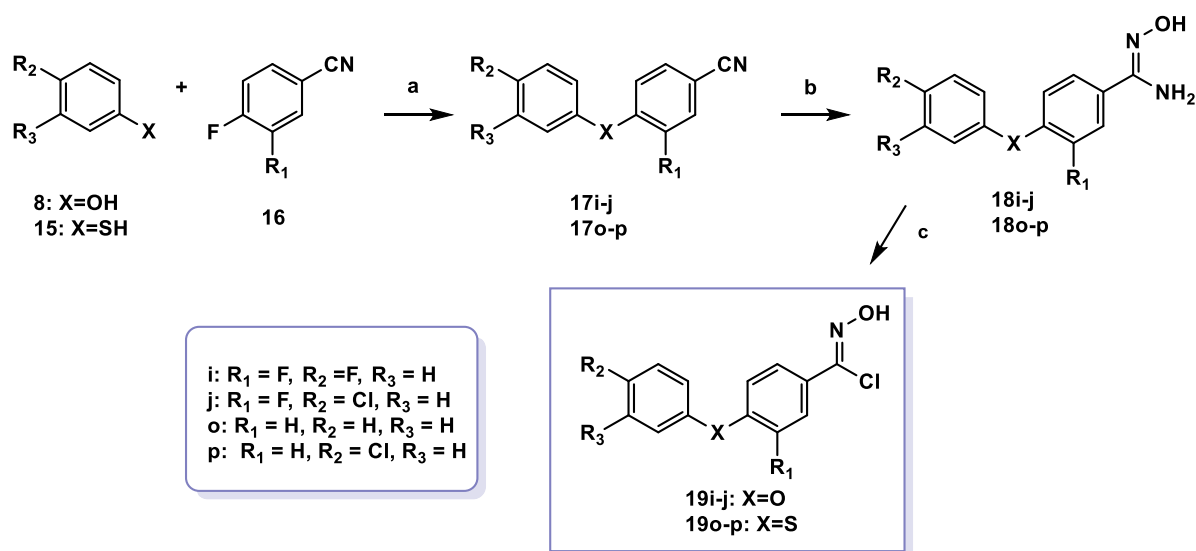


**Scheme 3.** General procedure A (GP-A). Reagents and conditions: a)  $K_2CO_3$ , DMSO, reflux,  $110^\circ C$ . b)  $NH_2OH.HCl$ ,  $NaOH$ ,  $EtOH/H_2O$ , r.t. 3h. c) N-chlorosuccinimide (NCS), ACN, DMF,  $60^\circ C$ , 2h.

Whereas compounds **13i-j** were synthesized using GP-B to obtain the desired chloro-oximes starting with a benzonitrile group instead of an aldehyde. GP-B began with a nucleophilic aromatic substitution reaction between 3,4-difluorobenzonitrile and phenols with desired substituents (scheme 4, procedure a) producing phenoxybenzonitriles **17i-j**.<sup>25</sup> These reacted with hydroxylamine hydrochloride (scheme 4, procedure b) producing amidoximes **18i-j** that were then chlorinated yielding chloro-oximes **19i-j**.<sup>26-27</sup>

Furthermore, considering that the design of the compounds synthesized in this study was based on a bioisosteric replacement of the amide group present in the drug benznidazole with the heterocyclic isoxazole ring, we designed three isoxazole compounds, **13o-q**, containing 4-phenylthiobenzene substituents. We proposed to investigate a novel series of sulfur-containing compounds by replacing a phenoxy benzene group, which has demonstrated activity against *T. cruzi* amastigotes in previous studies of 1,2,3-triazole analogs by our research group,<sup>14</sup> with its bioisostere phenylthio benzene, that have not yet been mentioned in the literature but may have the potential for antitrypanosomal activity. This is attributed to the fact that oxygen and sulfur are classical bioisosteres, implying that a bioisosteric replacement typically maintains the same biological activity of a compound. Additionally, it might reduce toxicity, modify the compound's activity, and impact its pharmacokinetic profile.<sup>24</sup>

Therefore, compounds **13o** and **13p** were synthesized via GP-B, beginning with a nucleophilic aromatic substitution reaction between 4-fluorobenzonitrile and phenols with desired substituents (scheme 4, procedure a) producing phenylthiobenzonitriles **17o-p**.<sup>25</sup> Next these reacted with hydroxylamine hydrochloride (scheme 4, procedure b) producing amidoximes **18o-p** which were then chlorinated affording chloro-oximes **19o-p**.<sup>26-27</sup>

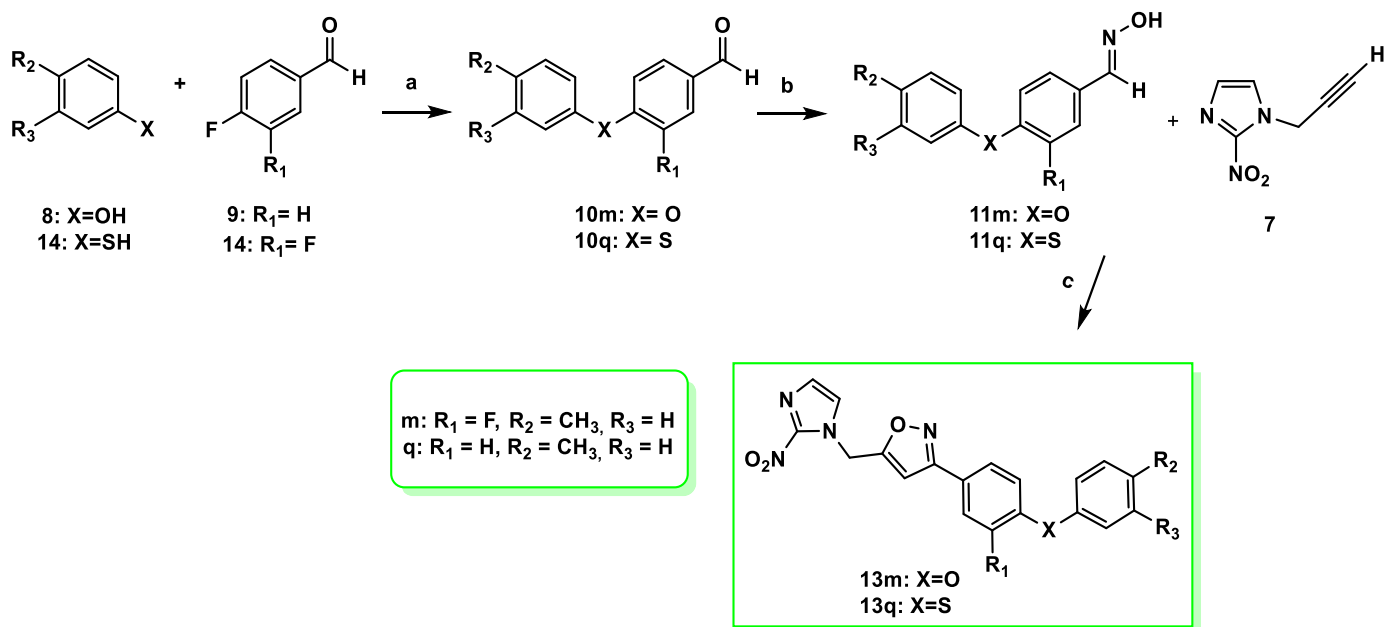


**Scheme 4.** General procedure B (GP-B). Reagents and conditions: a) K<sub>2</sub>CO<sub>3</sub>, DMSO, reflux, 110°C. b) NH<sub>2</sub>OH.HCl, K<sub>2</sub>CO<sub>3</sub>, MeOH, r.t. 2h. c) H<sub>2</sub>O, HCl, NaNO<sub>2</sub>, r.t., 2h.

Subsequently, reaction was performed between chloro-oximes **12a-l** and **12n-p** and terminal acetylene **7**, using a catalytic system of CuSO<sub>4</sub>·5H<sub>2</sub>O, sodium ascorbate, and KHCO<sub>3</sub>, in a solvent mixture of THF/CH<sub>2</sub>Cl<sub>2</sub> 1:1 (figure 2) yielding nitroimidazole isoxazoles **13a-l** and **13n-p** in moderate to good yields (29-81%) (Table 1).<sup>21</sup>

Next, a one-pot synthesis approach was tested to obtain compounds **13m** and **13q** by employing DBU (1,8-Diazabicyclo[5.4.0]undec-7-ene) to avoid the use of metallic catalysts and also attempt to spare extraction and purification processes.<sup>28</sup> Therefore, general procedure c (GP-C) was established starting with the synthesis of phenoxybenzaldehyde **10m** and phenylthiobenzaldehyde **10q** (procedure a, scheme 5). These were then converted into aldoximes **11m** and **11q** which were used as starting material for a one-pot synthesis of isoxazoles **13m** and **13q** (procedure c, scheme 5). Following this procedure, initially, chloro-oximes were generated *in situ* by adding N-

chlorosuccinimide (NCS) to a solution of the respective aldoxime, followed by the addition of DBU and terminal acetylene **7**, isoxazole compounds **13m** and **13q** were obtained with 36% and 34% yields, respectively.



**Scheme 5.** General procedure C (GP-C): synthesis of isoxazoles **13m** and **13q**. Reagents and conditions: a) K<sub>2</sub>CO<sub>3</sub>, DMSO, reflux, 110°C. b) NH<sub>2</sub>OH.HCl, NaOH, EtOH/H<sub>2</sub>O, r.t. 3h. c) 1: N-chlorosuccinimide (NCS), DMF, -10°C – 25°C, 2h. 2: DBU, terminal acetylene **7**.

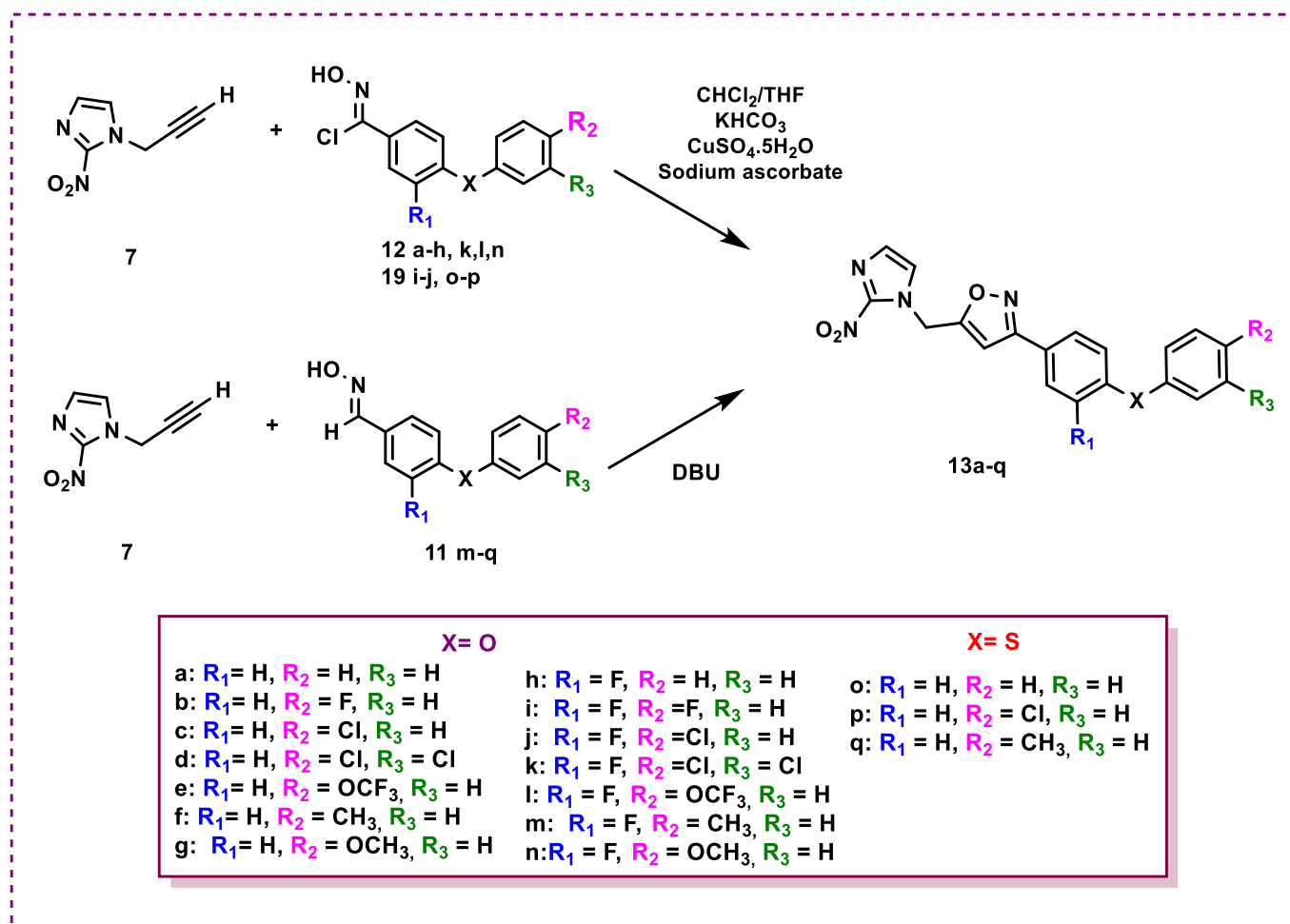


**Figure 2.** Synthesis of isoxazoles **13a-q**.

**Table 1.** Synthesis of nitroimidazole isoxazole analogs and yields.

| Compounds  | X | $\text{R}_1$ | $\text{R}_2$     | $\text{R}_3$ | Yield (%) |
|------------|---|--------------|------------------|--------------|-----------|
| <b>13a</b> | O | H            | H                | H            | 66        |
| <b>13b</b> | O | H            | F                | H            | 81        |
| <b>13c</b> | O | H            | Cl               | H            | 65        |
| <b>13d</b> | O | H            | Cl               | Cl           | 62        |
| <b>13e</b> | O | H            | OCF <sub>3</sub> | H            | 29        |
| <b>13f</b> | O | H            | CH <sub>3</sub>  | H            | 30        |

|            |   |   |                  |    |    |
|------------|---|---|------------------|----|----|
| <b>13g</b> | O | H | OCH <sub>3</sub> | H  | 77 |
| <b>13h</b> | O | F | H                | H  | 50 |
| <b>13i</b> | O | F | F                | H  | 61 |
| <b>13j</b> | O | F | Cl               | H  | 56 |
| <b>13k</b> | O | F | Cl               | Cl | 69 |
| <b>13l</b> | O | F | OCF <sub>3</sub> | H  | 46 |
| <b>13m</b> | O | F | CH <sub>3</sub>  | H  | 36 |
| <b>13n</b> | O | F | OCH <sub>3</sub> | H  | 54 |
| <b>13o</b> | S | H | H                | H  | 45 |
| <b>13p</b> | S | H | Cl               | H  | 64 |
| <b>13q</b> | S | H | CH <sub>3</sub>  | H  | 34 |

After synthesis, the nitroimidazole compounds were characterized by NMR analysis, hydrogen and carbon spectra were recorded by a Bruker 300 MHz spectrometer. The success of the cycloaddition reaction between the synthesized chloro-oximes and terminal acetylene was confirmed with the identification of two key signals in the spectra. The structural confirmation of the isoxazole ring in the compounds was verified by a singlet integrated to 1H at  $\delta$  6.0-7.0 ppm. Furthermore, a singlet integrated to 2H at approximately  $\delta$  5.8 ppm confirmed the formation of a methylene bridge joining the isoxazole ring and the nitroimidazole group (Figure 3).

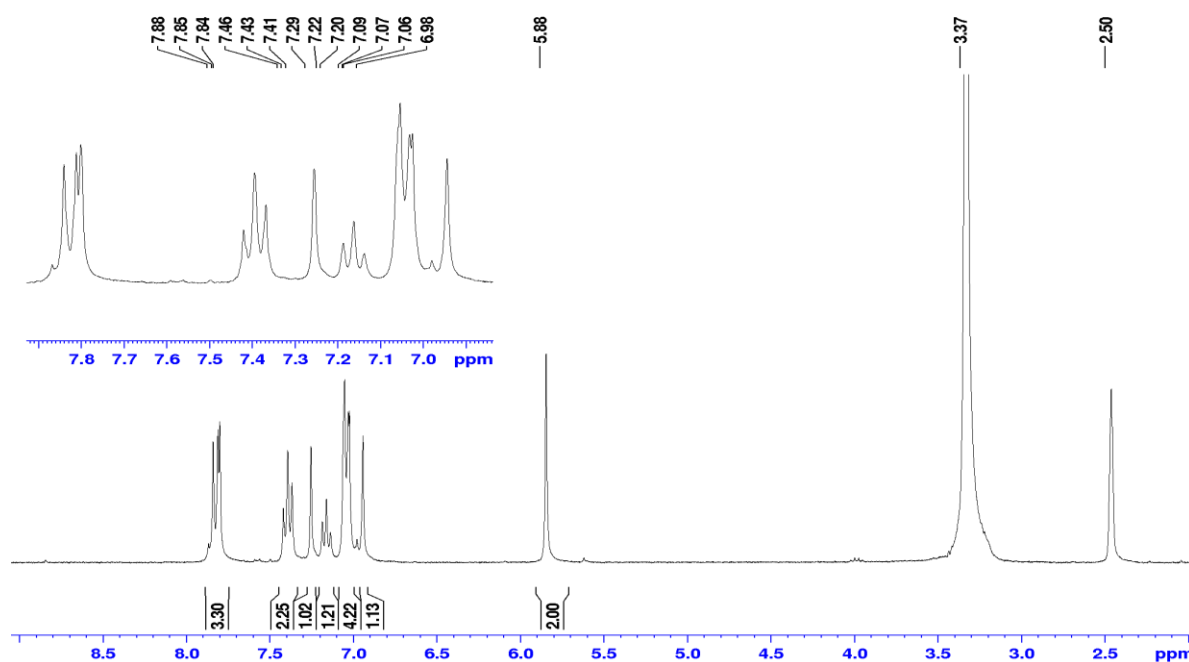


**Figure 3.** <sup>1</sup>H NMR spectrum (300 MHz, DMSO-*d*<sub>6</sub>) of compound **13a**.

### ***In vitro* Antitrypanosomal activity, cytotoxicity and SAR**

Table 2 displays the *in vitro* antitrypanosomal activity against *T. cruzi* amastigotes (Tulahuen lacZ strain). Drug discovery experts consider that a hit compound for CD should exhibit a half-maximal inhibitory concentration (IC<sub>50</sub>) of <10 μM against the intracellular forms of the parasite.<sup>29</sup> In this project, we report a novel series with 14 hit compounds, 12 of which showed greater potency than the reference drug benznidazole. Compounds were categorized as active (IC<sub>50</sub> < 4.0 μM), moderately active (IC<sub>50</sub> 4.0–60.0 μM), or inactive (IC<sub>50</sub> > 60.0 μM). The cytotoxicity evaluation and the determination of the selectivity index (SI) were done on LLCMK2 cells.<sup>30</sup>

To design the structure of these novel isoxazole compounds, traditional QSAR parameters, mainly Hansch's hydrophobicity constant ( $\pi$ ) and Hammett's substituent constant ( $\sigma$ ), were considered and used to plan each substituent. Using tools such as bioisosterism and Craig Plot to, thus, comprehend the role of each substituent group in the antitrypanosomal activity of this novel series of 2-nitroimidazole isoxazoles with diphenyl ether and thioether groups.<sup>31–34</sup>

Isoxazoles **13a–13q** were designed with diphenyl ether or thioether groups with different substituents in the *para* position. These substituents displayed diverse Hansch and Hammett

parameters. Hansch's hydrophobicity constant ( $\pi$ ) represents the behavior of a substituent on benzene derivatives by providing information about the substituent's hydrophobic lipophilic interactions ( $\pi^+$  when hydrophobic,  $\pi^-$  when hydrophilic); In contrast Hammett's substituent constant determines a substituent's electron-withdrawing or electron-donating property ( $\sigma^+$  when electron-withdrawing,  $\sigma^-$  when electron-donating).

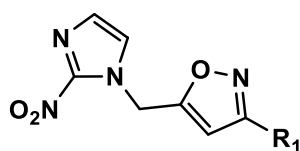


Table 2. Antitrypanosomal activity and cytotoxicity of compounds **13a-q**.

| Compounds  | LogP <sup>a</sup> | Hansch Constant   | Hammett Constant |                |  | Amastigotes IC <sub>50</sub> <sup>b</sup> (μM±SD) | LLC-MK2 CC <sub>50</sub> <sup>c</sup> (μM±SD) | SI <sup>d</sup> CC <sub>50</sub> /IC <sub>50</sub> |
|--|-------------------|-------------------|------------------|----------------|--|---|---|--|
|  |                   | π                 | σ <sub>p</sub>   | σ <sub>m</sub> |  |   |   |  |
| <b>13a:</b> R <sub>1</sub> = Ph-O-Ph                             | 4.02              | 0.00              | 0.00             | -              |  | 1,22 ± 0,73                                       | >100  | >82,2  |
| <b>13b:</b> R <sub>1</sub> = Ph-O-(4-F-Ph)                       | 4.18              | 0.14              | 0.06             | -              |  | 0,50 ± 0,51                                       | >100  | >199,4   |
| <b>13c:</b> R <sub>1</sub> = Ph-O-(4-Cl-Ph)                      | 4.70              | 0.71              | 0.23             | -              |  | 1,01 ± 1,13                                       | >100  | >99,0  |
| <b>13d:</b> R <sub>1</sub> = Ph-O-(3,4-di-Cl-Ph)                 | 5.30              | 1.25 <sup>f</sup> | 0.23             | 0.37           |  | 2,79 ± 0,93                                       | >100  | >35,9  |
| <b>13e:</b> R <sub>1</sub> = Ph-O-(4-OCF <sub>3</sub> -Ph)       | 4.99              | 1.04              | 0.35             | -              |  | 1,25 ± 0,71                                       | >100  | >80,1  |
| <b>13f:</b> R <sub>1</sub> = Ph-O-(4-CH <sub>3</sub> -Ph)        | 4.47              | 0.56              | -0.17            | -              |  | 1,77 ± 0,24                                       | >100  | >56,5  |
| <b>13g:</b> R <sub>1</sub> = Ph-O-(4-OCH <sub>3</sub> -Ph)       | 4.08              | -0.02             | -0.27            | -              |  | 0,64 ± 0,05                                       | >100  | >155,3   |
| <b>13h:</b> R <sub>1</sub> = (3-F-Ph)-O-(4-Ph)                   | 4.11              | 0.00              | 0.00             | -              |  | 3,18 ± 2,18                                       | >100  | >31,4  |
| <b>13i:</b> R <sub>1</sub> = (3-F-Ph)-O-(4-F-Ph)                 | 4.27              | 0.14              | 0.06             | -              |  | 1,42 ± 0,42                                       | >100  | >70,4  |
| <b>13j:</b> R <sub>1</sub> = (3-F-Ph)-O-(4-Cl-Ph)                | 4.79              | 0.71              | 0.23             | -              |  | 1,56 ± 0,69                                       | >100  | >64,1  |
| <b>13k:</b> R <sub>1</sub> = (3-F-Ph)-O-(3,4-di-Cl-Ph)           | 5.39              | 1.25 <sup>f</sup> | 0.23             | 0.37           |  | 8,50 ± 2,06                                       | >100  | >11,8  |
| <b>13l:</b> R <sub>1</sub> = (3-F-Ph)-O-(4-OCF <sub>3</sub> -Ph) | 5.08              | 1.04              | 0.35             | -              |  | 3,77 ± 0,07                                       | 55,6 ± 4.4                                    | >26,5  |
| <b>13m:</b> R <sub>1</sub> = (3-F-Ph)-O-(4-CH <sub>3</sub> -Ph)  | 4.56              | 0.56              | -0.17            | -              |  | 7,41 ± 3,22                                       | >100  | >13,5  |
| <b>13n:</b> R <sub>1</sub> = (3-F-Ph)-O-(4-OCH <sub>3</sub> -Ph) | 4.17              | -0.02             | -0.27            | -              |  | 3,54 ± 0,21                                       | >100  | >28,2  |
| <b>13o:</b> R <sub>1</sub> =Ph-S-Ph                              | 4.23              | 0.00              | 0.00             | -              |  | 20,55 ± 0,98                                      | >100  | >4,9   |
| <b>13p:</b> R <sub>1</sub> = Ph-S-(4-Cl-Ph)                      | 4.91              | 0.71              | 0.23             | -              |  | 11,09 ± 0,16                                      | >100  | >9,0   |
| <b>13q:</b> R <sub>1</sub> = Ph-S-(4-CH <sub>3</sub> -Ph)        | 4.68              | 0.56              | -0.17            | -              |  | 17,14 ± 0,24                                      | >100  | >5,8   |
| <b>BZN<sup>h</sup></b>   | 0.78              | -                 | -                | -              |  | 5,67 ± 0,83                                       | >100  | >17,6  |

a) LogP calculated using molinspiration software. b) Half-maximum inhibitory concentration (IC<sub>50</sub>) of *T. cruzi* intracellular amastigotes (Tulahuen strain); c) Cytotoxic concentration (CC<sub>50</sub>) on LLCMK2 cells; d) SI, selectivity index: CC<sub>50</sub> of LLCMK2 cells/IC<sub>50</sub> of intracellular amastigotes; e) SD: standard deviation. (f) Hansch's constant (Σπ observed), see ref. 34 g) Hammett's constant σ, see ref.34 h) Benznidazole (BZN) as reference drug.

The first synthesized compound of the diphenyl ether series **13a** (R<sub>1</sub>= Ph-O-Ph) presented an impressive IC<sub>50</sub> of 1.22μM, being 4.6-fold more active than the reference drug benznidazole (BZ) (IC<sub>50</sub> of 5.67μM). **13a** also exhibited a significantly higher SI of 82.2, which indicates the compound has a higher selectivity for parasites rather than mammalian cells. When comparing the structure of BZ and **13a**, as well as the other synthesized compounds in this series, BZ has a LogP of only 0.78



whilst **13a** has a much greater LogP of 4.02, as a result of the presence of two phenyl rings in its structure. Other than the bioisosteric replacement of the amide group in BZ for an isoxazole ring, the increased LogP may be a crucial factor for better activity of **13a** as well as the other compounds in this series because lipophilicity is an important physical-chemical property that affects a compound's cell permeability, especially when its targets are intracellular amastigote forms.

Although this isoxazole compound is unpublished in literature, it can be compared to its triazole congener with the same diphenyl ether substituent, which presented a promising activity with IC<sub>50</sub> of 6.6μM and a SI of 18.3. Our isoxazole analog **13a** was 5.4-fold more active against amastigote forms than its triazole analog.<sup>14</sup> Despite the structural and electronic similarities between 1,2,3-triazole and 3,5-isoxazole rings, a tendency of better activity of isoxazoles when compared to triazoles with the same substitution patterns has already been reported.<sup>12, 35</sup>

Next, we evaluated compounds containing lipophilic and electron-withdrawing substituents ( $\pi^+$ ,  $\sigma^+$ ). **13b** (R<sub>1</sub>= Ph-O-(4-F-Ph)) was the compound with the highest potency of all the synthesized compounds of this work with an IC<sub>50</sub> of 0.5μM. Moreover, **13b** also showed the highest safety profile with an excellent SI of 199.4. With a 4-Chloro substituent, **13c** (R<sub>1</sub>= Ph-O-(4-Cl-Ph)) showed the higher potency of the chlorine group when compared to its unsubstituted analog **13a**, exhibiting good activity with an IC<sub>50</sub> of 1.01μM and SI of 99.0; however, **13c** was 2-fold less active than its fluoro-substituted analog **13b**. When comparing these two substituent's parameters, analog **13c** with a 4-Cl group ( $\pi$  =0.71;  $\sigma$  =0.23) exhibited significantly higher lipophilic and electron-withdrawing properties than **13a** ( $\pi$  =0.14;  $\sigma$  =0.06).

Compound **13d** (Ph-O-(3,4-di-Cl-Ph)) had the addition of another chlorine substituent in the *meta* position that resulted in a reduction of antitrypanosomal activity (IC<sub>50</sub>=2.79μM) although it was still considered active, compared to analog **13c** bearing only one chlorine substituent (IC<sub>50</sub>=1.01μM). This reduction in activity may be due to the significantly higher lipophilicity profile (LogP=5.30;  $\pi$  =1.25) along with the increased electron-withdrawing effect and, perhaps, an unfavorable steric hindrance. The addition of an extra chloro in *meta* position did not boost antitrypanosomal activity

and a considerable reduction of the selectivity index of **13d** (SI= 35.9) was also observed in comparison to *para*-substituted **13c** (SI= 99.0).

Contrarily, Papadopoulou *et al* synthesized 3-nitrotriazole and nitroimidazole aryloxy-phenyl amides and reported that compounds with fluorine substituents were less active against *T. cruzi* amastigotes than their chlorine-substituted congeners.<sup>36</sup> The same was found by Carvalho *et al* when testing the antichagasic activity of nitroimidazole isoxazole derivatives, although these compounds did not present diphenyl ether substituents in their structures. Their 4-F-Ph nitroimidazole isoxazole derivative showed an IC<sub>50</sub> of 3.3μM with SI>15.3 and the 4-Cl-Ph derivative was 2.2-fold more active with an IC<sub>50</sub> of 1.5μM and a higher SI of 32.5. Nevertheless, their 3,4-*di*-chloro-substituted analog (IC<sub>50</sub>=2.2μM) also showed less activity compared to its monosubstituted analog (IC<sub>50</sub>=1.5μM), which corroborates our findings.<sup>12</sup>

In sequence, compound **13e** (Ph-O-(4-OCF<sub>3</sub>-Ph) also with considerable lipophilic and electron-withdrawing properties ( $\pi^+$ ,  $\sigma^+$ ) exhibited good activity with an IC<sub>50</sub> of 1.25μM and SI=80.1. Contrarily, 4-OCF<sub>3</sub>-Ph Isoxazole synthesized by Carvalho *et al* was considered one of the least active within electron-withdrawing ( $\sigma^+$ ) and lipophilic ( $\pi^+$ ) compounds, with an IC<sub>50</sub> of 15.2μM and low SI (>3.3); despite its rather high lipophilicity (LogP=3.23) compared to other  $\pi^+$ ,  $\sigma^+$  analogs, they concluded that lipophilicity was a non-determinant factor in the improvement of the antichagasic activity. However, in our synthesized compounds we observed an inversely proportional relationship between antitrypanosomal activity and LogP within  $\pi^+$ ,  $\sigma^+$  compounds, following the sequence from the most to least active: **13b** (4-F-Ph, LogP= 4.18) > **13c** (4-Cl-Ph, LogP= 4.70) > **13e** (4-OCF<sub>3</sub>-Ph, LogP= 4.99) > **13d** (3,4-*di*-Cl-Ph, LogP= 5.30). This suggests that there may be an ideal range of LogP for this set of compounds.

Compound **13f** (Ph-O-(4-CH<sub>3</sub>Ph)) with lipophilic and electron-donating properties ( $\pi$  =0.56,  $\sigma$  = -0.17) was then evaluated and also exhibited good activity (IC<sub>50</sub>= 1.77μM) and a lower, but satisfactory, selectivity index compared to most of the previous compounds (SI= 56.5) and considerable LogP of 4.47. In sequence compound **13g** (Ph-O-(4-OCH<sub>3</sub>Ph)) with slightly hydrophilic

and electron-donating properties ( $\pi = -0.02$ ,  $\sigma = -0.17$ ) showed relevant antitrypanosomal activity with an  $IC_{50}$  of  $0.64\mu M$ . **13g** was the second most potent of all the synthesized compounds and also presented the second highest selectivity against *T. cruzi* with a SI of 155,3.

Similarly, Carvalho *et al* also found that the (4-CH<sub>3</sub>Ph) isoxazole was less active and less selective than the methoxy-substituted analog (4-OCH<sub>3</sub>Ph), with an  $IC_{50}$  of  $9.3\mu M$ ; SI= 5.4 versus an  $IC_{50}$  of  $1.9\mu M$ ; SI= >25.6, respectively. Furthermore, they concluded that the 4-OCH<sub>3</sub> substituent was essential to antichagasic activity. As mentioned in their study, this finding also raised the possibility that these SAR tendencies could be attributed to the presence of different nitroheterocycle scaffolds since previous studies reported that 3-nitrotriazoles with 4-OCH<sub>3</sub> groups were considered less active than their congeners with lipophilic substituents like 4-Cl or 4-CH<sub>3</sub>.<sup>12, 30</sup>

Compounds **13a-g** were all considered active and more potent than reference drug benznidazole. This series of diphenyl ether substituted compounds was also more potent when compared to similar nitroimidazole isoxazole compounds previously published by our research group, without diphenyl ether substituents.<sup>12</sup> Analogs **13b** (R<sub>1</sub>= Ph-O-(4-F-Ph)) and **13g** (Ph-O-(4-OCH<sub>3</sub>Ph)) were highlighted as the most active of this work and also presented the best toxicity profile with the highest selectivity indexes (SI > 155), which may be due to the ability of these substituents to perform hydrogen bonds.

As for the (3-F)-Ph-O-Ph series, **13h-n** were synthesized with similar substituents as **13a-g**, but with the addition of a 3-Fluoro substituent in the first ring of the diphenyl ether group. The first compound of this series, **13h** (R<sub>1</sub>=(3-F-Ph)-O-(4-Ph)) was considered active with an  $IC_{50}$  of  $3.18\mu M$  but presented a low selectivity index of 31,4. In comparison with similar analog **13a** (R<sub>1</sub>= Ph-O-Ph,  $IC_{50}$ =  $1.22\mu M$ , SI= 82.2), **13h** displayed lower potency and a higher toxicity profile as a result of the inclusion of a *meta*-fluoro substituent. A discrete increase in lipophilicity (**13a**: LogP= 4.02; **13h**: LogP= 4.11) may explain this finding, as observed by Carvalho *et al* who suggested the existence of a minimal and maximal lipophilicity threshold for good antichagasic activity of their isoxazole compounds. Moreover, the 3,4-*di*-fluoro-substituted isoxazole tested in their research also

demonstrated low activity and unacceptable selectivity ( $IC_{50}$ = 6.5 $\mu$ M and SI=7.6); This result along with our observed findings indicates that, evidently, the presence of a fluoro-substituent in this position does not seem to improve antitrypanosomal activity in nitroimidazole isoxazole compounds. This same pattern was observed in the other synthesized compounds of this series, where (3-F)-substituted analogs showed considerably lower activity and selectivity than their congeners without a fluoro-substituent.

Compounds **13i-l** with lipophilic and electron-withdrawing substituents ( $\pi^+$ ,  $\sigma^+$ ) were evaluated in sequence and were considered active with  $IC_{50}$  values <4 $\mu$ M, except **13k** that exhibited moderate activity and low selectivity ( $IC_{50}$  = 8.50 $\mu$ M, SI= 11,8). **13i** ( $R_1$ = (3-F-Ph)- O-(4-F-Ph)) and **13j** ( $R_1$ = (3-F-Ph)-O-(4-Cl-Ph)), showed the best activity in this entire series with  $IC_{50}$  = 1.42 $\mu$ M, SI= 70.4 and  $IC_{50}$  = 1.56 $\mu$ M, SI= 64.1, respectively. Nevertheless, **13i** was considerably less active (2.8-fold) than its congener **13b** ( $R_1$ = Ph-O-(4-F-Ph)); the same was observed when comparing **13c** ( $R_1$ =(Ph-O-(4-Cl-Ph) and **13j** ( $R_1$ = (3-F-Ph)-O-(4-Cl-Ph)).

Analogously **13m** ( $R_1$ = (3-F-Ph)-O-(4-CH<sub>3</sub>-Ph)) with lipophilic and electron-donating properties ( $\pi^+$ ,  $\sigma^-$ ) was also 4-fold less active than **13f** (Ph-O-(4-CH<sub>3</sub>Ph)) with much lower selectivity. Likewise, with hydrophilic and electron-donating properties ( $\pi^-$ ,  $\sigma^-$ ), (3-F)-substituted **13n**  $R_1$ = (3-F-Ph)-O-(4-OCH<sub>3</sub>-Ph) exhibited 5.5-fold less activity and considerably lower SI than similar analog **13g** ( $R_1$ = Ph-O-(4-OCH<sub>3</sub>-Ph), which was the second most active of all the synthesized compounds.

Overall, the (3-F)-diphenyl ether compounds did not perform better or have a superior safety profile than their respective unsubstituted congeners. Despite maintaining the same substituents in the second phenyl ring, the inclusion of the (3-F)-substituent in the first phenyl ring clearly did not benefit antitrypanosomal activity or safety profile, which may be attributed to the increase of their lipophilicity profile.

Concerning diphenyl thioether substituted isoxazoles **13o-q**, these compounds exhibited the lowest antitrypanosomal activity of all the synthesized compounds of this work, besides presenting

the worst toxicity profile. **13o** ( $R_1 = \text{Ph-S-Ph}$ ) showed moderate activity with  $\text{IC}_{50}$  of  $20.55\mu\text{M}$  and very low SI of 4.9. **13p** ( $R_1 = \text{Ph-S-(4-Cl-Ph)}$ ) with a lipophilic and electron-withdrawing substituent ( $\pi^+$ ,  $\sigma^+$ ) showed improved activity ( $\text{IC}_{50} = 11.09\mu\text{M}$ ) in comparison with unsubstituted **13o**, nevertheless the toxicity profile remained unsatisfactory (SI= 9.0). Regarding compound **13q** ( $R_1 = \text{Ph-S-(4-CH}_3\text{-Ph)}$ ) with lipophilic and electron-donating properties ( $\pi^+$ ,  $\sigma^-$ ), this analog was moderately active with  $\text{IC}_{50}$  of  $17.14\mu\text{M}$ , while also displaying unsatisfactory selectivity index of 5.8.

The obtained results show that although Oxygen and Sulphur atoms are considered classical bioisosteres, in this series of nitroimidazole isoxazole compounds they did not exhibit similar biological activity against *T. cruzi* amastigote forms. This finding highlights the importance of the diphenyl ether group, which exhibited considerably better overall *in vitro* activity and toxicity profile than the diphenyl thioether group. The role of the ether link in antitrypanosomal activity was also discussed in Papadopoulos's study, which discovered that replacing a phenoxy group with a biphenyl group resulted in a 5.6-fold less potent analog.<sup>36</sup>

Overall, 17 nitroimidazole isoxazole compounds derivatives of benznidazole were synthesized with moderate to good yields (29%-81%) by three different synthetic routes, containing a series of phenoxy benzene or phenylthiol benzene substituents. All synthesized compounds are unpublished in literature, 12 of which showed higher potency than the reference drug benznidazole. Analog **13b** ( $R_1 = \text{Ph-O-(4-F-Ph)}$ ) was the most potent, and was 11-fold more active than benznidazole with an  $\text{IC}_{50}$  of  $0.50\mu\text{M}$ .

## Conclusions

A novel series of 3,5-isoxazole-2-nitroimidazole analogs were synthesized in moderate to good yields (29%-81%) by employing a 1,3-dipolar cycloaddition reaction, providing seventeen isoxazole compounds containing diphenyl ether and thioether substituents that have yet to be reported in the literature. Molecular modifications were designed based on bioisosterism of the drug benznidazole, with the replacement of an amide group by an isoxazole ring. Furthermore, an addition of diphenyl ether and thioether groups with substituents that exhibited varied Hansch's hydrophobicity constant ( $\pi$ ) and Hammett's substituent constant ( $\sigma$ ). The antitrypanosomal activity against amastigote forms and the cytotoxicity of the synthesized compounds were evaluated. The structure-activity relationship (SAR) of the compounds showed that 12 of our synthesized compounds were more active than the reference drug Benznidazole, with a substantially greater lipophilicity profile likely contributing to this result. **13a-g** all showed greater activity than benznidazole, but **13b** ( $R_1 = \text{Ph-O-(4-F-Ph)}$ ) and **13g** ( $R_1 = \text{Ph-O-(4-OCH}_3\text{-Ph)}$ ) were the most active of all the synthesized compounds with  $\text{IC}_{50}$  of  $0.50\mu\text{M}$  and  $0.64\mu\text{M}$ , respectively. Compounds **13h-n** were obtained to investigate if the incorporation of *meta*-substituted fluorine in the first phenyl ring of the diphenyl ether group would improve antitrypanosomal activity. Our findings showed the addition of a fluoro group in this position did not enhance antitrypanosomal activity, while also significantly lowering their selectivity index. With regards to compounds **13o-q**, because oxygen and sulfur are classical bioisosteres, we proposed a bioisosteric replacement of the diphenyl ether by a diphenyl thioether group aiming to maintain or improve antitrypanosomal activity. Nonetheless, these analogs did not exhibit good antitrypanosomal activity and were considered moderately active with  $\text{IC}_{50}$  values ranging from  $11\mu\text{M}$  to  $20.55\mu\text{M}$ , besides showing an undesirable toxicity profile. The results of this study show that this novel series of nitroimidazole isoxazole compounds with diphenyl ether groups are very promising and further research is necessary to evaluate their performance *in vivo*. Other examples will also be synthesized and evaluated in order to obtain a better understanding of the SAR of these novel compounds.

## Experimental

### General Procedures and Reagents

Anhydrous solvents were dried and distilled according to standard methods before use. All chemicals used for synthesis were of reagent grade and used without purification unless indicated otherwise. The reactions were monitored using thin-layer chromatography on prepared plates (silica gel 60 F254 on aluminum). Chromatograms were examined under both 254 and 360 nm ultraviolet light. Flash-column chromatography was performed on silica gel 60 (particle size 200–400 mesh ASTM, purchased from Aldrich). The  $^1\text{H}$  and  $^{13}\text{C}$  NMR spectra were recorded in  $\text{CDCl}_3$  and  $\text{DMSO}-d_6$  solutions by a Bruker 300 MHz spectrometers. Chemical shifts ( $\delta$ ) are indicated in parts per million (ppm) downfield from tetramethylsilane or deuterated solvent ( $\text{CDCl}_3$   $^1\text{H}$   $\delta$  7.27 and  $^{13}\text{C}$   $\delta$  77.0 ppm; dimethyl sulfoxide ( $\text{DMSO}$ )- $d_6$   $^1\text{H}$   $\delta$  2.5 and  $^{13}\text{C}$   $\delta$  39.51 ppm) as the internal standard. Additional data are included in the supporting information.

### Synthesis of diphenyl ether isoxazole nitroimidazole analogs

#### Synthesis of Terminal acetylene **7**

##### Synthesis of 2-aminoimidazole **4**

To a solution of 2-aminoacetaldehyde dimethyl acetal (105g, 1 mol) in water, methylthiourea hemisulfate (139 g, 1 mol) was added and kept under stirring at room temperature. The mixture was progressively heated until it reached 75°C, then agitated for another hour at this temperature. In vacuum, the solvent was withdrawn until a viscous residue was produced. The residue was dissolved in water, and sulfuric acid was added to achieve a pH of 1.0 before being heated to 95°C and stirred for another 30 minutes. The solvent was evaporated in vacuum, and 200 mL of ethanol at -5°C was added to the residue. 29 g of a white solid was recovered in 59% yield after vacuum filtering.

### Synthesis of 2-nitroimidazole **5**

At -5°C, an aqueous solution of sodium nitrite (4.1 g, 60 mmol in 10 mL of water) was added dropwise to a solution of 2-aminoimidazole hemisulfate (1.57 g, 5.9 mmol) and fluoroboric acid (7 mL, 53 mmol) and stirred for 30 minutes. The reaction mixture was then poured over a copper sulfate solution (29.7 g, 119 mmol) at -5°C. The mixture was then agitated for 24 hours at room temperature after the addition of more sodium nitrite (4.1 g, 60 mmol in 10 mL of water). To obtain the purified product we applied a separation technique based on the acid-base properties of the product. First, to remove the excess of copper salts from the medium, the pH of the solution was corrected to 13.0 using NaOH at which an insoluble precipitate of Cu(OH)<sub>2</sub> was formed and was then removed by vacuum filtration, whilst the nitroimidazole compound was unprotonated and therefore soluble in the aqueous solution. Next the filtered solution containing the product was acidified using HCl to a pH of 1.0, at which the nitroimidazole compound was protonated and formed a precipitate in the aqueous solution, it was then vacuum filtered and obtained in 80% yield (6.51g) as a yellow solid.

### Synthesis of propargyl-2-nitroimidazole **7**

Propargyl bromide (0.8 mL, 5.31 mmol 80% in toluene) was added to a suspension of 2-nitroimidazole (0.5g, 4.42 mmol) and potassium carbonate (0.85g, 6.19 mmol) in dry acetone (10 mL). The mixture was stirred at room temperature for 16 hours. The reaction was filtered, the solvent was removed under vacuum, and the residue was purified using flash chromatography. The product was obtained in 80% yield (4.0 g) as a yellow liquid (NMR <sup>1</sup>H, 300MHz, DMSO-d<sub>6</sub>) 3.56 (t, 1H, *J* 2.46 Hz), 5.24 (*d*, 2H, *J* 2.78 Hz), 7.17 (*d*, 1H, *J* 0.9 Hz), 7.71 (*d*, 1H, *J* 0.70 Hz).

### General procedure A (GP- A): synthesis of Isoxazoles **13 a-h, k, l, n**

#### Synthesis of diphenyl ether aldehydes **10a-h, k, l, n**

Phenolic compounds with various substituents (1 eq., 20 mmol), 4-fluorobenzaldehyde (1 eq., 20 mmol), potassium carbonate (3 eq., 60 mmol), and dimethylsulfoxide (28 mL) were poured into a



reaction flask equipped with magnetic stirring and a condenser. The mixture was heated to 110 °C and the conversion of the compounds to the desired product was monitored by TLC. Upon completion, the resulting mixture was dissolved in ethyl acetate (150 mL) and washed with distilled water (100 mL). The aqueous phase was then extracted with ethyl acetate (3 x 50 mL). The organic phases were combined, dried over anhydrous magnesium sulfate, filtered and concentrated under reduced pressure to give the diphenyl ether aldehyde products as colorless to light yellow liquids.

#### Synthesis of diphenyl ether aldoximes **11a-h, k, l, n**

Hydroxylamine hydrochloride (18 mmol, 1.2 eq.) was added to a solution of phenoxy benzaldehyde **10a-h, k, l, n** (15 mmol, 1.0 eq.) in water/ethanol 95% (10 mL:10 mL) under stirring. The reaction mixture was then agitated for 3 hours to room temperature after a solution of NaOH (18 mmol, 1.2 eq.) in water (18 mL) was added dropwise. The product was extracted with ethyl acetate (3 x 30 mL) and washed with brine (3 x 30 mL). The solvent was removed under low pressure after the organic phase was dried over anhydrous MgSO<sub>4</sub>.

#### Synthesis of diphenyl ether Chloro-oximes **12a-h, k, l, n**

Under magnetic stirring and heat, aldoxime **11a-h, k, l, n** (10mmol, 1 eq.), acetonitrile (50 mL), and 20% N-chlorosuccinimide (2 mmol, 0.2 eq.) were added to a two-neck flask equipped with a nitrogen atmosphere and heating mantle until the system reached 60 ° C. Then, the heating was turned off, and the remaining NCS (8 mmol, 1 eq.) dissolved in 10mL of DMF was progressively added to the reaction, so that the temperature did not rise over 60°C. The heat was switched on after the addition of the NCS and the reaction was agitated at 60°C for 2 hours. The reaction mixture was then diluted with ethyl acetate (3 x 30 mL) and rinsed with water (8 x 30 mL). The solvent was removed under low pressure and the organic phase was dried over anhydrous MgSO<sub>4</sub>. Flash chromatography was used to purify the products, yielding Chloro-oximes **12a-h, k, l, n**

## Synthesis of diphenyl ether nitroimidazole isoxazoles **13a-h, k, l, n**

To a solution of the respective chloro-oxime of interest **12a-h, k, l, n** (3 mmol, 1.0 equiv.) and the acetylene (3.3 mmol, 1.1 equiv.) in CH<sub>2</sub>Cl<sub>2</sub>/THF (50:50, 5 mL/mmol), CuSO<sub>4</sub>·5H<sub>2</sub>O (0.19 mmol), sodium ascorbate (0.52 mmol) and KHCO<sub>3</sub> (30 mmol, 10 equiv.) were added. The mixture was stirred at room temperature for 48 hours. Extraction was carried out using ethyl acetate (3 x 30 mL) and rinsed with an NaCl saturated solution (3 x 30 mL). The solvent was removed under low pressure after the organic phase was dried over anhydrous MgSO<sub>4</sub>. The product was purified using flash chromatography and was then subjected to recrystallization in ethanol.

### 5-((2-nitro-1H-imidazol-1-yl)methyl)-3-(4-phenoxyphenyl)isoxazole (**13a**)

Yellow solid, yield 66%; <sup>1</sup>H NMR (300 MHz, DMSO-d<sub>6</sub>) δ 5.88 (*s*, 2H), 6.98 (*s*, 1H), 7.04-7.11(*m*, 4H), 7.19 (*t*, 1H), 7.29 (*d*, 1H, *J* 0.88 Hz), 7.37-7.47 (*m*, 2H), 7.78-7.93 (*m*, 3H); <sup>13</sup>C NMR (75 MHz, DMSO-d<sub>6</sub>) δ 45.2, 101.5, 117.7, 118.7, 119.8, 123.4, 124.6, 128.6, 128.7, 129.0, 130.6, 156.1, 159.1, 162.0, 167.7.

### 3-(4-(4-fluorophenoxy)phenyl)-5-((2-nitro-1H-imidazol-1-yl)methyl)isoxazole (**13b**)

Yellow solid, yield 81%; <sup>1</sup>H NMR (300 MHz, DMSO-d<sub>6</sub>) δ 5.88 (*s*, 2H), 6.98 (*s*, 1H), 7.05 (*d*, 2H *J* 8.74 Hz), 7.11-7.19 (*m*, 2H), 7.22-7.32 (*m*, 3H), 7.80-7.90 (*m*, 3H); <sup>13</sup>C NMR (75 MHz, DMSO-d<sub>6</sub>) δ 45.2, 101.5, 117.0, 117.3, 118.4, 122.0, 123.3, 128.7, 129.1, 152.0, 157.5, 159.5, 160.6, 159.1, 162.0, 167.7.

### 3-(4-(4-chlorophenoxy)phenyl)-5-((2-nitro-1H-imidazol-1-yl)methyl)isoxazole (**13c**)

Yellow solid, Yield 65%. <sup>1</sup>H NMR (300 MHz, DMSO-d<sub>6</sub>) δ 5.88 (*s*, 2H), 7.00 (*s*, 1H), 7.07-7.14 (*m*, 4H), 7.30 (*d*, 1H, *J* 0.87 Hz), 7.47 (*d*, 2H, *J* 8.74 Hz), 7.82-7.90 (*m*, 3H); <sup>13</sup>C NMR (75 MHz, DMSO-d<sub>6</sub>) δ 45.2, 101.5, 119.2, 121.4, 123.8, 128.4, 128.6, 128.7, 129.1, 130.5, 155.2, 158.6, 161.9, 167.8.

3-(4-(3,4-dichlorophenoxy)phenyl)-5-((2-nitro-1H-imidazol-1-yl)methyl)isoxazole (**13d**)

Yellow solid, Yield 62%; <sup>1</sup>H NMR (300 MHz, DMSO-d<sub>6</sub>) δ 5.85 (s, 2H), 6.98 (s, 1H), 7.01-7.08 (m, 1H), 7.13 (d, 2H, *J* 8.56 Hz), 7.25 (d, 1H, *J* 0.85 Hz), 7.35 (d, 1H, *J* 2.73 Hz), 7.61 (d, 1H, *J* 8.47 Hz), 7.76-7.89 (m, 3H); <sup>13</sup>C NMR (75 MHz, DMSO-d<sub>6</sub>) δ 45.2, 101.6, 119.7, 119.8, 121.4, 124.4, 126.5, 128.6, 128.7, 129.2, 132.1, 132.6, 144.8, 156.0, 158.0, 161.9, 167.8.

5-((2-nitro-1H-imidazol-1-yl)methyl)-3-(4-(4-(trifluoromethoxy)phenoxy)phenyl)isoxazole (**13e**)

Yellow solid, yield 29%. <sup>1</sup>H NMR (300 MHz, DMSO-d<sub>6</sub>) δ 5.89 (s, 2H), 7.00 (s, 1H), 7.07 (d, 1H, *J* 8.7 Hz), 7.10-7.22 (m, 3H), 7.29 (d, 1H, *J* 0.88 Hz), 7.42 (d, 2H, *J* 8.27), 7.81-7.96 (m, 3H); <sup>13</sup>C NMR (75 MHz, DMSO-d<sub>6</sub>) δ 45.2, 101.59, 118.2, 119.4, 121.0, 123.5, 124.0, 128.6, 128.7, 129.2, 130.2, 144.5, 155.2, 158.5, 161.9, 167.7.

5-((2-nitro-1H-imidazol-1-yl)methyl)-3-(4-(p-tolyloxy)phenyl)isoxazole (**13f**) Yellow solid, yield 30%. <sup>1</sup>H NMR (300 MHz, DMSO-d<sub>6</sub>) δ 2.30 (s, 3H), 5.88 (s, 2H), 6.90-7.06 (m, 5H), 7.17-7.31 (m, 3H), 7.78-7.88 (m, 3H); <sup>13</sup>C NMR (75 MHz, DMSO-d<sub>6</sub>) δ 20.7, 45.2, 101.5, 118.3, 120.0, 122.9, 128.6, 128.7, 129.0, 131.0, 133.9, 144.7, 153.6, 159.6, 162.0, 167.6.

3-(4-(4-methoxyphenoxy)phenyl)-5-((2-nitro-1H-imidazol-1-yl)methyl)isoxazole (**13g**)

Pale-yellow solid, yield 77%. <sup>1</sup>H NMR (300 MHz, DMSO-d<sub>6</sub>) δ 3.76 (s, 3H), 5.87 (s, 2H), 6.91-7.10 (m, 7H), 7.29 (d, 1H, *J* 0.79 Hz), 7.78-7.86 (m, 3H); <sup>13</sup>C NMR (75 MHz, DMSO-d<sub>6</sub>) δ 45.1, 55.8, 101.5, 115.6, 117.7, 121.7, 122.6, 128.6, 128.7, 128.9, 144.7, 148.8, 156.5, 160.3, 162.0, 167.6.

3-(3-fluoro-4-phenoxyphenyl)-5-((2-nitro-1H-imidazol-1-yl)methyl)isoxazole (**13h**)

Pale yellow solid yield 50%. <sup>1</sup>H NMR (300 MHz, DMSO-d<sub>6</sub>) δ 5.89 (s, 2H), 7.0-7.08 (m, 3H), 7.12-7.25 (m, 2H), 7.30 (d, 1H, *J* 0.77 Hz), 7.41 (t, 2H, *J* 7.41 Hz), 7.72 (d, 1H, *J* 7.70 Hz), 7.80-7.94 (m,

2H).  $^{13}\text{C}$  NMR (75 MHz, DMSO- $d_6$ )  $\delta$  44.8, 101.2, 117.8, 119.0, 120.6, 123.1, 123.6, 128.2, 128.3, 128.8, 129.8, 144.21, 154.8, 158.1, 161.6, 167.4.

3-(4-(3,4-dichlorophenoxy)-3-fluorophenyl)-5-((2-nitro-1H-imidazol-1-yl)methyl)isoxazole (**13k**)  
Pale yellow solid yield 69%.  $^1\text{H}$  NMR (300 MHz, DMSO- $d_6$ )  $\delta$  5.90 (s, 2H), 7.01-7.13 (m, 2H), 7.24-7.36 (m, 3H), 7.65 (d, 1H,  $J$  8.94), 7.76 (d, 1H,  $J$  8.59), 7.85 (s, 1H), 7.93 (d, 1H,  $J$  11.65).  $^{13}\text{C}$  NMR (75 MHz,  $\text{CDCl}_3$ )  $\delta$  44.5, 102.3, 115.7, 116.0, 117.0, 119.4, 122.1, 123.5, 123.6, 125.6, 125.7, 127.2, 129.0, 131.1, 133.3, 144.6, 144.7, 152.4, 155.6, 155.7, 161.30, 161.33, 165.4.

3-(3-fluoro-4-(4-(trifluoromethoxy)phenoxy)phenyl)-5-((2-nitro-1H-imidazol-1-yl)methyl)isoxazole (**13l**)  
Pale yellow solid 46%.  $^1\text{H}$  NMR (300 MHz,  $\text{CDCl}_3$ )  $\delta$  5.77 (s, 2H), 6.61 (s, 1H), 7.00 (d, 2H,  $J$  9Hz), 7.08 (t, 1H,  $J$  8Hz), 7.14-7.32 (m, 5H), 7.48 (d, 1H,  $J$  8Hz), 7.62 (d, 1H,  $J$  9Hz).  $^{13}\text{C}$  NMR (75 MHz,  $\text{CDCl}_3$ )  $\delta$  44.4, 102.3, 115.6, 115.9, 118.7, 118.8, 121.65, 121.66, 122.7, 123.44, 123.48, 125.0, 125.1, 126.1, 129.0, 144.94, 144.96, 145.4, 145.6, 152.4, 154.9, 155.7, 161.41, 161.44, 165.3

3-(3-fluoro-4-(4-methoxyphenoxy)phenyl)-5-((2-nitro-1H-imidazol-1-yl)methyl)isoxazole (**13n**)  
Pale yellow solid 54%.  $^1\text{H}$  NMR (300 MHz,  $\text{CDCl}_3$ )  $\delta$  3.78 (s, 3H), 5.75 (s, 2H), 6.58 (s, 1H), 6.83-7.02 (m, 5H), 7.17-7.30 (m, 3H), 7.39 (d, 1H,  $J$  8Hz), 7.58 (d, 1H,  $J$  8Hz).  $^{13}\text{C}$  NMR (75 MHz,  $\text{CDCl}_3$ )  $\delta$  44.4, 55.6, 102.3, 114.9, 115.2, 115.5, 119.3, 120.2, 123.1, 123.1, 126.1, 129.0, 149.1, 151.7, 155.0, 156.4, 161.6, 164.9.

General procedure B (GP-B): synthesis of nitroimidazole isoxazoles **13i-j** and **13o-p**

Synthesis of diphenyl ether and thioether benzonitriles **17i-j**, **17o-p**

4-Fluorobenzonitrile or 3,4-difluorobenzonitrile (20 mmol, 1 eq.), phenols with substituents of interest (20 mmol, 1 eq.), potassium carbonate (30 mmol, 1.5 eq.) and dimethylsulfoxide (20 mL) were poured into a flask equipped with magnetic stirring and a reflux condenser. The mixture was

heated to 110 °C and the conversion of the phenolic compound to the desired product was monitored by TLC analyses. Upon completion, the reaction medium was dissolved in ethyl acetate (150 mL) and washed with distilled water (100 mL). The aqueous phase was extracted twice with ethyl acetate (50 mL). The organic phases were combined, dried over anhydrous magnesium sulfate, filtered and concentrated under reduced pressure to give the benzonitrile product as a white solid.

#### Synthesis of diphenyl ether and thioether amidoximes **18i-j**, **18o-p**

Potassium carbonate (22.5 mmol 1.5 eq.) and hydroxylamine hydrochloride (37.5 mmol, 2.5 eq.) were added to a solution of nitriles **17i-j**, **17o-p** (15 mmol, 1 eq.) in dry methanol, and the mixture was agitated at reflux for 2 hours under a nitrogen atmosphere. The solution was then vacuum-concentrated, diluted with water (50 mL), and extracted using ethyl acetate (3 x 30 mL). The organic phases were dried with MgSO<sub>4</sub>, filtered, and concentrated in vacuo to yield amidoximes.

#### Synthesis of diphenyl ether and thioether chloro-oximes **19i-j**, **19o-p**

Amidoximes **18i-j**, **18o-p** (10 mmol, 1 eq.) were dissolved in a mixture of concentrated hydrochloric acid (10 mL, 1 eq.) and water (50 mL) at room temperature. Sodium nitrite (11.5 mmol, 1.15 eq.) was dissolved in 5 mL of water and then was added dropwise to the mixture. The system was stirred for 2 h. At the end of the reaction, as verified by TLC, the system was neutralized with sodium bicarbonate and the material was vacuum filtered and washed with water.

#### Synthesis of diphenyl ether and thioether nitroimidazole isoxazoles **13i-j** and **13o-p**

To a solution of the respective chloro-oxime of interest **19i-j**, **19o-p** (3 mmol, 1.0 eq.) and the acetylene (3.3 mmol, 1.1 eq.) in CH<sub>2</sub>Cl<sub>2</sub>/THF (50:50, 5 mL/mmol), CuSO<sub>4</sub>·5H<sub>2</sub>O (0.19 mmol), sodium ascorbate (0.52 mmol) and KHCO<sub>3</sub> (30 mmol, 10 equiv.) were added. The mixture was stirred at room temperature for 48 hours. Extraction was carried out using ethyl acetate (3 x 30 mL) and rinsed with an NaCl saturated solution (3 x 30 mL). The solvent was removed under low pressure

after the organic phase was dried over anhydrous MgSO<sub>4</sub>. The product was purified using flash chromatography and was then subjected to recrystallization in ethanol.

3-(3-fluoro-4-(4-fluorophenoxy)phenyl)-5-((2-nitro-1H-imidazol-1-yl)methyl)isoxazole (**13i**)

White solid 61%. <sup>1</sup>H NMR (300 MHz, CDCl<sub>3</sub>)  $\delta$  5.76 (*s*, 2H), 6.60 (*s*, 1H), 6.93- 7.09 (*m*, 5H), 7.19-7.31 (*m*, 3H), 7.44 (*d*, 1H, *J* 8 Hz), 7.60 (*d*, 1H, *J* 9 Hz). <sup>13</sup>C NMR (75 MHz, CDCl<sub>3</sub>)  $\delta$  44.4, 102.3, 115.4, 115.7, 116.3, 116.6, 119.8, 119.9, 120.4, 123.2, 123.3, 124.1, 124.2, 126.1, 129.0, 146.5, 146.7, 152.0, 155.3, 157.5, 160.7, 161.4, 165.1.

3-(4-(4-chlorophenoxy)-3-fluorophenyl)-5-((2-nitro-1H-imidazol-1-yl)methyl)isoxazole (**13j**)

Pale yellow solid yield 56%. <sup>1</sup>H NMR (300 MHz, DMSO-d<sub>6</sub>)  $\delta$  5.90 (*s*, 2H), 7.04-7.12 (*m*, 3H), 7.22-7.32 (*m*, 2H), 7.45 (*d*, 2H, *J* 8.92 Hz), 7.73 (*d*, 1H, *J* 8.59), 7.80-7.96 (*m*, 2H). <sup>13</sup>C NMR (75 MHz, DMSO-d<sub>6</sub>)  $\delta$  45.2, 101.7, 116.0, 116.3, 119.7, 122.5, 124.3, 124.3, 125.8, 128.1, 128.6, 128.7, 130.4, 144.7, 144.9, 152.1, 155.4, 155.5, 161.2, 168.2.

5-((2-nitro-1H-imidazol-1-yl)methyl)-3-(4-(phenylthio)phenyl)isoxazole (**13o**)

Yellow solid, yield 45%. <sup>1</sup>H NMR (300 MHz, DMSO-d<sub>6</sub>)  $\delta$  5.88 (*s*, 2H), 7.00 (*s*, 1H), 7.26-7.47 (*m*, 8H), 7.78-7.85 (*m*, 3H). <sup>13</sup>C NMR (75 MHz, DMSO-d<sub>6</sub>)  $\delta$  31.1, 45.2, 101.6, 126.8, 128.0, 128.6, 128.7, 130.0, 130.2, 132.6, 133.3, 139.19, 162.0, 167.9.

3-(4-((4-chlorophenyl)thio)phenyl)-5-((2-nitro-1H-imidazol-1-yl)methyl)isoxazole (**13p**)

Yellow solid, yield 64%. <sup>1</sup>H NMR (300 MHz, DMSO-d<sub>6</sub>)  $\delta$  5.89 (*s*, 2H), 7.01 (*s*, 1H), 7.29 (*s*, 1H), 7.34-7.51 (*m*, 6H), 7.79-7.88 (*m*, 3H). <sup>13</sup>C NMR (75 MHz, DMSO-d<sub>6</sub>)  $\delta$  45.22, 101.66, 127.28, 128.21, 128.63, 128.71, 130.20, 130.70, 132.95, 133.38, 133.82, 138.22, 144.81, 161.97, 167.98.

General procedure C (GP-C): synthesis of Isoxazoles **13m** and **13q** via DBU

#### Synthesis of aldehydes **10m** and **10q**

Phenolic compounds with various substituents (1 eq., 20 mmol), 4-fluorobenzaldehyde (1 eq., 20 mmol), potassium carbonate (3 eq., 60 mmol), and dimethylsulfoxide (28 mL) were poured into a reaction flask equipped with magnetic stirring and a condenser. The mixture was heated to 110 °C and the conversion of the compounds to the desired product was monitored by TLC. Upon completion, the resulting mixture was dissolved in ethyl acetate (150 mL) and washed with distilled water (100 mL). The aqueous phase was then extracted with ethyl acetate (3 x 50 mL). The organic phases were combined, dried over anhydrous magnesium sulfate, filtered and concentrated under reduced pressure to give the diphenyl ether and thioether aldehyde products as colorless to light yellow liquids.

#### Synthesis of diphenyl ether aldoximes **11m** and **11q**

Hydroxylamine hydrochloride (18 mmol, 1.2 eq.) was added to a solution of phenoxy benzaldehyde **10m** and 4-(phenylthiol)benzaldehyde **10q** (15 mmol, 1.0 eq.) in water/ethanol 95% (10 mL:10 mL) under stirring. The reaction mixture was then agitated for 3 hours to room temperature after a solution of NaOH (18 mmol, 1.2 eq.) in water (18 mL) was added dropwise. The product was extracted with ethyl acetate (3 x 30 mL) and washed with brine (3 x 30 mL). The solvent was removed under low pressure after the organic phase was dried over anhydrous MgSO<sub>4</sub>.

#### Synthesis of diphenyl ether nitroimidazole isoxazoles via DBU **13m** and **13q**

N-chlorosuccinimide (3.6mmol, 1.2 eq.) was added to a stirred solution of aldoximes (3mmol, 1 equiv.) in DMF (10 mL) at -10°C and warmed until it reached room temperature, then the reaction was stirred for 2 h. The reaction was then agitated for 8 hours after DBU (3 mmol, 1 equiv.) and the terminal acetylene (3.6 mmol, 1.2 equiv.) were added. After the reaction was completed, as

verified by TLC, water (50 mL) was added and the product was extracted with ethyl acetate (3 x 30 mL). The organic phase was recovered and dried using anhydrous MgSO<sub>4</sub>, the solvent was evaporated under reduced pressure. The product was purified using flash chromatography, yielding compounds **13m** and **13q**.

3-(3-fluoro-4-(p-tolyloxy)phenyl)-5-((2-nitro-1H-imidazol-1-yl)methyl)isoxazole (**13m**)

White solid, yield 36%. <sup>1</sup>H NMR (300 MHz, CDCl<sub>3</sub>)  $\delta$  2.32(*s*, 3H), 5.76 (*s*, 2H), 6.59 (*s*, 1H), 6.91 (*d*, 2H, *J* 8Hz), 6.98 (*t*, 1H, *J* 8Hz), 7.14 (*d*, 2H, *J* 8Hz), 7.18-7.30 (*m*, 3H), 7.41 (*d*, 1H, *J* 9Hz), 7.59 (*d*, 1H, *J* 9Hz). <sup>13</sup>C NMR (75 MHz, CDCl<sub>3</sub>)  $\delta$  20.72, 44.47, 102.38, 115.33, 115.60, 118.47, 120.39, 123.19, 123.23, 123.65, 123.75, 126.12, 129.08, 130.41, 133.82, 153.82, 161.64, 165.04.

5-((2-nitro-1H-imidazol-1-yl)methyl)-3-(4-(p-tolylthio)phenyl)isoxazole (**13q**)

White solid, yield 34%. <sup>1</sup>H NMR (300 MHz, CDCl<sub>3</sub>)  $\delta$  2.35 (*s*, 3H), 5.76 (*s*, 2H), 6.63 (*s*, 1H), 7.17-7.28 (*m*, 5H), 7.52 (*d*, 2H, *J* 8Hz), 7.69 (*d*, 2H, *J* 8Hz), 7.70 (*d*, 2H, *J* 8Hz), 7.83 (*d*, 2H, *J* 8Hz). <sup>13</sup>C NMR (75 MHz, CDCl<sub>3</sub>)  $\delta$  21.3, 44.4, 102.4, 125.0, 125.1, 126.2, 127.6, 129.0, 130.2, 130.4, 141.9, 142.1, 144.1, 148.2, 161.8, 165.4.

## Biological methods

### Antitrypanosomal assay

Initially, 5x10<sup>3</sup> LLC-MK2 cells/well were infected with trypomastigotes in 96-well plates at a parasite/cell ratio of 10:1. After 48 hours, plates were washed twice with PBS before adding compounds in a serial dilution range of 100  $\mu$ M to 0.78  $\mu$ M in fresh RPMI 1640 medium (Sigma-Aldrich®). As a control, infected untreated cells (100 percent infection control) were employed. Following 72 hours of incubation, amastigote viability tests were performed using 50  $\mu$ L of PBS containing 2% Triton X-100 and 200  $\mu$ M CPRG. Tulahuen lacZ strain expressing galactosidase enzyme were used, which catalyzes the yellow reagent of CPRG into a red chromophore that can be



easily detected by absorbance at 570 nm after 4 hours at 37°C (microplate reader -Synergy™H1). The percentage of amastigotes inhibition (IC50) was calculated as  $100 - (\text{absorbance of treated infected cells}) / (\text{absorbance mean of untreated infected cells}) \times 100$ .

#### Cytotoxicity assay

To assess chemical cytotoxicity, MTT (3-(4,5-Dimethyl-2-thiazolyl)-2,5-diphenyl-2Htetrazolium bromide, Sigma-Aldrich®)-based kit reagents were employed. LLC-MK2 cells were incubated in 96-well plates for 48 hours at a concentration of  $5 \times 10^3$  cells/well. Cells were then washed twice with PBS (Sigma-Aldrich®) before being incubated with compounds in a serial dilution from 200 µM to 1.56 µM in fresh RPMI 1640 medium (Sigma-Aldrich®). After 72 hours, 50 µL of MTT solution (2.0 mg/mL) was added to each well, and the plates were incubated for another 4 hours at 37 °C. The resultant formazan crystals were dissolved in DMSO (50 µL/well) and measured at 570 nm 30 minutes later in a Synergy H1 microplate reader. Cytotoxic concentration of 50% (CC50) was calculated based on a dose-response curve excluding DMSO cytotoxicity (>1%) of the untreated control.

### Supplementary Information

Supplementary Information (spectral data) is available in annexes.

### Acknowledgments

We gratefully acknowledge financial support received from the Conselho Nacional de Desenvolvimento Científico e Tecnológico (CNPq), Coordenação de Aperfeiçoamento de Pessoal de Nível Superior (CAPES) and Fundação de Apoio ao Desenvolvimento do Ensino, Ciência e Tecnologia do Estado de Mato Grosso do Sul (FUNDECT).

## References


1. World Health Organization, [https://www.who.int/health-topics/chagas-disease#tab=tab\\_1](https://www.who.int/health-topics/chagas-disease#tab=tab_1), accessed in June 2022.
2. World Health Organization, [https://www.who.int/news-room/fact-sheets/detail/chagas-disease-\(american-trypanosomiasis\)](https://www.who.int/news-room/fact-sheets/detail/chagas-disease-(american-trypanosomiasis)), accessed in June 2022.
3. Conteh, L.; Engels, T.; Molyneux, D. H.; *The Lancet*. **2010**, 375, 239–247. [[https://doi.org/10.1016/S0140-6736\(09\)61422-7](https://doi.org/10.1016/S0140-6736(09)61422-7)].
4. Schmunis, G. A.; Yadon, Z. E.; *Acta Trop.* **2010**, 115, 14. [<https://doi.org/10.1016/j.actatropica.2009.11.003>].
5. Pérez-Molina, J. A.; Molina, I.; *The Lancet*. **2018**, 391, 82. [[https://doi.org/10.1016/S0140-6736\(17\)31612-4](https://doi.org/10.1016/S0140-6736(17)31612-4)].
6. Perez, C. J.; Lymbery, A. J.; Thompson, R. C. A.; *Trends in Parasitology* **2015**, 31, 595. [<https://doi.org/10.1016/j.pt.2015.06.006>].
7. Jackson, Y.; Alirol, E.; Getaz, L.; Wolff, H.; Combescure, C.; Chappuis, F.; *Clin. Infect. Dis.* **2010**, 51, 69. [<https://doi.org/10.1086/656917>].
8. Bermudez, J.; Davies, C.; Simonazzi, A.; Real, J. P.; Palma, S.; *Acta trop.* **2016**, 156, 1. [<https://doi.org/10.1016/j.actatropica.2015.12.017>].
9. Müller Kratz, J.; Garcia Bournissen, F.; Forsyth, C. J.; Sosa-Estani, S.; *Expert Rev. Clin. Pharmacol.* **2018**, 11, 943. [<https://doi.org/10.1080/17512433.2018.1509704>].
10. Kannigadu, C.; N'Da, D., *Curr. Pharm. Des.* **2020**, 26, 4658. [<http://dx.doi.org/10.2174/1381612826666200331091853>].
11. Deeks, E. D. *Drugs* **2019**, 79, 215. [<https://doi.org/10.1007/s40265-019-1051-6>].
12. Carvalho, D. B.; Costa, P. A.; Portapilla, G. B.; das Neves, A. R.; Shiguemoto, C. Y.; Pelizaro, B. I.; Baroni, A. C.; *Eur. J. Med. Chem.* **2023**, [<https://doi.org/10.1016/j.ejmech.2023.115451>].

13. Sysak, A.; Obmińska-Mrukowicz, B.; *Eur. J. Med. Chem.* **2017**, *137*, 292.  
[<https://doi.org/10.1016/j.ejmech.2017.06.002>].
14. Assunção, E. L.; Carvalho, D. B.; das Neves, A. R.; Kawasoko Shiguemotto, C. Y.; Portapilla, G. B.; de Albuquerque, S.; Baroni, A. C.; *Chem. Med. Chem.* **2020**, *15*, 2019.  
[<https://doi.org/10.1002/cmdc.202000460>].
15. Burdinski, D.; Lub, J.; Pikkemaat, J. A.; Langereis, S.; Grill, H.; Hoere, W.; *Chem. Biodiversity*. **2008**, *5*, 1505. [<https://doi.org/10.1002/cbdv.200890139>].
16. Agrawal, K. C.; Bears, K. B.; Sehgal, R. K.; Brown, J. N.; Rist, P. E.; *J. Med. Chem.* **1979**, *2526*, 583. [<https://doi.org/10.1021/jm00191a025>].
17. Yap, S.; Woodman, O. L.; Crack, P. J.; Williams, S. J.; *Bioorg. Med. Chem. Lett.* **2011**, *21*, 5102. [<https://doi.org/10.1016/j.bmcl.2011.03.040>].
18. Foyer, G.; Chanfi, B. H.; Virieux, D.; David, G.; Caillol, S. *Eur. Polym. J.* **2016**, *77*, 65.  
[<https://doi.org/10.1016/j.eurpolymj.2016.02.018>].
19. Abele, E.; Lukevics, E.; *Org. Prep. Proced. Int.* **2000**, *32*, 235.  
[<https://doi.org/10.1080/00304940009355921>].
20. Kuruba, B. K.; Vasanthkumar, S.; *Tetrahedron* **2017**, *73*, 3860.  
[<https://doi.org/10.1016/j.tet.2017.05.055>].
21. Trefzger, O. S.; Barbosa, N. V.; Scapolatempo, R. L.; das Neves, A. R.; Ortale, M. L.; Carvalho, D. B.; Baroni, A. C.; *Arch. Pharm.* **2020**, *353*, 1900241.  
[<https://doi.org/10.1002/open.202100141>].
22. Gillis, E. P.; Eastman, K. J.; Hill, M. D.; Donnelly, D. J., & Meanwell, N. A.; *J. Med. Chem.* **2015**, *58*, 8315. [<https://doi.org/10.1021/acs.jmedchem.5b00258>].
23. Hagmann, W. K.; *J. Med. Chem.* **2008**, *v. 51*, *15*, 4359, . [<https://doi.org/10.1021/jm800219f>].
24. Lima, L. M.; Barreiro, E. J. *Curr. Med. chem.* **2005**, *12*, 23.  
[<https://doi.org/10.2174/0929867053363540>].

25. Tangallapally, R. P; Yendapally, R.; Lee, R. E.; Lenaerts, A. J.; Lee, R. E.; *J. med. Chem.* **2005**, 48, 8261. [<https://doi.org/10.1021/jm050765n>].
26. Vörös, A.; Mucsi, Z.; Baán, Z.; Timári, G.; Hermech, I.; Mizsey, P.; Finta, Z.; *Org. Biomol. Chem.* **2014**, 12, 8036. [<https://doi.org/10.1039/C4OB00854E>].
27. Gobis, K., Foks; H., Kędzia, A.; Wierzbowska M.; Zwolska, Z.; *J. Heterocycl. Chem.* **2009**, 46, 1271. [<https://doi.org/10.1002/jhet.251>].
28. Mohammed, S.; Vishwakarma, R. A.; Bharate, S. B.; *RSC Adv.* **2015**, 5, 3470.[<https://doi.org/10.1039/C4RA14694H>].
29. Katsuno, K.; Burrows, J.N.; Duncan, K.; Hooft van Huijsduijnen, R.; Kaneko, T.; Kita, K.; Mowbray, C.E.; Schmatz, D.; Warner, P.; Slingsby, B.T.; *Nat. Rev. Drug. Discov.* **2015**, 751.[<https://doi.org/10.1038/nrd4683>].
30. Papadopoulou, M.V.; Bloomer, W.D.; Lepesheva, G.I.; Rosenzweig, H.S.; Kaiser, M.; B.; Aguilera-Venegas, Wilkinson, S.R.; Chatelain, E.; Ioset, J.R.; *J. Med. Chem.* **2015**, 58, 1307.[<https://doi.org/10.1021/jm5015742>].
31. Patrick, G.L.; *An Introduction to Medicinal Chemistry*, 5th Ed., Oxford University Press, 2013.
32. Craig, P.N.; *J. Med. Chem.***1971**, 14, 680. [<https://doi.org/10.1021/jm00290a004>].
33. Ertl, P.; *J. Cheminform.* **2020**, 12, 8. [<https://doi.org/10.1186/s13321-020-0412-1>].
34. Hansch, C.; Leo, A.; Unger, S. H.; Kim, K. H.; Nikaitani, D.; Lien, E. J.; *J. Med. Chem.* **1973** , 16, 1207.[<https://doi.org/10.1021/jm00269a003>].
35. das Neves, A.R.; Trefzger, O.S.; Barbosa, N.V.; Honorato, A.M.; Carvalho, D.B.; Moslaves, I.S.; Kadri, M.C.T.; Yoshida, N.C.; Kato, M.J.; Arruda, C.C.P.; Baroni, A.C.M.; *Chem. Biol. Drug. Des.* **2019**, 94, 2004. [<https://doi.org/10.1111/cbdd.13609>].
36. Papadopoulou, M.V.; Bloomer, W.D.; Rosenzweig, H.S.; O'Shea, I.P.; Wilkinson, S.R.; Kaiser, M.; Chatelain, E.; Ioset, J-R.; *Bioorg. Med. Chem.* **2015**. [<http://dx.doi.org/10.1016/j.bmc.2015.08.014>].

## Supplementary Information

### Synthesis and Antitrypanosomal activity of novel Nitroimidazole Isoxazole derivatives with Diphenyl ether and thioether substituents

*Larissa B. B. Santos,<sup>a</sup> Diego B. Carvalho,<sup>a</sup> Gisele B. Portapilla,<sup>b</sup> Sergio de Albuquerque<sup>b</sup>  
and Adriano C. M. Baroni,  <sup>\*a</sup>*

<sup>a</sup> *Laboratório de Síntese e Química Medicinal (LASQUIM), Faculdade de Ciências Farmacêuticas,  
Alimentos e Nutrição, Universidade Federal do Mato Grosso do Sul, UFMS, Campo Grande, Mato  
Grosso do Sul, CEP 79051-470, Brazil*

<sup>b</sup> *Departamento de Análises Clínicas, Toxicológicas e Bromatológicas, Faculdade de Ciências  
Farmacêuticas de Ribeirão Preto – Universidade de São Paulo, Ribeirão Preto, São Paulo, CEP 14040-900,  
Brazil*

---

\* [adriano.baroni@ufms.br](mailto:adriano.baroni@ufms.br)

#### Spectral data

5-((2-nitro-1H-imidazol-1-yl)methyl)-3-(4-phenoxyphenyl)isoxazole (**13a**)

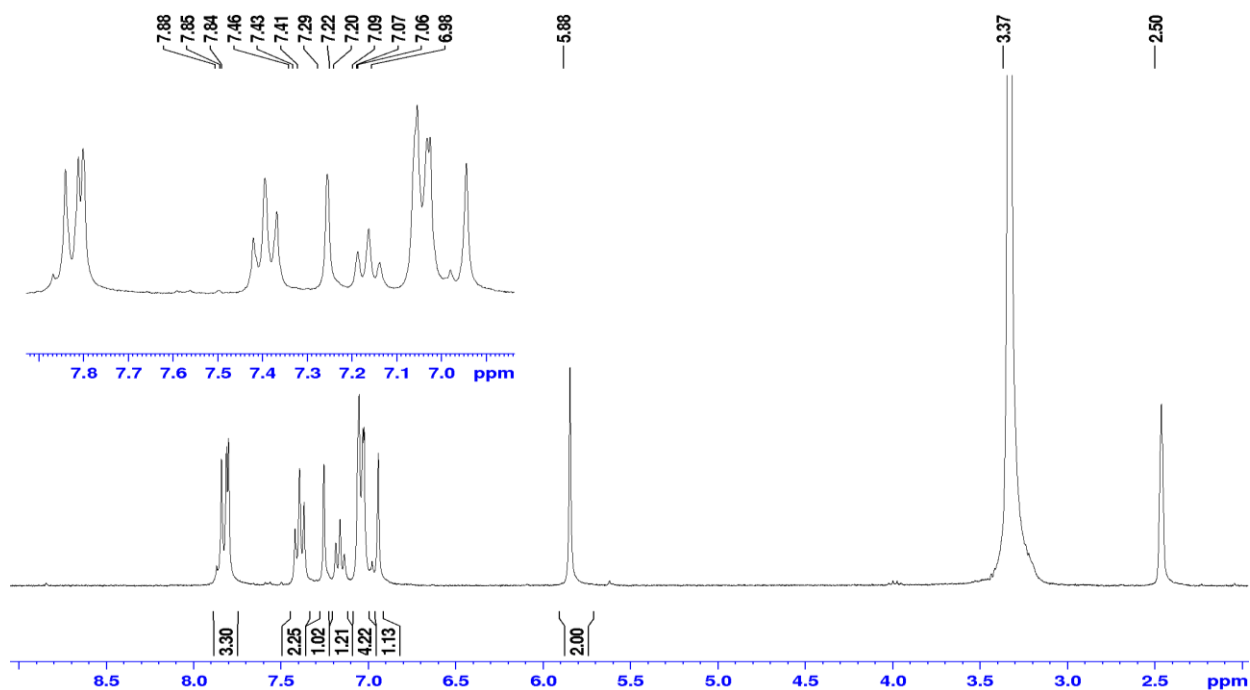


Figure S1. <sup>1</sup>H NMR spectrum (300 MHz, DMSO-d<sub>6</sub>) of compound **13a**.

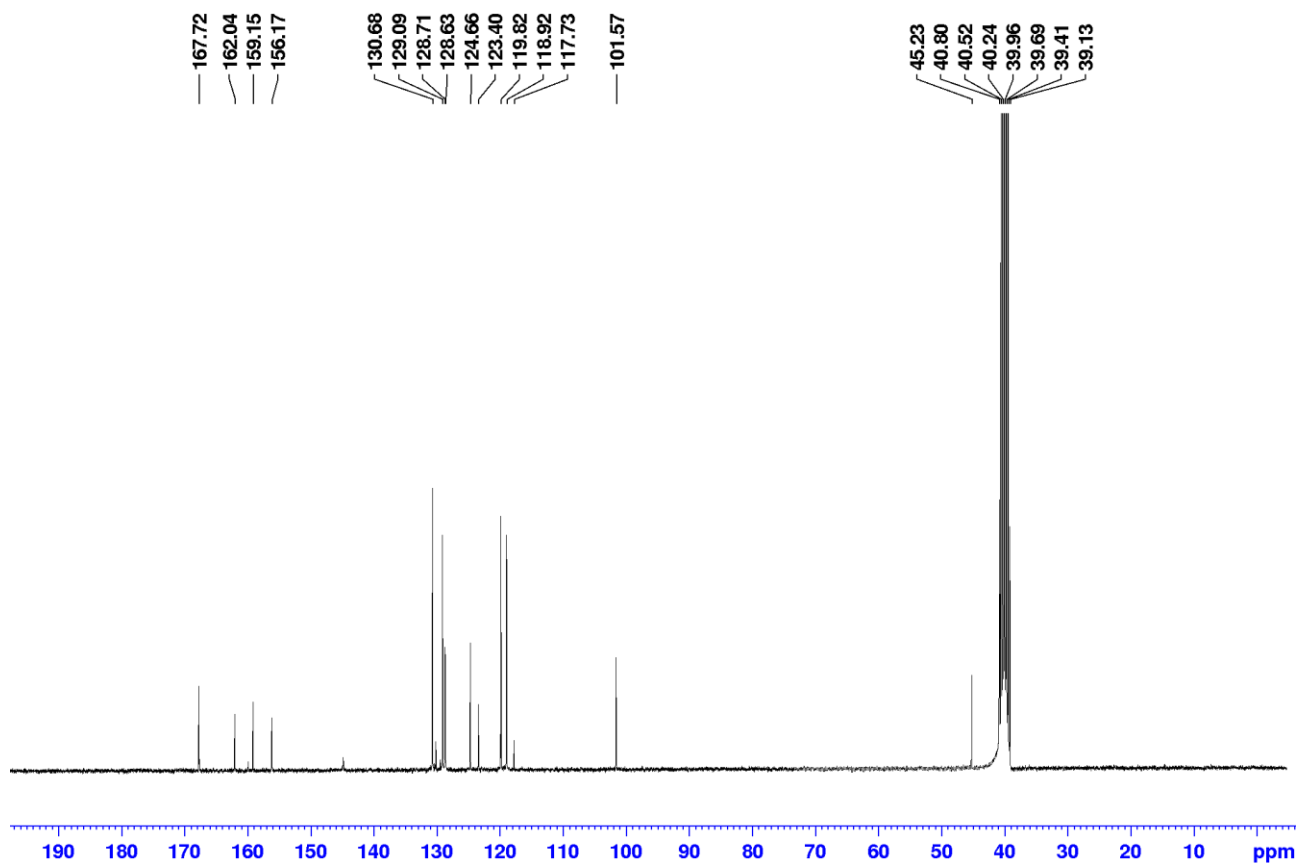


Figure S2. <sup>13</sup>C NMR spectrum (75 MHz, DMSO-d<sub>6</sub>) of compound **13a**.

3-(4-(4-fluorophenoxy)phenyl)-5-((2-nitro-1H-imidazol-1-yl)methyl)isoxazole (**13b**)

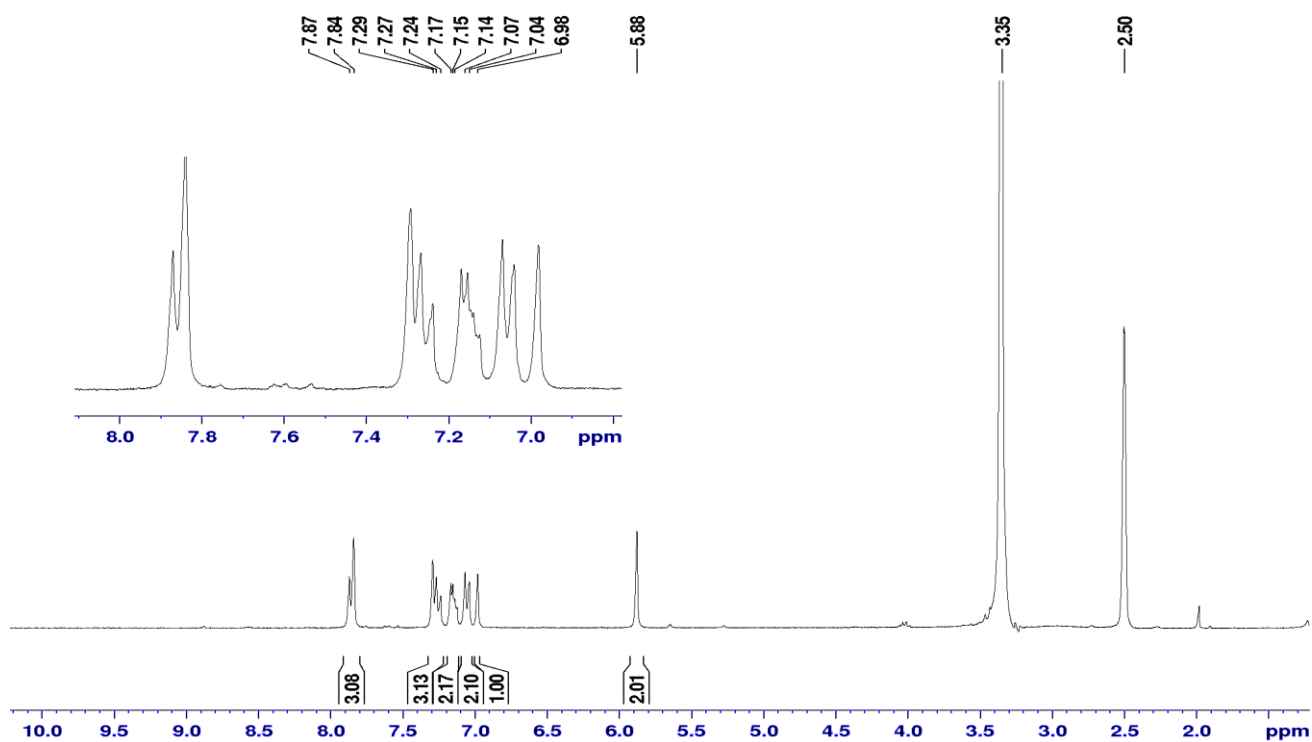


Figure S3. <sup>1</sup>H NMR spectrum (300 MHz, DMSO-d<sub>6</sub>) of compound **13b**.

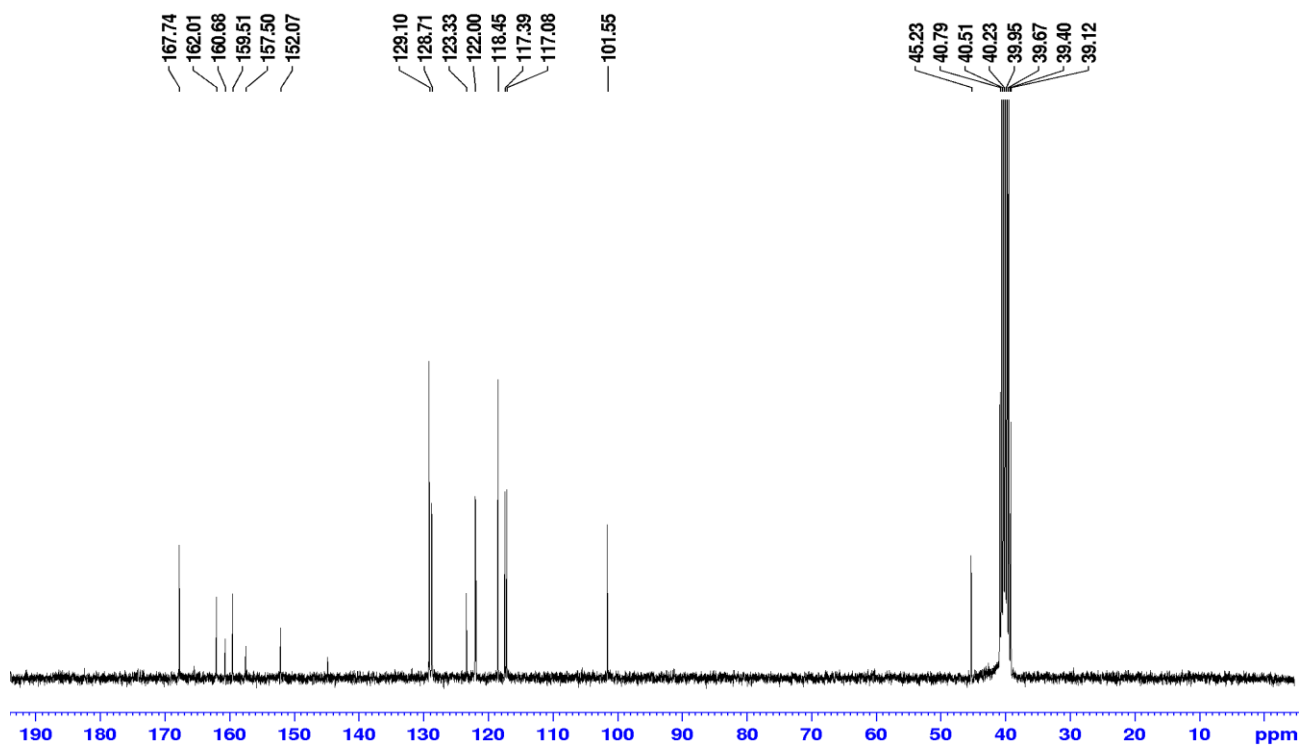


Figure S4. <sup>13</sup>C NMR spectrum (75 MHz, DMSO-d<sub>6</sub>) of compound **13b**.

3-(4-(4-chlorophenoxy)phenyl)-5-((2-nitro-1H-imidazol-1-yl)methyl)isoxazole (**13c**)

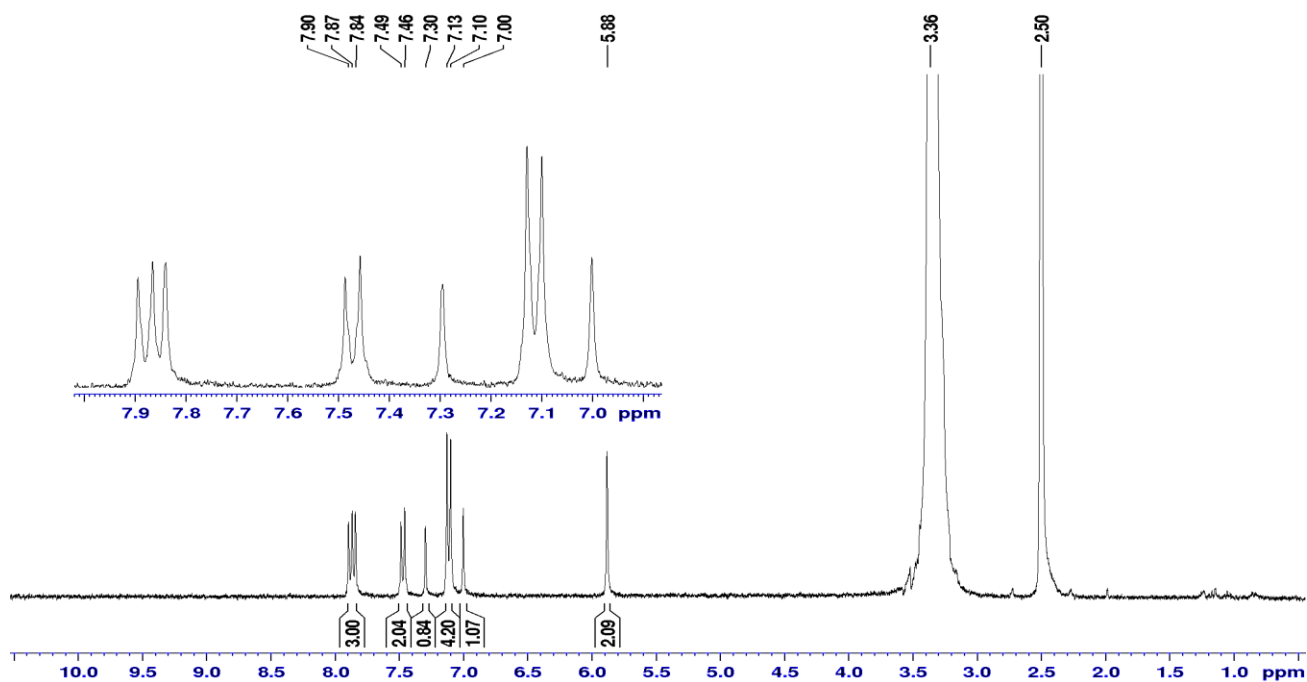


Figure S5. <sup>1</sup>H NMR spectrum (300 MHz, DMSO-d<sub>6</sub>) of compound **13c**.

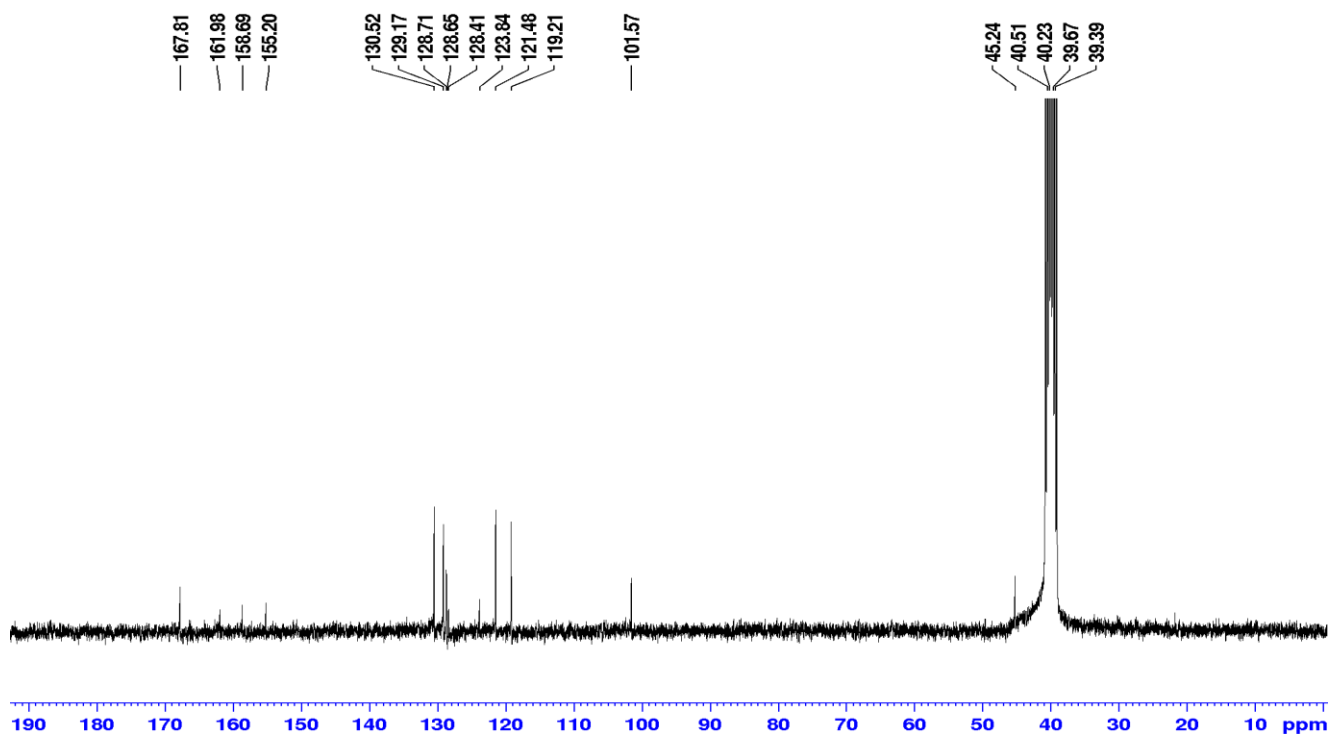


Figure S6. <sup>13</sup>C NMR spectrum (75 MHz, DMSO-d<sub>6</sub>) of compound **13c**.



3-(4-(3,4-dichlorophenoxy)phenyl)-5-((2-nitro-1H-imidazol-1-yl)methyl)isoxazole (**13d**)

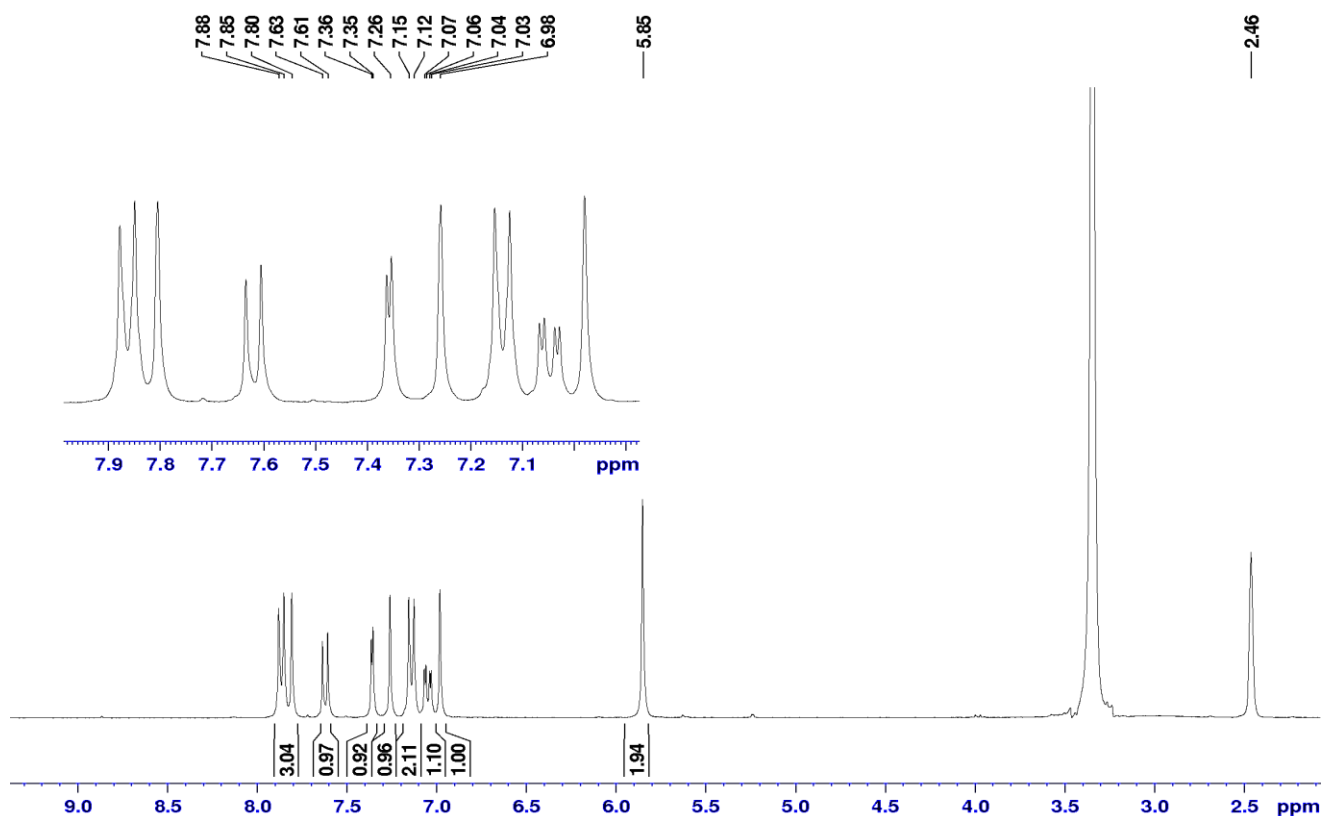


Figure S7. <sup>1</sup>H NMR spectrum (300 MHz, DMSO-d<sub>6</sub>) of compound **13d**.

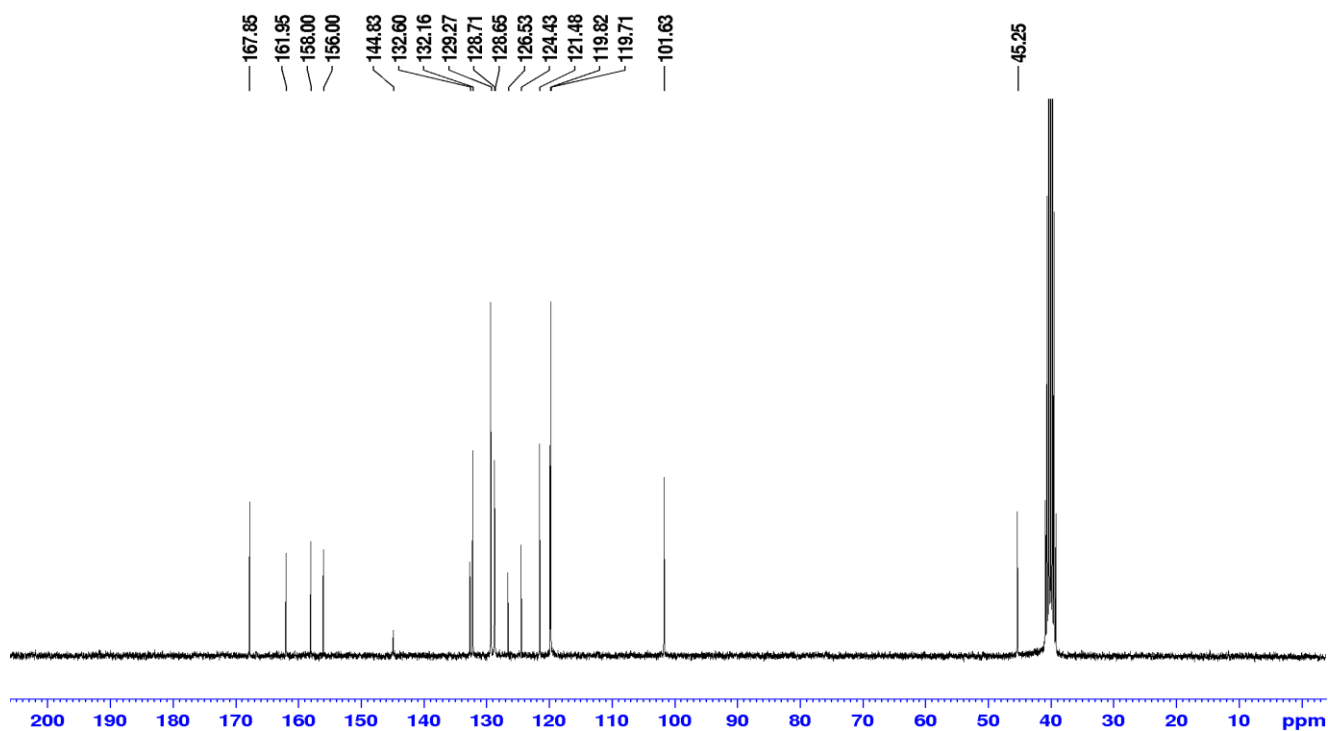


Figure S8. <sup>13</sup>C NMR spectrum (75 MHz, DMSO-d<sub>6</sub>) of compound **13d**.

5-((2-nitro-1H-imidazol-1-yl)methyl)-3-(4-(4-(trifluoromethoxy)phenoxy)phenyl)isoxazole (**13e**)

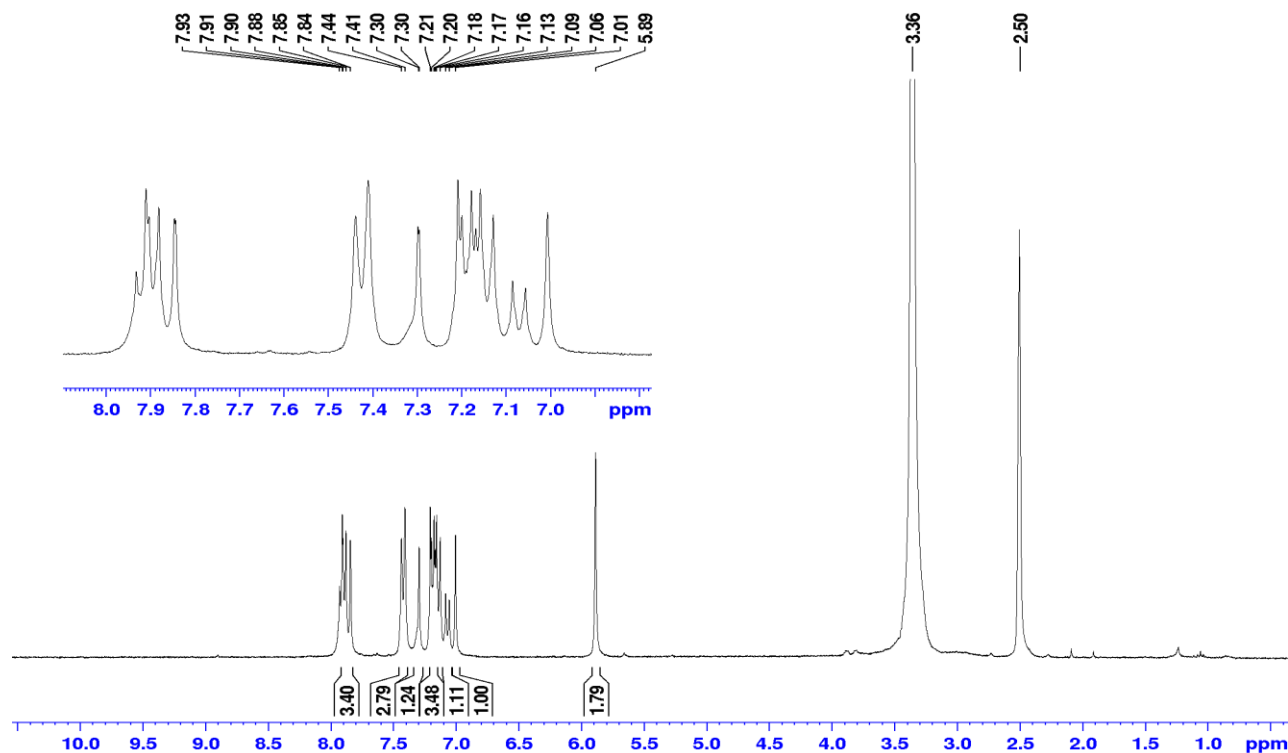


Figure S9. <sup>1</sup>H NMR spectrum (300 MHz, DMSO-d<sub>6</sub>) of compound **13e**.

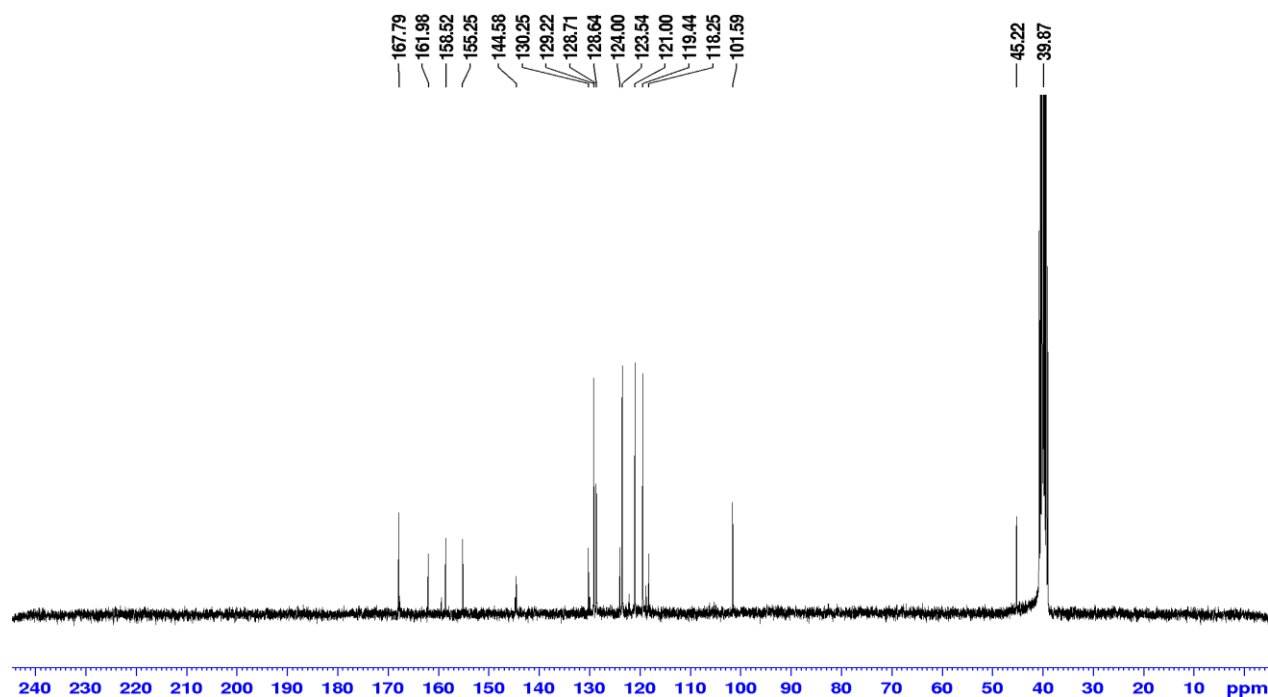


Figure S10. <sup>13</sup>C NMR spectrum (75 MHz, DMSO-d<sub>6</sub>) of compound **13e**.

5-((2-nitro-1H-imidazol-1-yl)methyl)-3-(4-(p-tolyloxy)phenyl)isoxazole (**13f**)

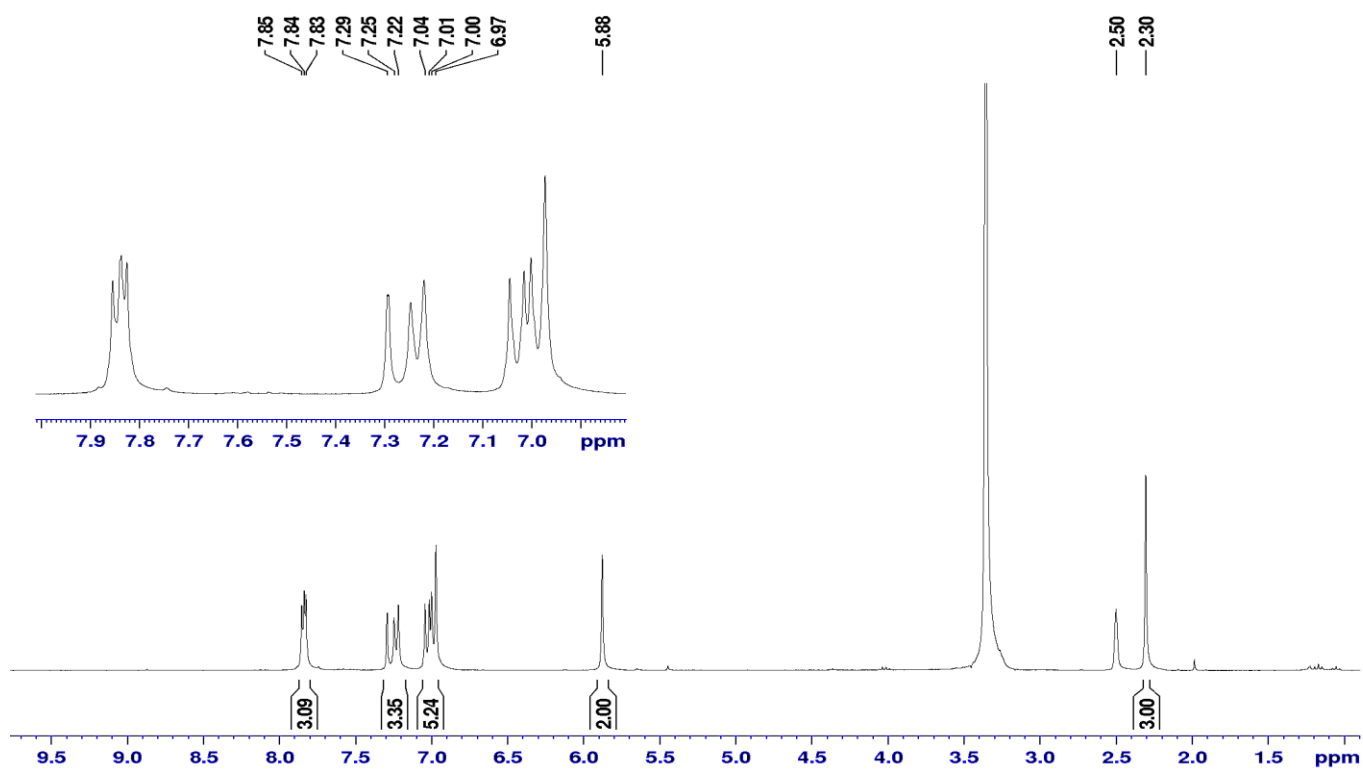


Figure S11. <sup>1</sup>H NMR spectrum (300 MHz, DMSO-d<sub>6</sub>) of compound **13f**.

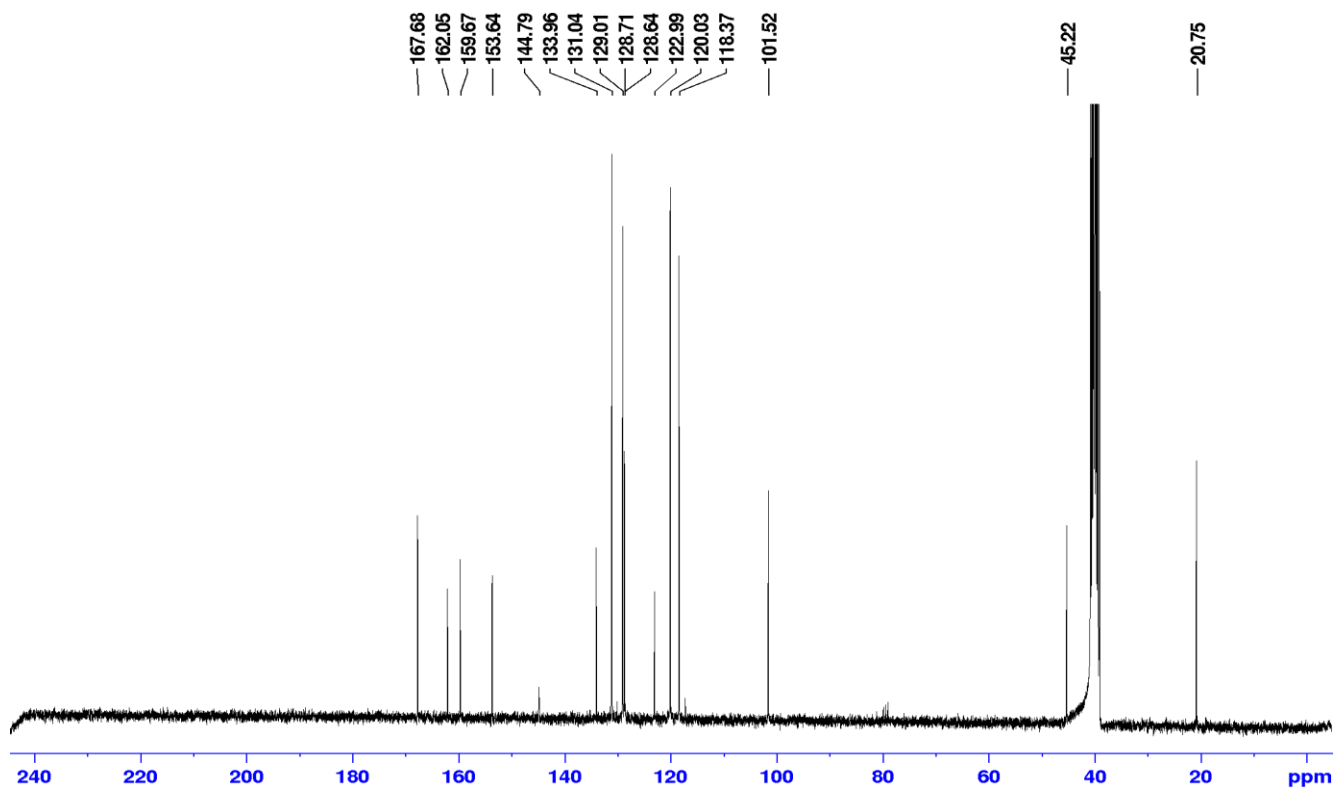


Figure S12. <sup>13</sup>C NMR spectrum (75 MHz, DMSO-d<sub>6</sub>) of compound **13f**.

3-(4-(4-methoxyphenoxy)phenyl)-5-((2-nitro-1H-imidazol-1-yl)methyl)isoxazole (**13g**)

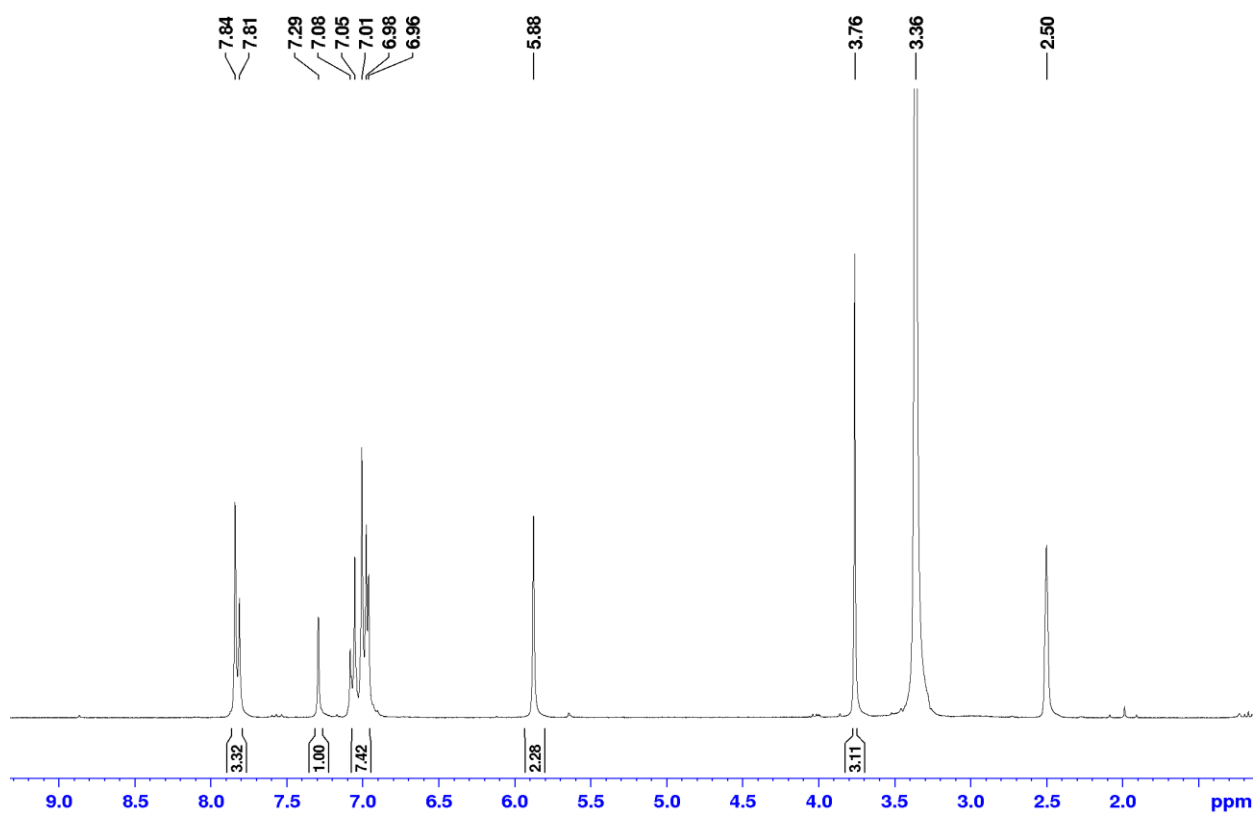


Figure S13. Figure S9. <sup>1</sup>H NMR spectrum (300 MHz, DMSO-d<sub>6</sub>) of compound **13g**.

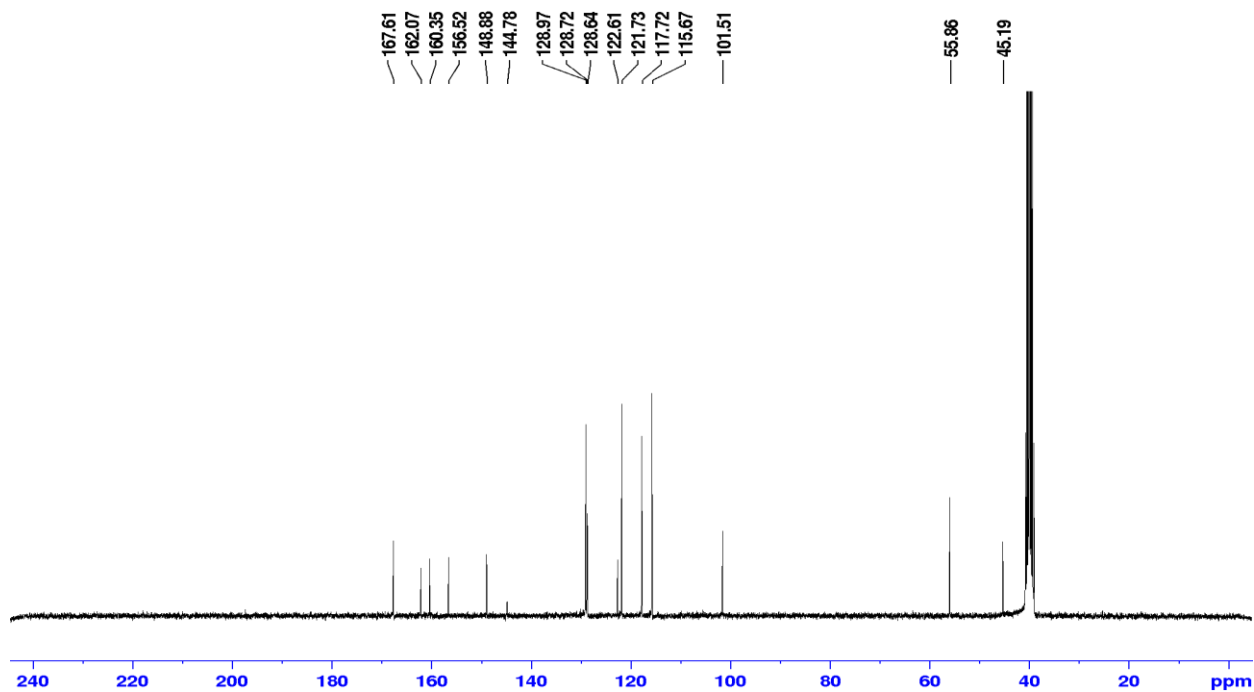


Figure S14. <sup>13</sup>C NMR spectrum (75 MHz, DMSO-d<sub>6</sub>) of compound **13g**.

3-(3-fluoro-4-phenoxyphenyl)-5-((2-nitro-1H-imidazol-1-yl)methyl)isoxazole **13h**.

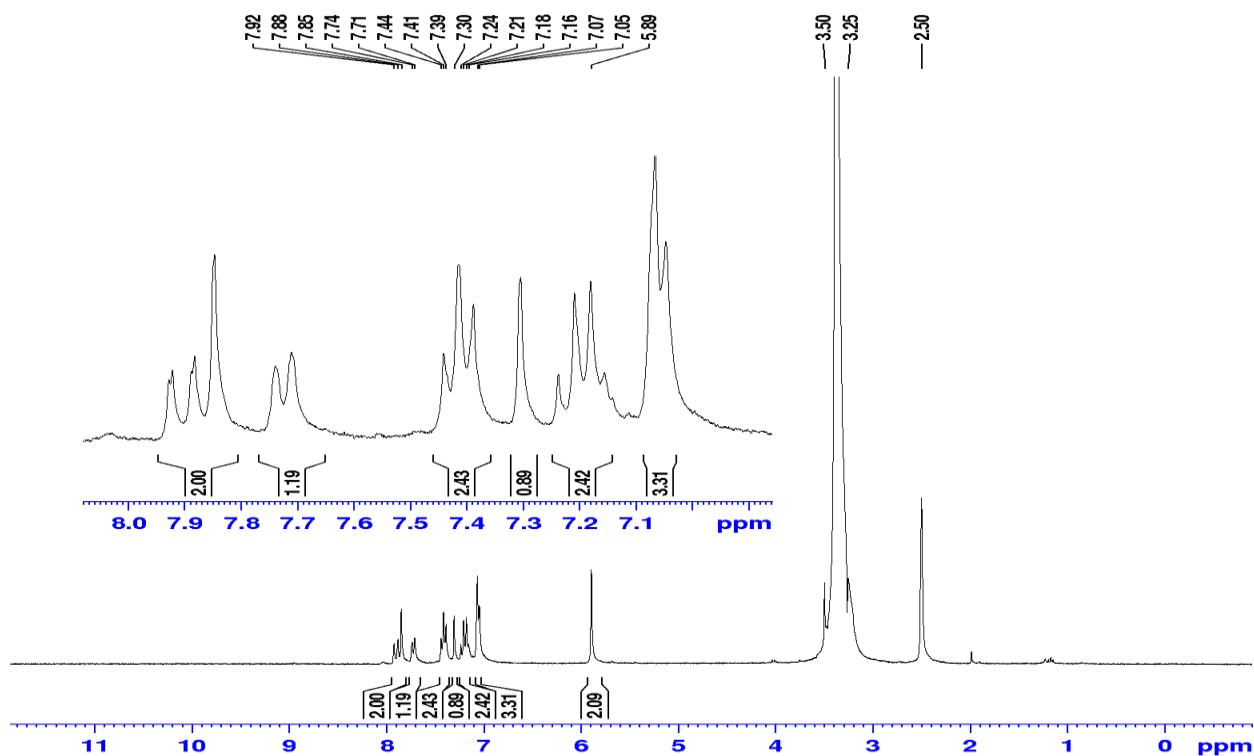


Figure S15. <sup>1</sup>H NMR spectrum (300 MHz, DMSO-d<sub>6</sub>) of compound **13h**.

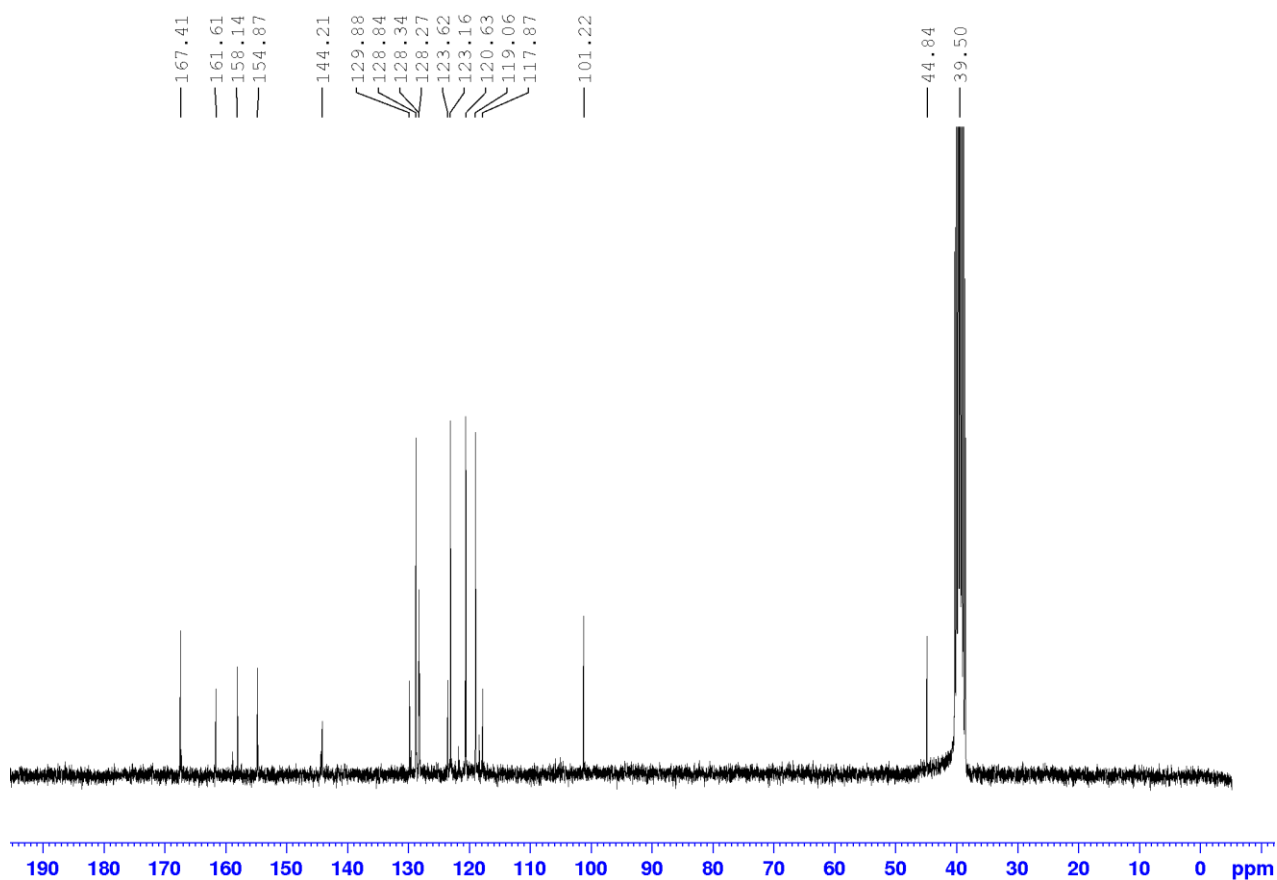


Figure S16. <sup>13</sup>C NMR spectrum (75 MHz, DMSO-d<sub>6</sub>) of compound **13h**.

3-(3-fluoro-4-(4-fluorophenoxy)phenyl)-5-((2-nitro-1H-imidazol-1-yl)methyl)isoxazole **13i**.

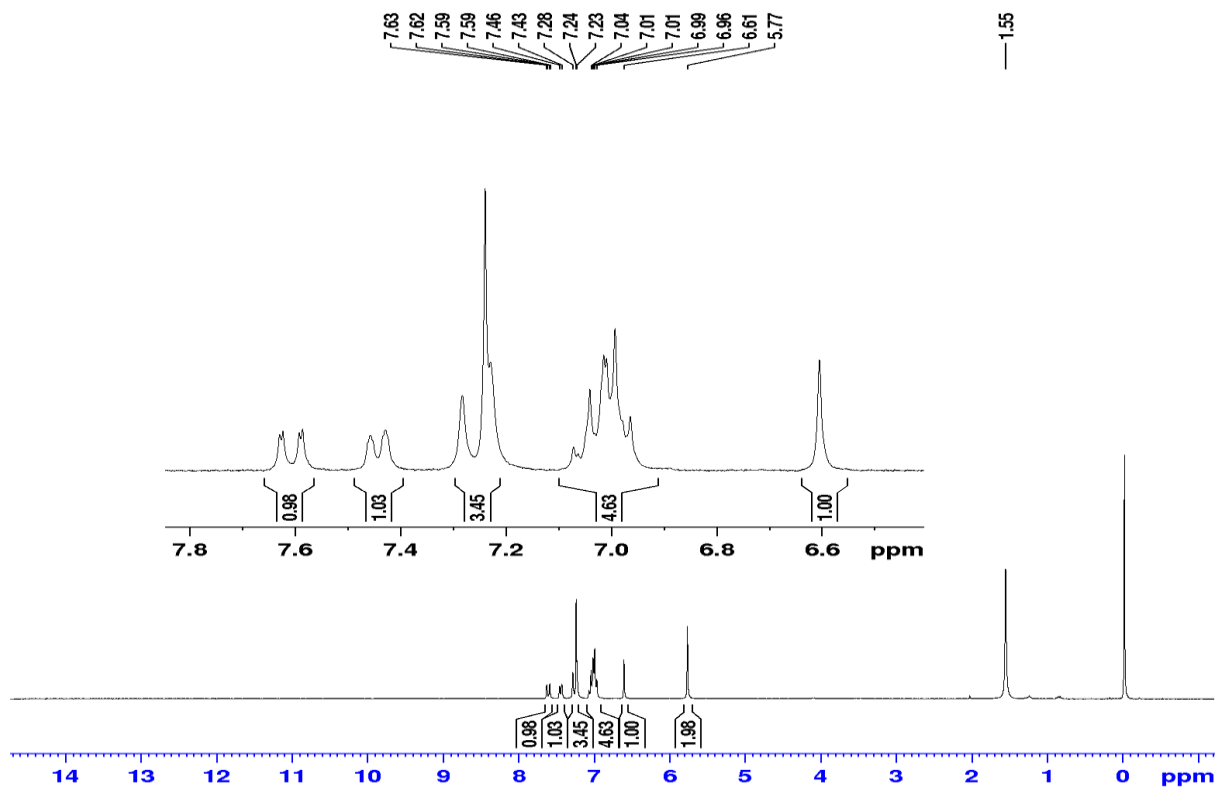


Figure S17. <sup>1</sup>H NMR spectrum (300 MHz, CDCl<sub>3</sub>) of compound **13i**.

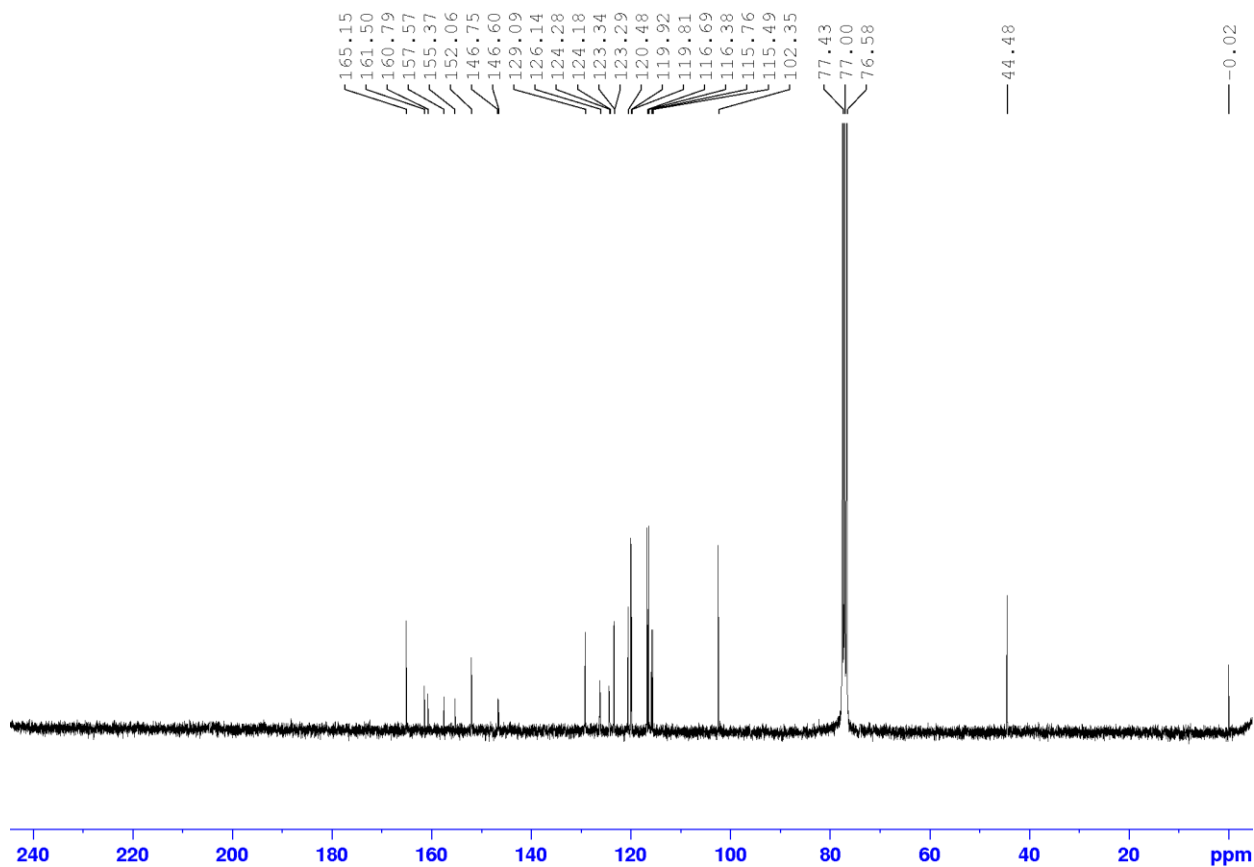


Figure S18. <sup>13</sup>C NMR spectrum (75 MHz, CDCl<sub>3</sub>) of compound **13i**.

3-(4-(4-chlorophenoxy)-3-fluorophenyl)-5-((2-nitro-1H-imidazol-1-yl)methyl)isoxazole **13j**.

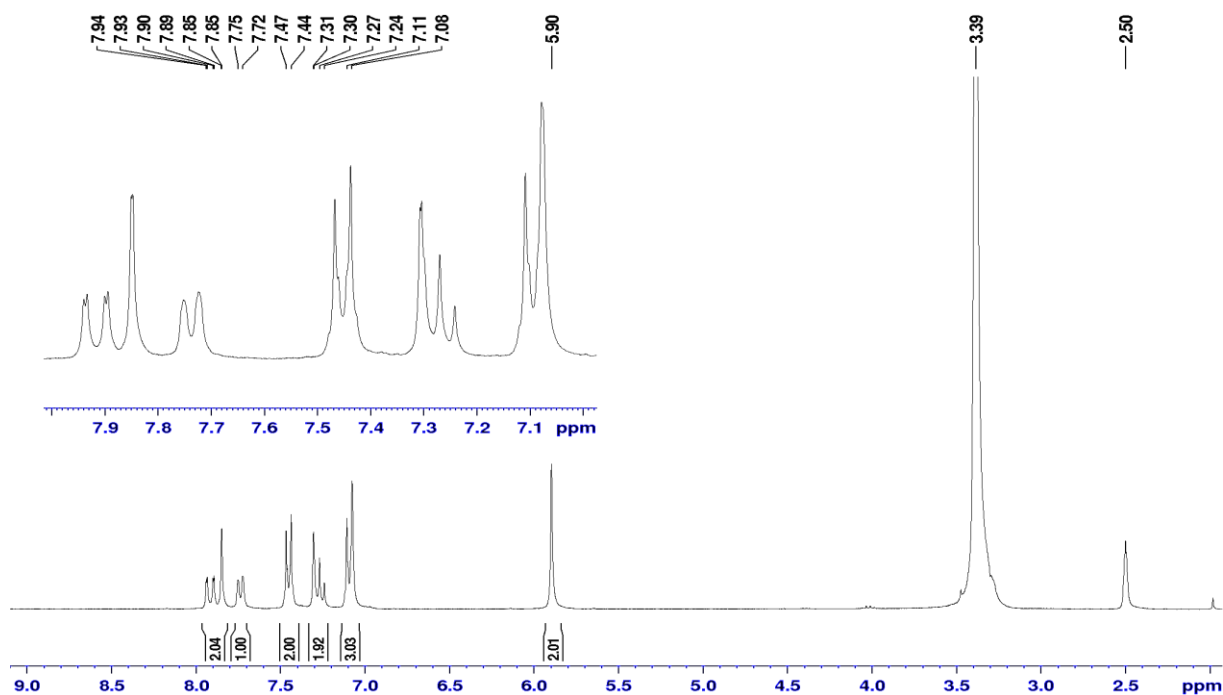


Figure S19. <sup>1</sup>H NMR spectrum (300 MHz, DMSO-d<sub>6</sub>) of compound **13j**.

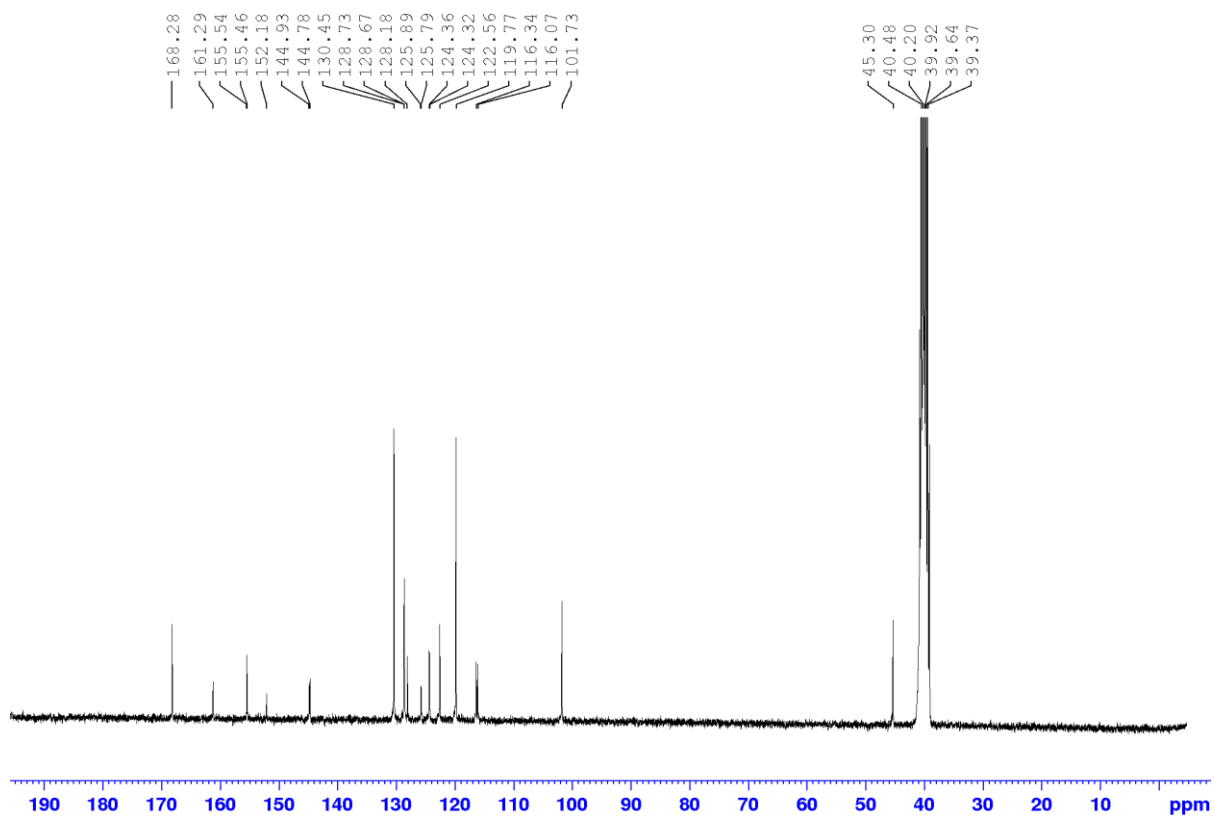


Figure S20. <sup>13</sup>C NMR spectrum (75 MHz, DMSO-d<sub>6</sub>) of compound **13j**.

3-(4-(3,4-dichlorophenoxy)-3-fluorophenyl)-5-((2-nitro-1H-imidazol-1-yl)methyl)isoxazole **13k**.

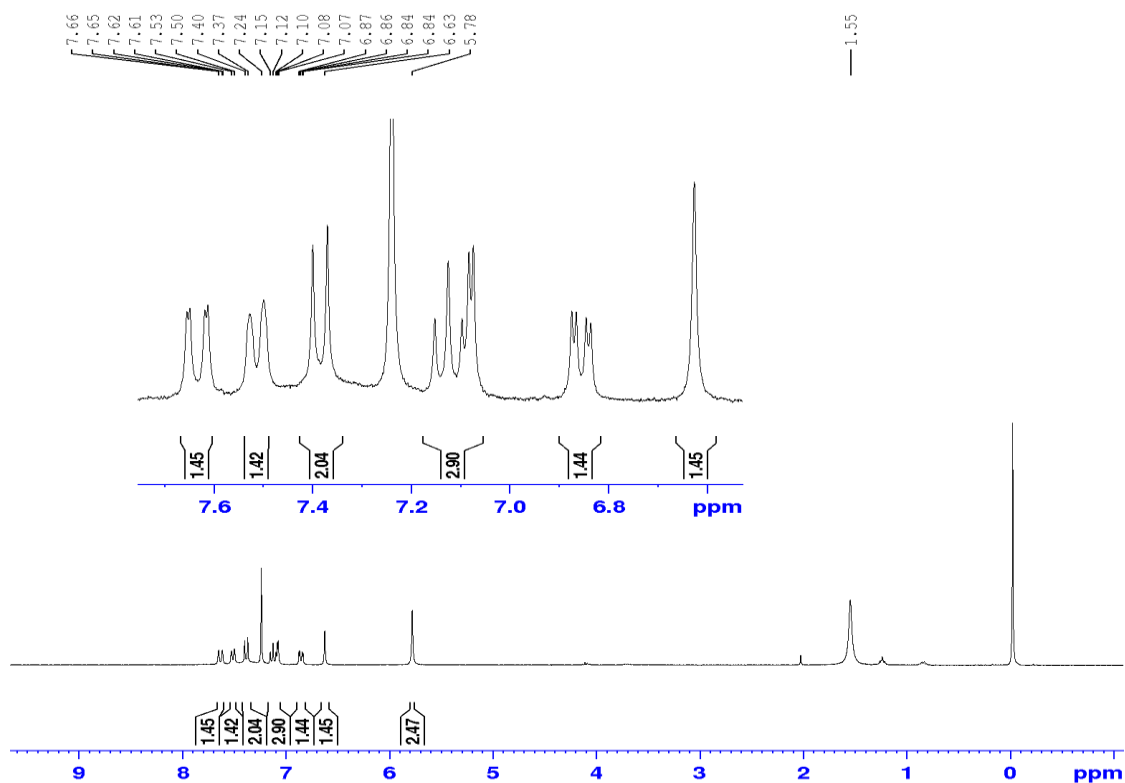


Figure S21. <sup>1</sup>H NMR spectrum (300 MHz, CDCl<sub>3</sub>) of compound **13k**.

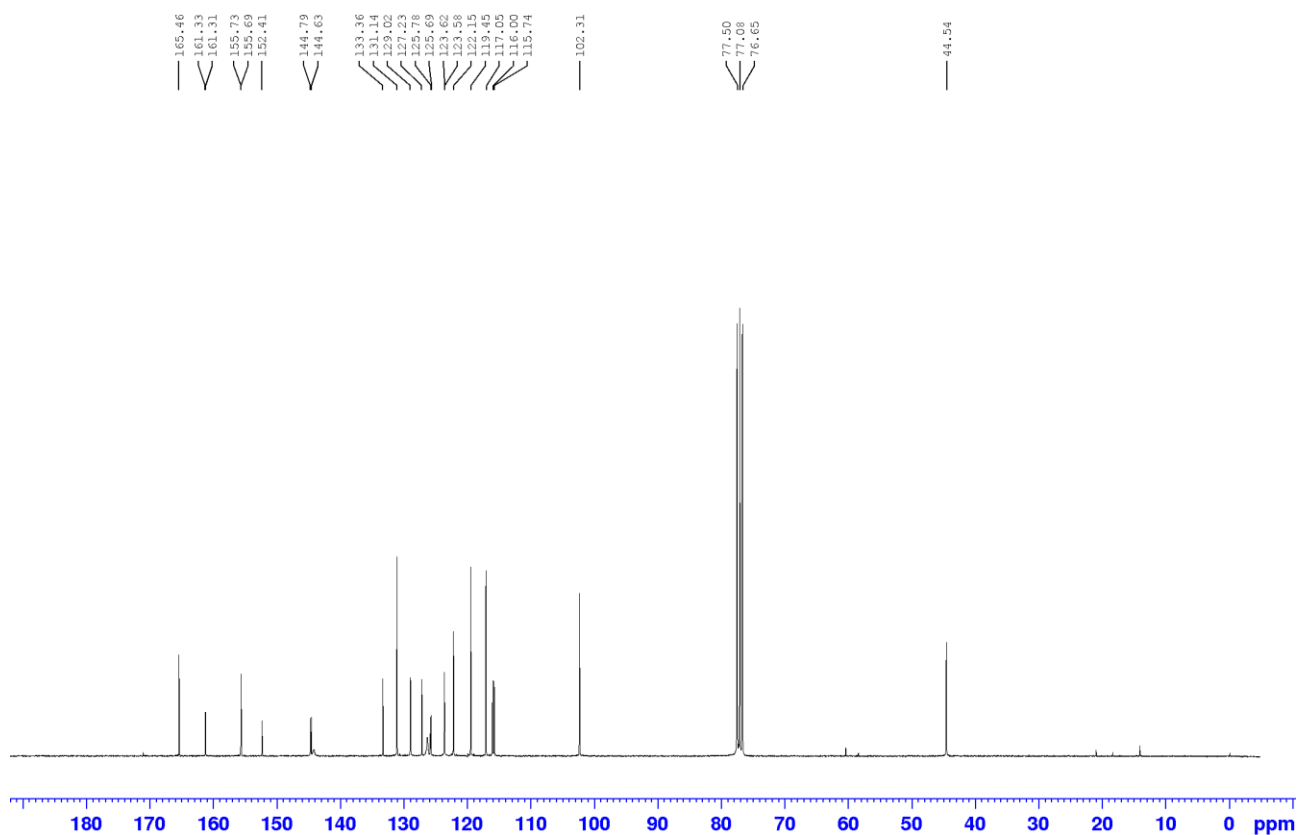


Figure S22. <sup>13</sup>C NMR spectrum (75 MHz, CDCl<sub>3</sub>) of compound **13k**.



3-(3-fluoro-4-(4-(trifluoromethoxy)phenoxy)phenyl)-5-((2-nitro-1H-imidazol-1-yl)methyl)isoxazole  
(**13l**)

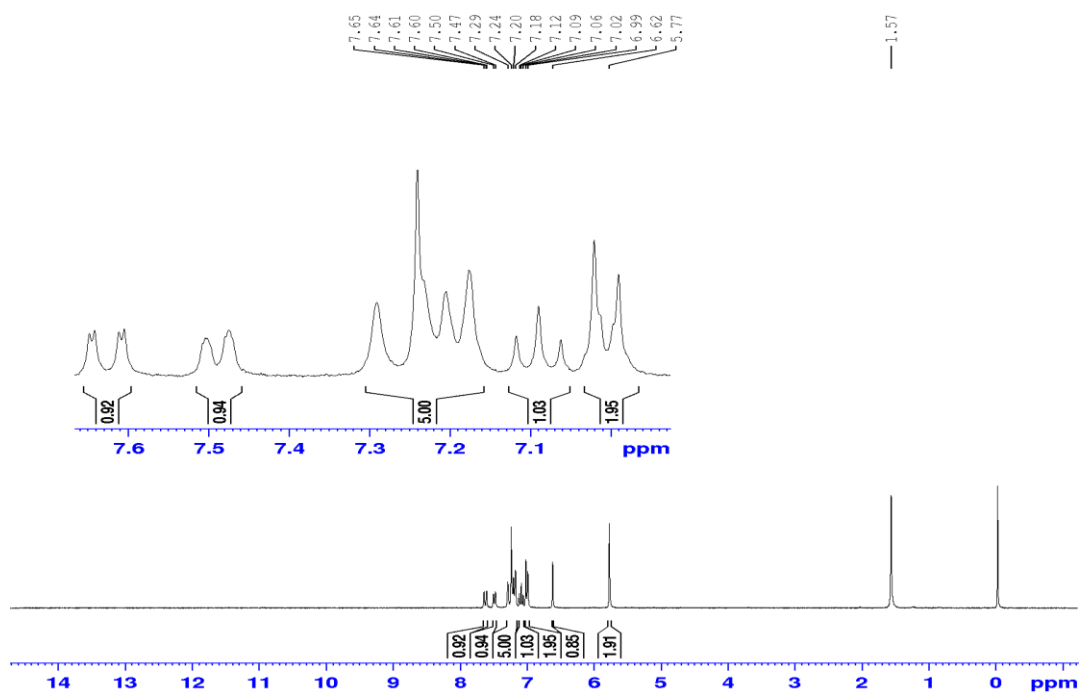


Figure S23. <sup>1</sup>H NMR spectrum (300 MHz, CDCl<sub>3</sub>) of compound **13l**.

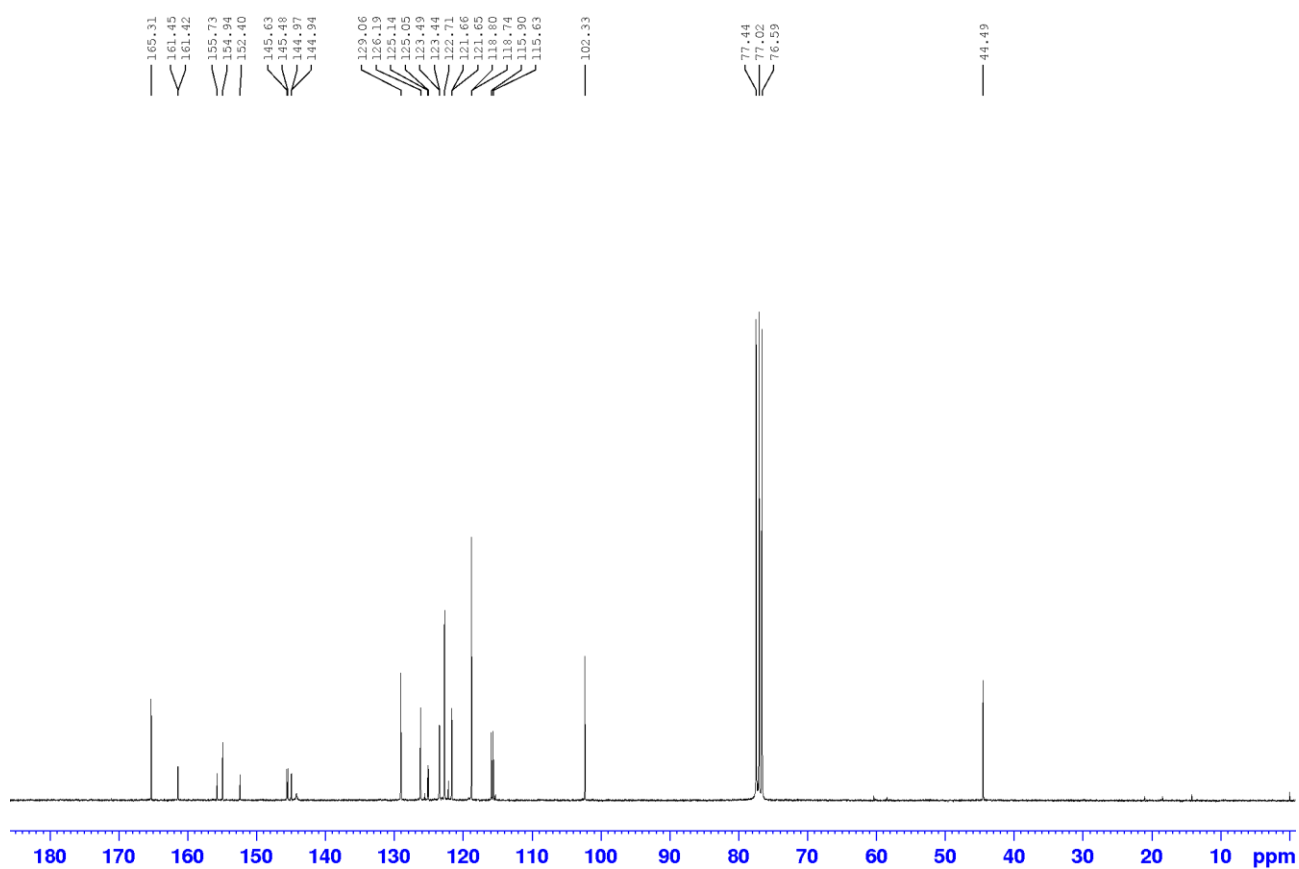


Figure S24. <sup>13</sup>C NMR spectrum (75 MHz, CDCl<sub>3</sub>) of compound **13l**.

3-(3-fluoro-4-(p-tolyloxy)phenyl)-5-((2-nitro-1H-imidazol-1-yl)methyl)isoxazole (**13m**)

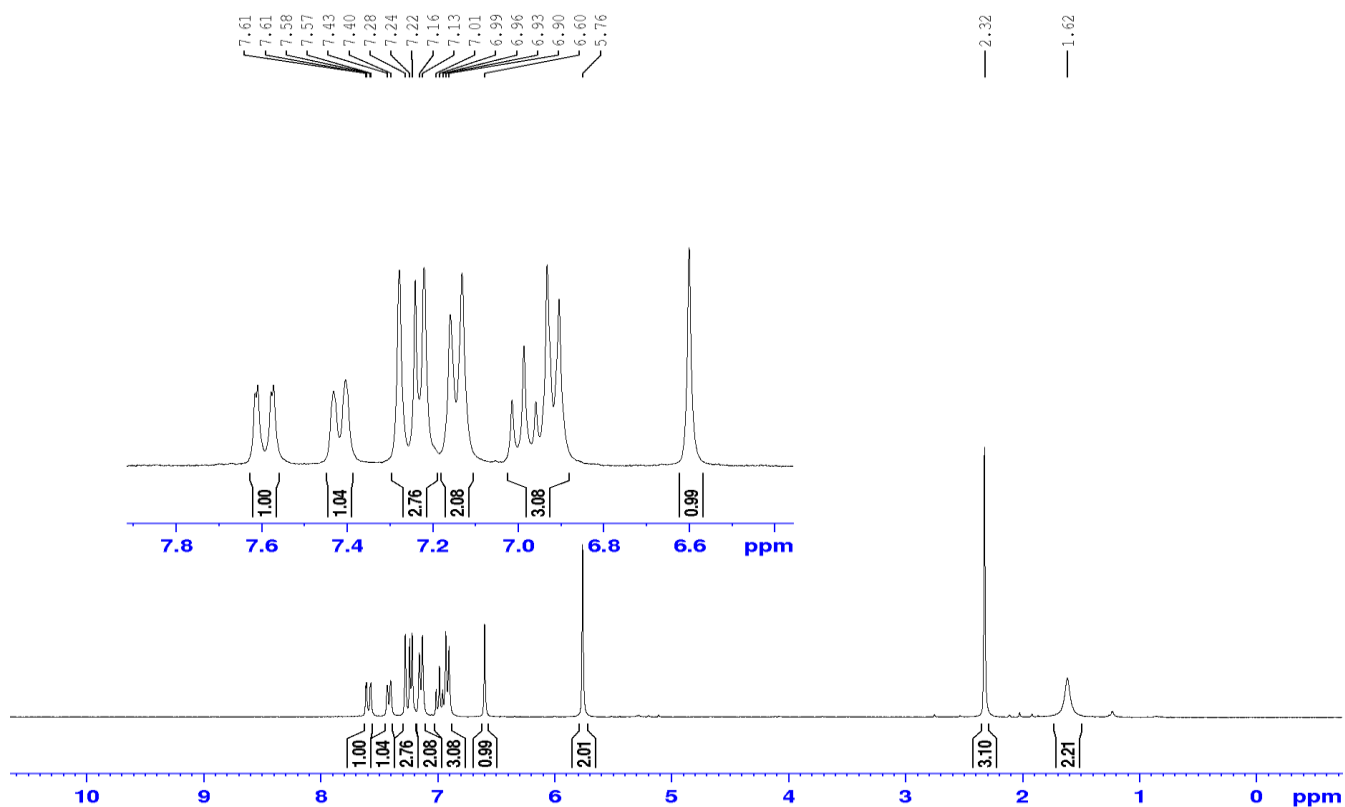


Figure S25. <sup>1</sup>H NMR spectrum (300 MHz, CDCl<sub>3</sub>) of compound **13m**.

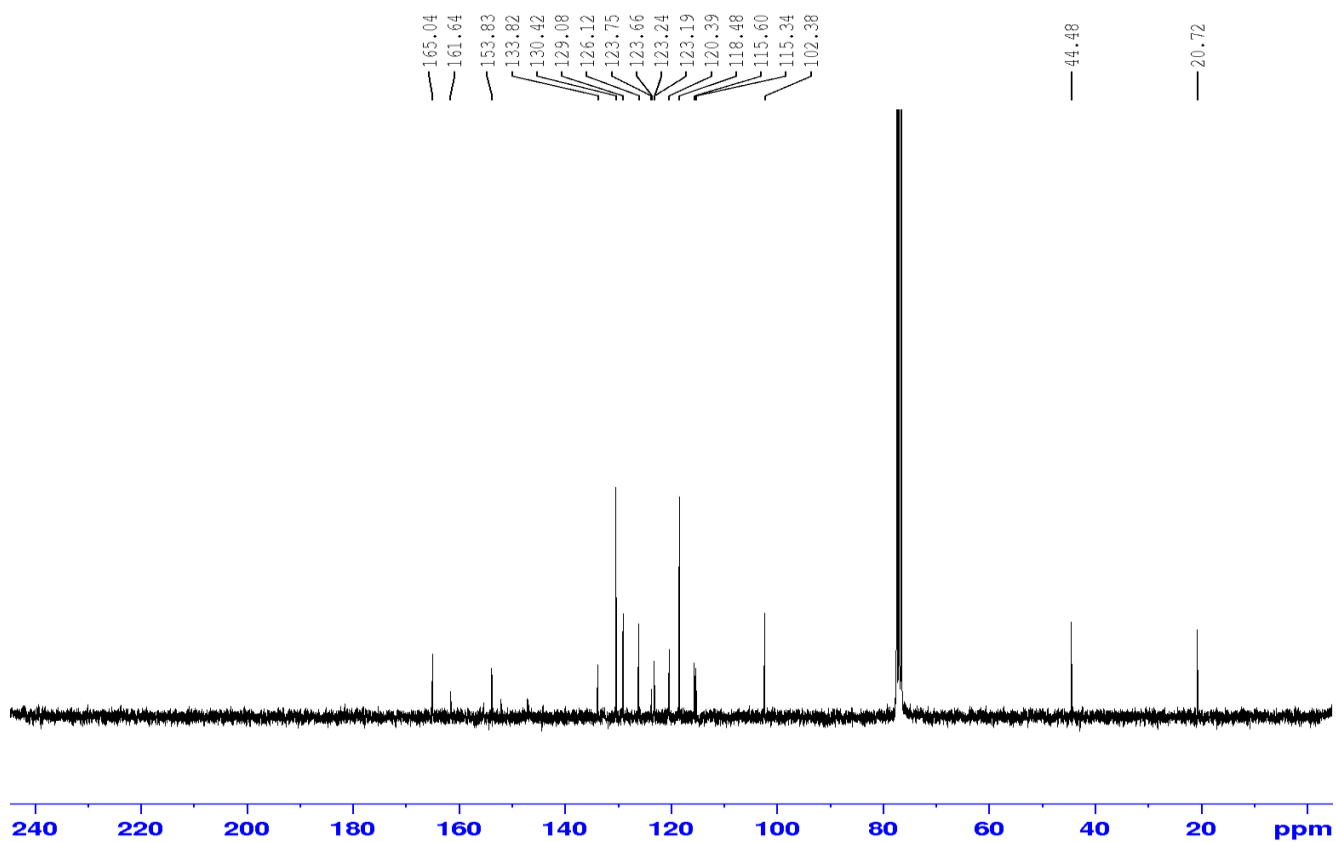


Figure S26. <sup>13</sup>C NMR spectrum (75 MHz, CDCl<sub>3</sub>) of compound **13m**.

3-(3-fluoro-4-(4-methoxyphenoxy)phenyl)-5-((2-nitro-1H-imidazol-1-yl)methyl)isoxazole (**13n**)

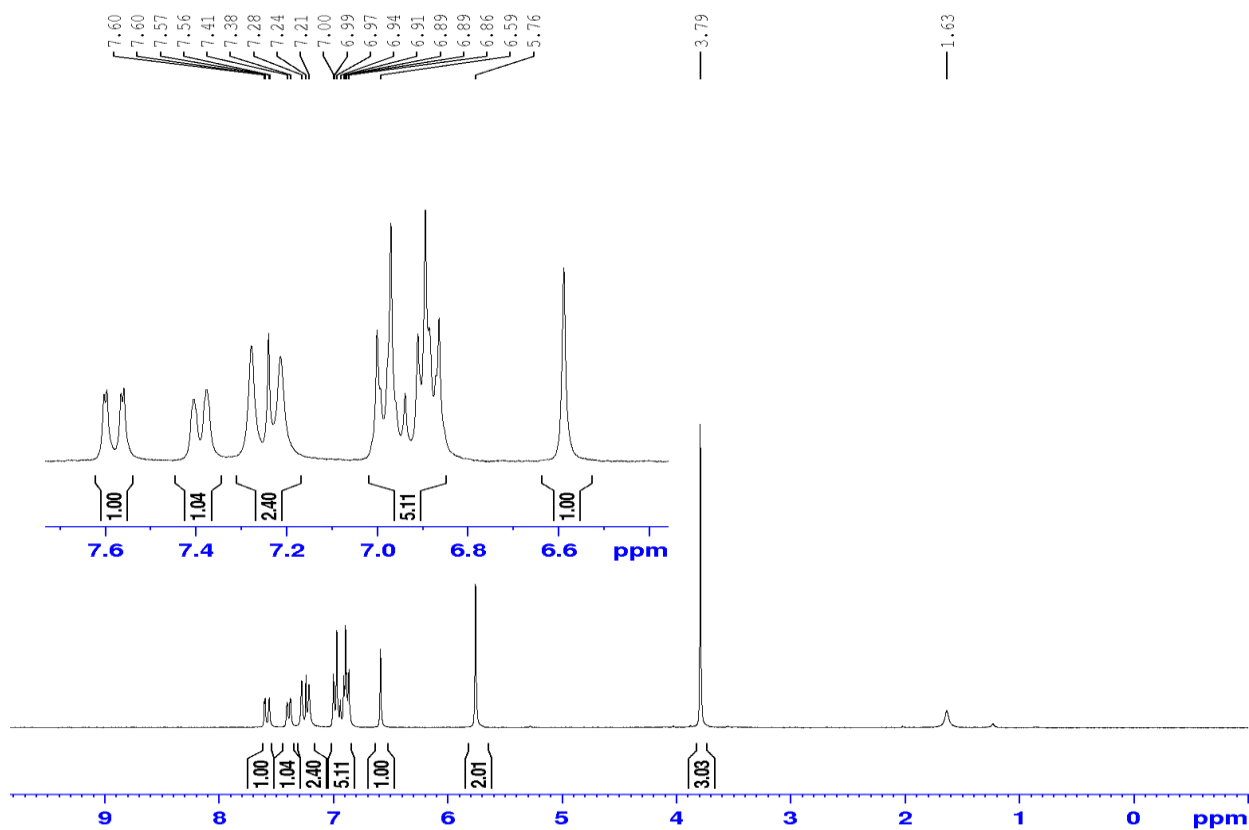


Figure S27. <sup>1</sup>H NMR spectrum (300 MHz, CDCl<sub>3</sub>) of compound **13n**.

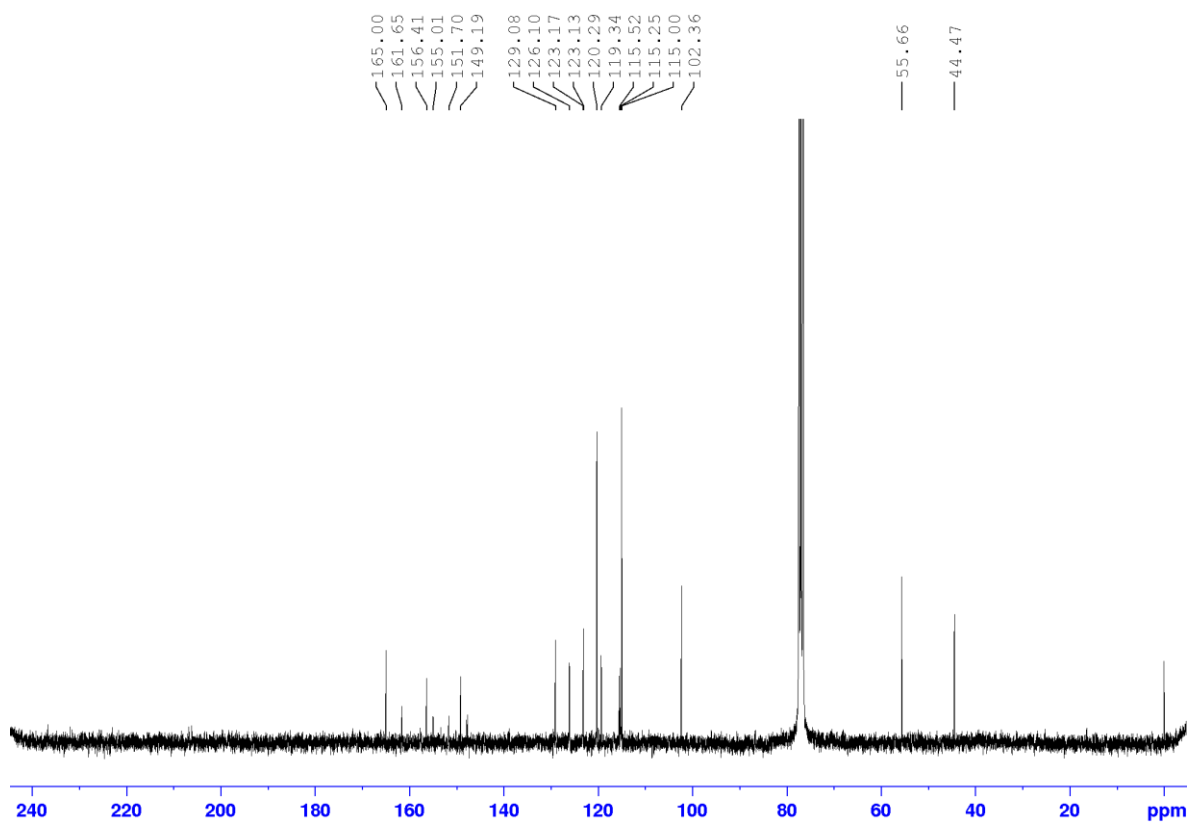


Figure S28. <sup>13</sup>C NMR spectrum (75 MHz, CDCl<sub>3</sub>) of compound **13n**.

5-((2-nitro-1H-imidazol-1-yl)methyl)-3-(4-(phenylthio)phenyl)isoxazole (**13o**)

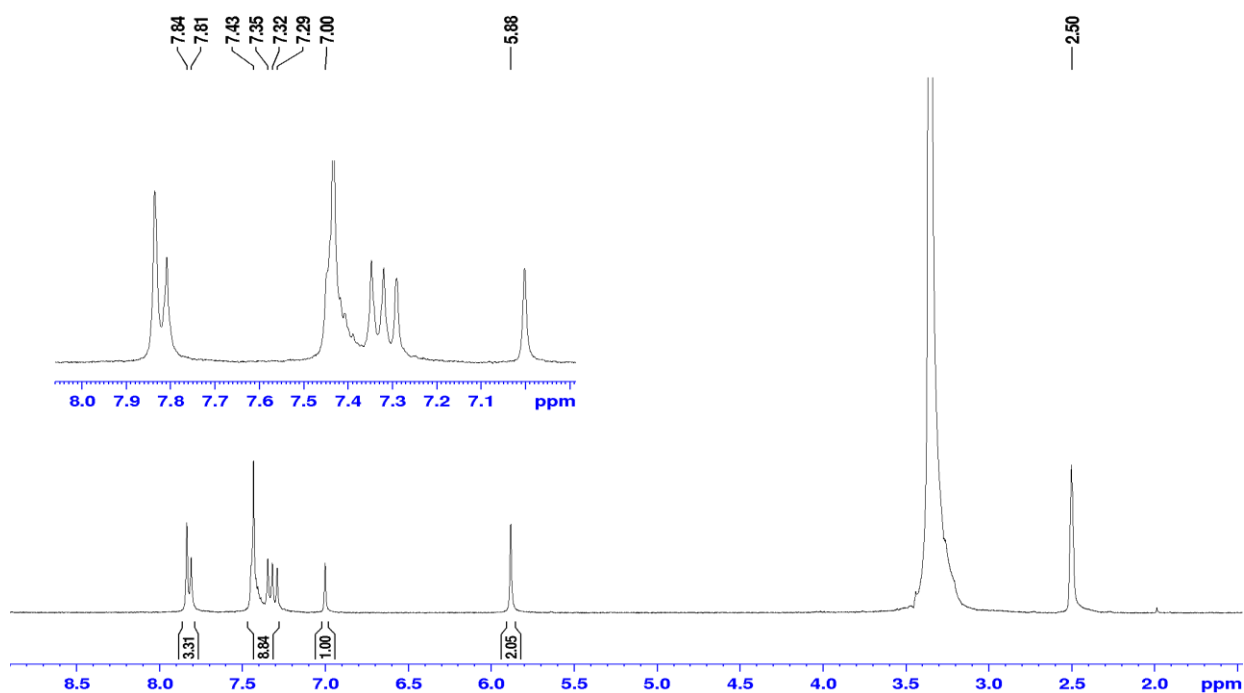


Figure S29. <sup>1</sup>H NMR spectrum (300 MHz, DMSO-d<sub>6</sub>) of compound **13o**.

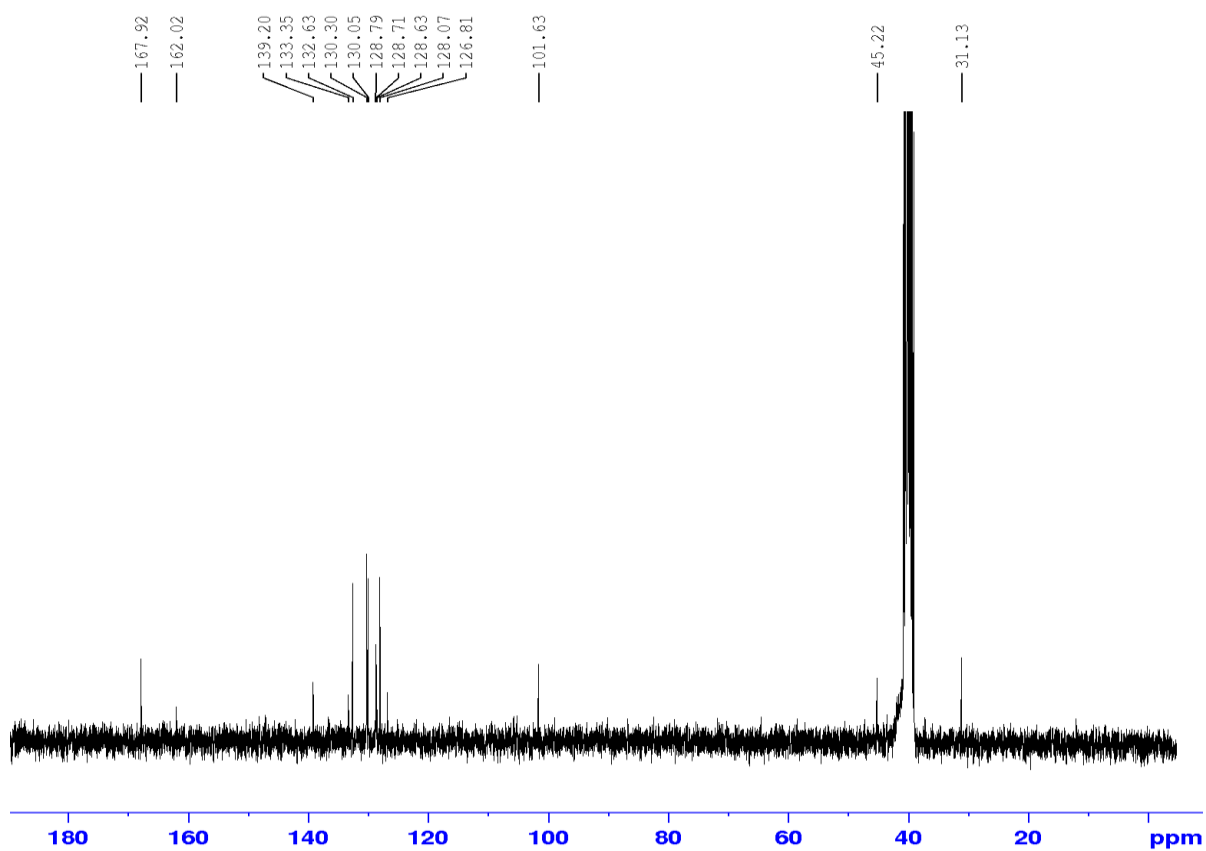


Figure S30. <sup>13</sup>C NMR spectrum (75 MHz, DMSO-d<sub>6</sub>) of compound **13o**.

3-(4-((4-chlorophenyl)thio)phenyl)-5-((2-nitro-1H-imidazol-1-yl)methyl)isoxazole (**13p**)

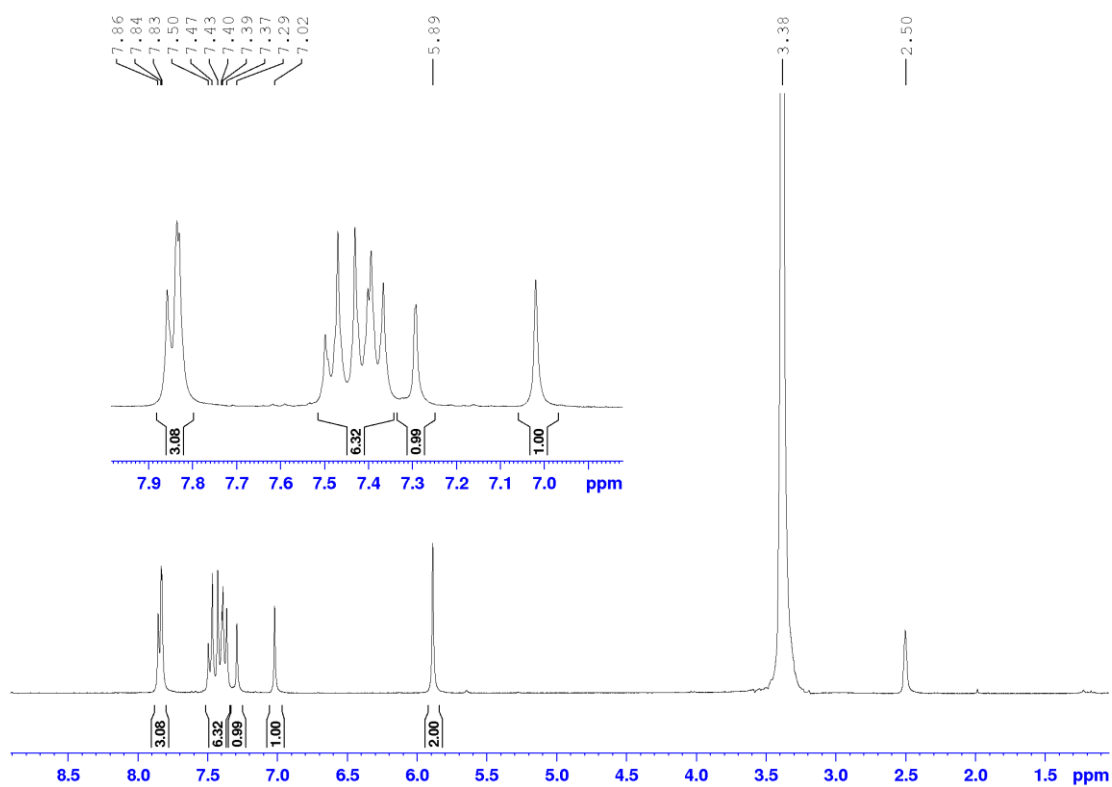


Figure S31. <sup>1</sup>H NMR spectrum (300 MHz, DMSO-d<sub>6</sub>) of compound **13p**.

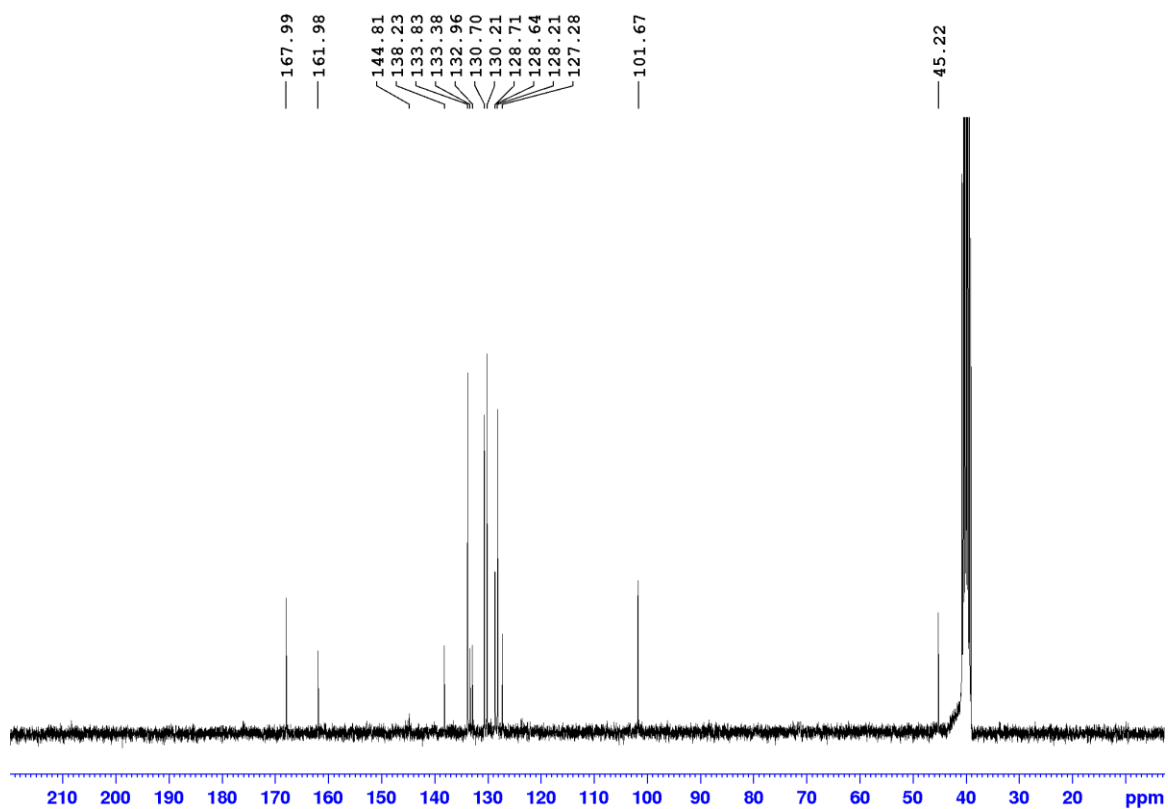


Figure S32. <sup>13</sup>C NMR spectrum (75 MHz, DMSO-d<sub>6</sub>) of compound **13p**.

5-((2-nitro-1H-imidazol-1-yl)methyl)-3-(4-(p-tolylthio)phenyl)isoxazole (**13q**)

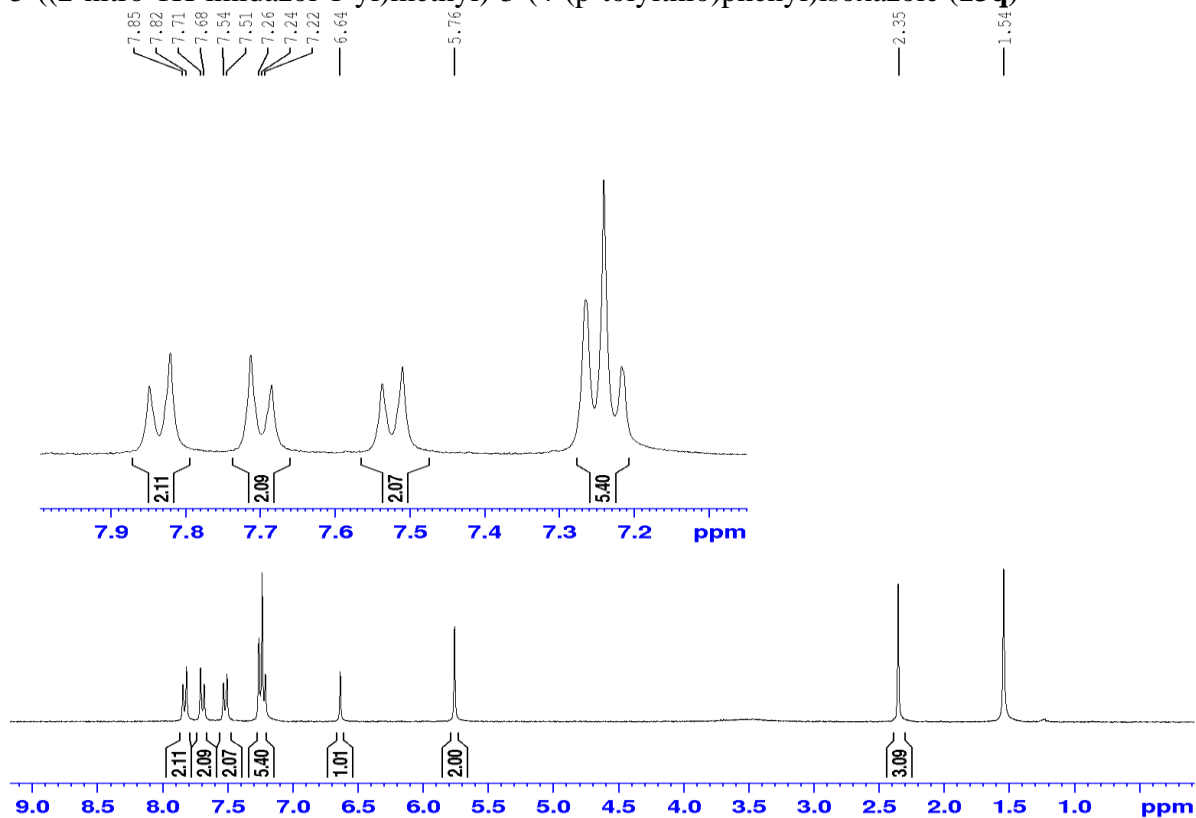


Figure S33. <sup>1</sup>H NMR spectrum (300 MHz, CDCl<sub>3</sub>) of compound **13q**.

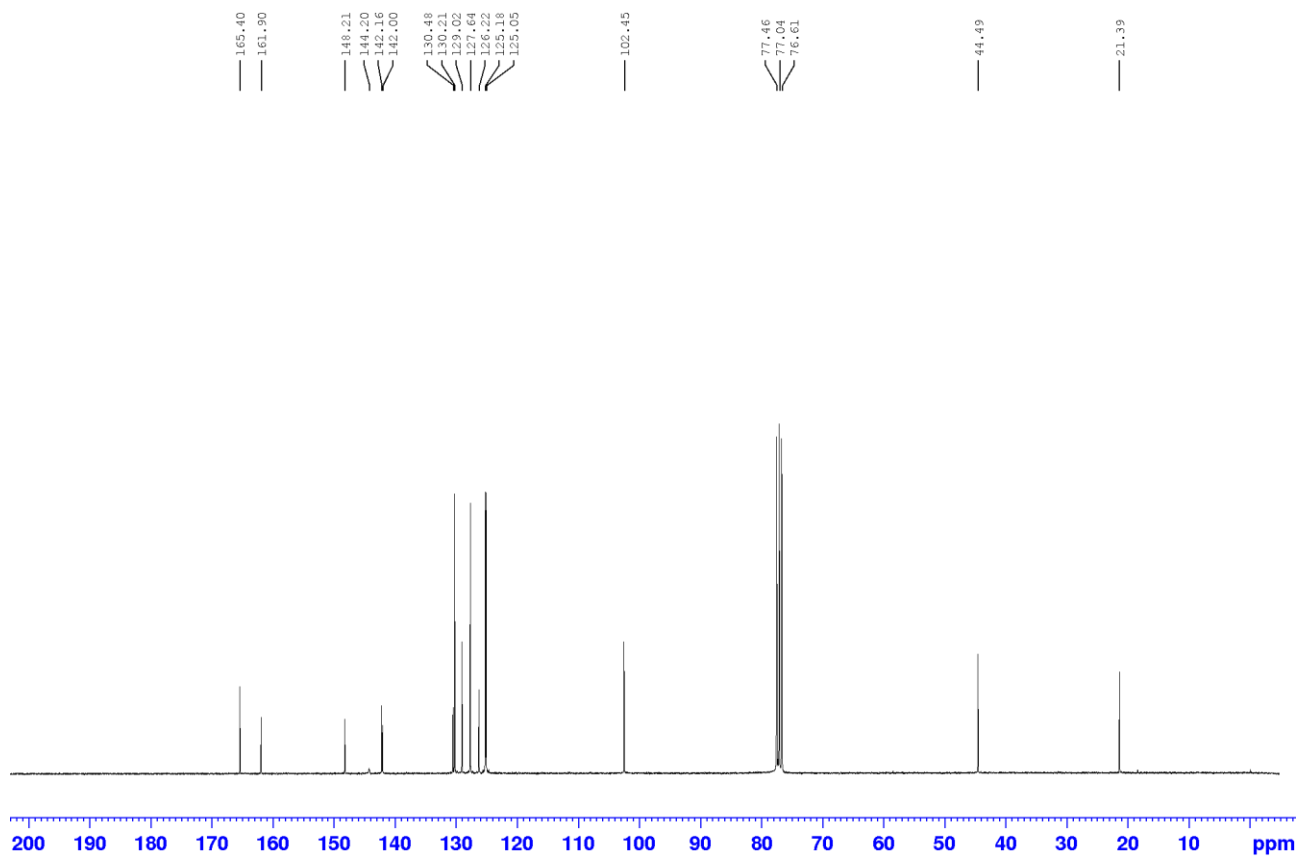


Figure S34. <sup>13</sup>C NMR spectrum (75 MHz, CDCl<sub>3</sub>) of compound **13q**.